Immunocamouflage of Red Blood Cells by means of Layer-by-Layer Self-Assembly Technique for Medical Transfusion

Sania Mansouri

BioMedical Engineering Department
McGill University
Montreal, Canada

Submitted October 2010

A thesis submitted to McGill University, Faculty of Graduate and Postdoctoral Studies, in partial fulfilment of the requirements of the degree of doctor of philosophy.

To my parents...

ABSTRACT

Shortages in the blood supply have potential life-threatening consequences for patients requiring rapid and urgent blood transfusion. Different attempts described in the literature to produce universal blood have drawbacks and still induce the activation of the immune system. We report here new means of universal red blood cells (RBCs) production using the Layer-by-Layer (LbL) self-assembly technique for the deposition of chitosan-graft-phosphorylcholine (CH-PC), poly-L-lysine-graft-polyethylene glycol (PLL-PEG), hyaluronic acid (HA) and alginate (AL) onto functional and non-fixed RBCs. This idea was based on previous findings where fixed RBCs have been used as template for LbL multilayer assembly for the production of hollow capsules. The aim of this thesis, therefore, was to coat fresh and functional red blood cells (RBCs) with a multilayered polymeric shell.

The natural polyelectrolytes, CH-PC, HA, PLL-PEG and AL were successfully assembled in a well-designed multilayer system on non-fixed RBCs in a two-dimensional (2-D) model through the electrostatic LbL assembly technique. A systematic study of constructs formed by two pairs of oppositely charged biocompatible polyelectrolytes has been performed. By modulating the film composition and build-up conditions, such as incorporating the protein-repulsive polyelectrolyte PLL-PEG, adjusting the film thickness and the multilayer permeability, cell recognition by the anti-A antibody is prevented.

The main goal of this thesis was to develop a multilayer shell on non-fixed and functional RBCs in suspension. The design in suspension involved, CH-PC, PLL-PEG and AL that were successfully assembled in a nano-organized shell on non-fixed RBCs through the electrostatic LbL self-assembly technique. The RBCs' shape, morphology were not affected by the polyelectrolytes multilayers build-up. The multilayered nanoshell succeeded in preventing anti-A, anti-B, anti-Lewis y and anti-CD44 antibodies interactions with their specific antigens on the RBC membrane. Moreover, the RBCs maintained their initial role after

their coating which is to carry oxygen. This research has demonstrated that LbL assembly of polyelectrolytes can be used as means to induce immunocamouflage of RBC antigens. As a preliminary step toward the clinical application of such universal red blood cells, an in vivo study was conducted to evaluate the safety and integrity of coated mice RBCs. The coated mice RBCs survived in bloodstream and did not trigger the immune system. These results represent a significant step toward the potential use of the coated RBCs as a universal blood in medical transfusion.

RÉSUMÉ

Les pénuries dans l'approvisionnement de sang ont des conséquences potentiellement mortelles pour les patients nécessitant une transfusion de sang rapide et urgente. Différentes tentatives de production de sang universel décrites dans la littérature présentent des inconvénients et induisent toujours l'activation du système immunitaire. Dans cette étude, nous rapportons une nouvelle stratégie de production de sang universel via la technique de déposition de couche par couche (CpC) de polymères tel que le chitosane-greffé-phosphorylcholine (CH-PC), la poly-L-lysine-greffé-polyéthylène glycol (PLL-PEG), l'acide hyaluronique (HA) et l'alginate (AL) sur les globules rouges (GR) fonctionnels et non-fixés. Cette idée est basée sur des résultats antérieurs, où les globules rouges ont été utilisés comme matrice pour l'auto-assemblage de multicouches pour la production de capsules creuses. L'objectif de cette thèse, était donc d'enrober des GR fonctionnels et non-fixés avec une multicouche polymérique.

Les polyélectrolytes naturels, CH-PC, HA, PLL-PEG et AL ont été assemblés dans un système de multicouches sur les globules rouges non fixés dans un modèle deux-dimensions (2-D) via la technique d'assemblage électrostatique CpC. Une étude systématique des constructions formées par deux paires de polyélectrolytes biocompatibles de charges opposées a été effectuée. Par la modulation de la composition du film et les conditions de construction des CpC, telles que l'incorporation de PLL-PEG qui a la propriété de répulsion des protéines et en ajustant l'épaisseur du film et par conséquent la perméabilité de la multicouche, la reconnaissance par l'anticorps anti-A est empêchée.

L'objectif principal de cette thèse était de développer une multicouche polymérique sur des GR non fixés et fonctionnels en suspension. Le design en suspension incluant CH-PC, PLL-PEG et AL qui ont été assemblés avec succès dans une multicouche nano-organisée sur des GR non fixés par la technique d'auto-assemblage électrostatique de CpC. La forme et la morphologie des GR

n’ont pas été affectées par les multicouches de polymères. Les multicouches polymériques ont réussi à empêcher les anticorps anti-A, anti-B, anti-lewis y et anti-CD44 d’interagir avec leurs antigènes spécifiques à la surface des GR. De plus, les GR enrobés ont maintenu leur rôle initial de transporter l’oxygène. Cette recherche a démontré que l'assemblage de polyélectrolytes par la technique de CpC peut être utilisé comme un moyen d'induire l’immunocamouflage des antigènes érythrocytaires. Comme une étape préliminaire vers l'application clinique de ces GR universels, une étude *in vivo* a été réalisée pour évaluer la biocompatibilité et l'intégrité des GR de souris enrobés. Les GR enrobés ont survécu dans le sang et n’ont pas déclenché pas le système immunitaire chez la souris. Ces résultats représentent une étape importante vers l’application de ces GR universels en transfusion sanguine.

.

ACKNOWLEDGMENTS

First and foremost I would like to acknowledge the dedicated and supportive supervision of Prof. Maryam Tabrizian and Prof. Françoise Winnik. Each has taught me a great deal throughout the past few years, and neither has failed to make time for me and to motivate me. The combination of their outstanding laboratories proficiency, critical thinking, patience, and kindness has enabled me to complete this work. Not enough can be said to properly credit their support, dedication, and generosity. I would like to add that Prof. Maryam Tabrizian and Prof. Françoise Winnik have a wonderful working relationship, which allowed me to capitalize immensely on the synergies between the two research groups. I thank them for giving me the opportunity to work on a project I truly enjoy. I extend my gratitude to Prof. Tabrizian for the numerous opportunities to travel and share my work at national and international conferences. You have been a constant source of motivation for me in the completion of my Ph.D. I want to thank you for the invaluable time spent in your office discussing the problems encountered during my thesis. I would like to specify that Prof. Françoise Winnik has been my research mentor since I started my master. Without your support and guidance, I won't be standing where I stand today.

I would also like to acknowledge the members of my Ph.D. committee, Dr. Satya Prakash, Dr. Yahye Merhi and Dr. Isabelle Cloutier for their insightful comments, guidance and suggestions during the numerous meetings of my Ph.D.

Also many thanks go to Dr. Yahye Merhi from Montreal Heart Institute for his kindness, availability, for providing me with red blood cells, and for his help in conducting the *in vitro* and *in vivo* studies. I want to thank all his group members for their availability and patience, especially Dr. Jean-François Théorêt for the long hours spent on the flow cytometry and for his very helpful advice.

I want to address my sincere gratitude to all the students from Prof. Tabrizian's group and from Prof. Winnik's group. A special thank to Lidija Malic for her

help in editing my manuscripts and thesis, for her encouragement, advice on many matters and invaluable friendship. I want to thank Jamal Daoud, Xuyen Hoa, Nicholas Duceppe and Ziyad Haidar for their friendship and all the good time spent together. A special thanks to Charbel Diab, Rodolphe Obeid, Zhimei Miao and Pei Lian Ma for their help in polymer synthesis and friendship. My gratitude goes to Dr. Julien Fatisson for the advice throughout my thesis. My appreciation goes to Line Mongeon for sharing her remarkable skills with SEM and AFM and Dr. Fereshteh Azari for her invaluable help with the TEM. I would like to acknowledge Pina Sorrini, Lina Vuch, Nadia Morrone, and Andrew Pearce for their administrative assistance.

And to my parents, my brothers and sisters, I owe the maximum gratitude for their support, patience and understanding. I would like to thank my husband Ali for his understanding and encouragement during the down period of the last few years. Special thanks to the smiles and laughs of my little angel Nadia.

Finally, I would like to acknowledge the funding agencies that contributed to this work: Fonds de la Recherche de la Santé du Québec (FRSQ), Natural Sciences and Engineering Council of Canada-discovery grant, the Canadian Institutes for Health Research-regenerative medicine nano-medicine grant and FQRNT-Centre for Biorecognition and Biosensors.

TABLE OF CONTENTS

LIST OF FIGURES AND TABLES

2-D	Two dimension
AFM	Atomic force microscopy
AGM	Aorta-gonad mesonephros
AIHA	Autoimmune hemolytic anemia
AL	Alginate
ATP	Adenosine triphosphate
ATR-FTIR	Attenuated total reflection Fourier transform infrared spectroscopy
BCR	B Cell Antigen Receptor
BFU-E	Burst forming unit-erythroid
BSA	Bovine serum albumin protein
BTC	Benzotriazole carbonate
CFU-E	Colony forming unit- erythroid
CH	Chitosan
CH-PC	Chitosan-graft-phosphorylcholine
CLP	Common lymphoid progenitor
CMC	Carboxymethyl cellulose
CMP	Myeloid progenitor
CN	Cyanuric chloride
CO_2	Carbon dioxide
C-shell	Camouflage shell
D	Dissipation
DAT	Direct antiglobulin tests
DCs	Dendritic cells
DDA	Degree of deacetylation
DEXs	Dextran sulphate
DMPA	L-R-dimyristoylphosphatidic acid
DNA	Deoxyribonucleic acid
ECO	Enzyme-converted group-B-to-group-O
EDC	1-Ethyl-3-[3-dimethylaminopropyl]carbodiimide hydrochloride
Epo	Erythropoietin
ESCs	Embryonic stem cells
FC	Free cholesterol
FITC	Fluorescein isothiocyanate
Gal	Galactose
GalNAc	*N*-acetylgalactosamine
GlcNAc	*N*-acetylglucosamine.
GMP	Granulocyte-myeloid progenitors
GP-A	Glycophorin A
GPC	Gel permeation chromatography
GPI	Glycosylphosphatidylinositol
GR	Grafting ratio

HA	Hyaluronic acid
HbF	Foetal hemoglobin
HCO_3^-	Bicarbonate ions
HFN	Human fibronectin
HIV	Human immunodeficiency virus
HSA	Human serum albumin
HSCs	Hematopoietic stem cells
IB	Ibuprofen
IEP	Isoelectric point
IgG	Immunoglobulin G
IgM	Immunoglobulin M
LbL	Layer-by-Layer
L-PC	Lysophosphatidylcholine
L-PE	Lysophosphatidylethanolamine
MB	Molecular beacon
MEP	Megakaryocytic/erythroid progenitors
mPEG	Methoxypoly(ethylene glycol)
MPP	Multipotent progenitors
MTT	3-(4,5-Dimethylthiazol-2-yl)-2,5-diphenyltetrazolium bromide
NHS	N-hydroxylsuccinimide
NK	Natural killer cells
NOD/SCID	Non-obese diabetic/severe combined immunodeficient
O_2	Oxygen
ON	Orthochromatic normoblasts
OWLS	Optical waveguide lightmode spectroscopy
PA	Phosphatidic acid
PAA	Poly(acrylic acid)
PAH	Poly(allylamine hydrochloride)
PBS	Phosphate buffer saline
PC	Phosphatidylcholine
PDDA	Poly(diallyl dimethylammonium) chloride
PE	Phosphatidylethanolamine
PEG	Polyethylene glycol
PEI	Polyethyleneimine
PEM	Polyelectrolyte multilayer
PI	Phosphatidylinositol
PIP2	PI-4,5-bisphosphate
PIP	PI-monophosphate
PLL	Poly-L-lysine
PLL-HBr	Poly(L-lysine) hydrobromide
PLL-PEG	Poly-L-lysine-*graft*-polyethylene glycol
PLTs	Platelets
PMA	Poly(α,β-l-malic acid)
ProEB	Proerythroblasts

PS	Phosphatidylserine
P-shell	Protecting shell
PSS	Poly(sodium-4-styrene sulfonate)
QCM-D	Quartz-crystal microbalance with the dissipation factor
RBCs	Red blood cells
RETs	Reticulocytes
RNA	Ribonucleic acid
SAR	Scanning angle reflectometry
SDS	Sodium dodecyl sulphate
SI	Supporting information
SM	Sphingomyelin
SP	Succinimidyl propionate
TCR	T cell antigen receptor
TEM	Transmission electron microscopy
TIRF	Total internal relflection fluorescence
VP-SEM	Variable pressure scanning electron microscopy
WBC	White blood cells
WSCH	Water-soluble chitosan

CONTRIBUTIONS OF AUTHORS

This thesis is presented as a collection of manuscripts written by the candidate with the guidance and collaboration of the co-authors. The manuscripts are based on experimental data generated from experiments designed and executed by the candidate who was also responsible for data collection and analysis. Dr. F. M. Winnik and Dr. M. Tabrizian appear as co-authors on the manuscripts to reflect their supervisory role during the execution of the work and their involvement in the manuscript preparation. Dr Y. Merhi was involved in this work scientifically as collaborator by providing the candidate with the red blood cells and facilities in conducting experiments. Dr. J. Fatisson performed the quartz crystal microbalance data modelization in the first manuscript. Dr Z. Miao synthesized chitosan-*graft*-phosphoryl choline and poly-L-lysine-*graft*-poly(ethylene glycol) used in this work.

CHAPTER 1: INTRODUCTION

1.1 State of the field: The need for universal blood

Blood transfusion is one of the most noteworthy success stories in modern medicine. The progress of this now widespread and commonly accepted clinical practice can be attributed to a long history of genius, innovation, and controversy. The earliest references to the clinical applications of blood can be traced back to ancient Egypt and Rome.[1] These early civilizations commonly practiced bleeding of patients due to the belief that there was a strong connection between blood and spirituality. Historically, blood was thought to be the source of life. An animal's liver, the organ that contains the most blood in the body, was considered the greatest offering to the divinities. Many centuries later, the life-saving potential of blood transfusion was recognized. In 1665 Dr. Richard Lower performed the first successful transfusion of blood from one dog to another. About two ounces of blood were transferred via syringe with no apparent harmful effects.[2] After several failed xenotransfusions, the pioneering work by James Blundell in 1829 shifted the interest from animal-human transfusions to human-human transfusions; Blundell is credited for the rebirth of scientific blood transfusion owing to his unbiased approach. However, the lack of information and understanding of human blood groups led to baffling observations of hemolysis and cross-type reactions. These reactions were finally explained by a scientist named Dr. Karl Landsteiner. In 1900, Landsteiner demonstrated that the serum of one human being can agglutinate the red blood cells (RBCs) of another human being.[1] These findings led to the discovery of

ABO blood groups and the understanding of blood group compatibility: only the blood of two individuals bearing the same blood group could be mixed.

These breakthroughs spurred further historical advances in the field on blood transfusion. The time of Great Wars was a remarkable catalyst for transfusion development due to heightened interest in using blood transfusions to address casualties. While the field has grown ever since, despite the significant progress enabled by modern medicine, numerous problems associated with the risk of transfusion of homologous blood, still exist today. Some of these problems include the time-consuming blood-type analysis and crossmatch tests, the transmission of viral disease (human immunodeficiency virus (HIV) and hepatitis), the fatal hemolytic transfusion reactions, the lack of donors, and the emerging pathogens.[3] The recognition of the high risk associated with the transmission of HIV through unsafe blood transfusions led to the introduction of blood safety interventions in the mid-1980s, with a particular focus on the testing of donated blood for HIV. The modern techniques used to screen for infectious agents have rendered blood supplies in the United States, Canada and other developed countries safer than ever. For instance, the current estimated risk of transfusion transmission in Canada for HIV is 1 per 7.8 million donations, for hepatitis C virus is 1 per 2.3 million donations, for hepatitis B virus is between 1 per 153,000, and for malaria is three cases in 10 years.[4] Estimated risks in the United States are somewhat higher for most but not all major transfusion-transmitted infections.

While testing of blood is essential, the first and the most important line of defence is the collection of blood from the safest possible donors. However, the lack of donors, the time and the cost associated with the collection of blood, one of the world's most vital commodities makes the implementation of the defence strategy challenging. For instance, the Canadian Health Care system strongly depends on the blood supply which is replenished each year by an average of 850 000 blood units with the mean cost of blood collection, production, and distribution of US$202.74 per unit.[5]

In emergency situations, such as acute bleeding (35% of patients) and the augmentation of oxygen delivery (25% of patients) [6], the universal donor type, blood group O, is highly desirable for rapid transfusion. This high demand of blood group O often leads to very short supply. Due to potential shortages of human blood, recent attention has been given to alternatives like autologous blood donation and blood substitutes.

Currently, a majority of clinical substitutes for blood are plasma volume expanders that do not provide oxygen (O_2) transport. However, even when blood volume is preserved, severe loss of red cell mass can be fatal due to O_2 deprivation which can eventually lead to cell death and organ failure. Although a "blood substitute" cannot duplicate the whole blood functionality, including the hemostasis and immunity, it can potentially prevent cell death by delivering O_2. For instance, hemoglobin found inside red blood cells is capable of sustaining life by reversibly binding dissolved O_2 in the lungs (oxygenation) and subsequently releasing it in the tissues (deoxygenation). Therefore, the aim of

the research directed towards the development of a blood substitute is to duplicate the physiological properties of hemoglobin in RBCs. As such, the requirements for a potential blood substitute would include low O_2 affinity, prolonged circulation time accompanied with slow removal by the reticuloendothelial system, low toxicity, non-complement activation, and long-term stability.

Up-to-date, several approaches are employed to generate universal RBCs; RBCs production from stem cells *ex-vivo*, the removal of the group-specific carbohydrate antigens from the RBCs by selective enzymatic digestion and the masking of these antigens by conjugating nonantigenic polymers to RBCs. A common shortcoming of these approaches is their inability to prevent the patients from developing alloimmunization against blood group antigens.

The objective of this thesis is to obtain functional RBCs that do not trigger alloimmunization reactions against blood group antigens. The methodology selected is to coat RBCs by the Layer-by-Layer (LbL) deposition of two oppositely charged polyelectrolytes. By using efficient deposition strategies, LbL films can be assembled onto cells that modify and control their biointerfacial properties without affecting their function.

1.2 Thesis outline

This research project is comprised of three major tasks: (1) development and optimization of the coating and immunocamouflage of RBCs deposited on a flat surface "the two-dimension (2D) model" (2) development and optimization of the coating of RBCs maintained in suspension; and demonstration of their biologic activities such as cell hemolysis, cell viability and oxygen uptake (3) assessment of the coated RBCs immunocamouflage, complement activation and stability *in vitro* and biocompatibility *in vivo*. The description and conclusions from each of these parts are presented as published, accepted for publication or submitted articles in chapter 8, 9, and 10. Prior to the presentation of these articles, the rationale and hypothesis are stated and objectives are identified in chapter 2. RBC characteristics are reviewed in chapter 3, including the membrane characteristic. An overview of the immune system is presented in chapter 4. In chapter 5, the various approaches to produce universal red blood cells are overviewed. LbL technique principles are presented in chapter 6. A published review paper forms chapter 7 which provides further background knowledge of the LbL self-assembly technique of polyelectrolytes on 2-D surfaces as well as on colloidal systems.

Chapter 11 summarizes the main contributions of this work and discusses the future perspectives. The cumulative references, copyright waivers and paper reprints, the research compliance certificates and the author's curriculum vitae are available at the end of the thesis.

CHAPTER 2: RATIONALE, HYPOTHESIS AND OBJECTIVES

2.1 Rationale

For a long time, blood transfusion has been subject to the constraint of blood group compatibility. Blood transfusion critically depends on the availability and safety of the transfused material. The LbL self-assembly technique of oppositely charged polymers offers a simple technique to modify the RBCs' surface in order to prevent the activation of the immune system and hence to produce a universal blood. This project constitutes a new challenge to be carried out in the biomedical application of multilayers for immunocamouflage of red blood cells.

2.2 Challenges

The main challenges lie in the production of viable and functional RBCs that do not aggregate in suspension and the prevention of antibody binding onto the modified RBCs. The coating process has to be carried out at physiological pH and ionic strength in order to keep the integrity of the RBCs. Another challenge in this project is to determine a proper polymer combination capable of inducing the immunocamouflage and preventing the adhesion and recognition of the coated RBCs by the antibodies while maintaining the RBCs viability and functionality.

2.3 Opportunities

The strategy followed in order to address these challenges is to use the LbL self-assembly technique which is a method of producing thin films from oppositely

charged species deposited in succession. This method is simple and versatile compared to other techniques of thin film preparation, such as Langmuir-Blodgett deposition. No special apparatus is required for LbL construction, and the multilayer build-up can be made under mild physiological conditions. Film assembly can be described as the kinetic trapping of charged polymers from solution on charged surface. Multilayer formation is possible due the charge reversal on the film surface after each polyion adsorption step. Surface charge depends on the last adsorbed layer, permitting a degree of control over surface and interface properties. Several layers of polyelectrolytes applied in succession form strong coating.

Polymers, namely chitosan-*graft*-phosporylcholine (CH-PC), poly-L-lysine-*graft*-polyethylene glycol (PLL-PEG), hyaluronic acid (HA) and alginate (AL) used in this thesis are biocompatible and biodegradable, which makes them good candidates for the LbL self-assembly on non-fixed RBCs. Additionally, it has been shown that the conversion of primary amine into secondary amine of chitosan can increase the chitosan pKa to 7.2 permitting a charged modified chitosan at physiological pH.

2.4 Hypothesis

We hypothesize that RBCs' antigens can be camouflaged via the LbL deposition technique of natural polyelectrolytes on RBCs for their potential application in medical transfusion. The polyelectrolyte candidates to perform the coating via LbL technique are chitosan-*graft*-phosporylcholine (CH-PC), poly-L-lysine-*graft*-polyethylene glycol (PLL-PEG), hyaluronic acid (HA) and alginate (AL)

because of the tunability of their physicochemical properties which will allow to counterbalance the film repulsive properties to antibodies and the film permeability to nutrient and oxygen uptake.

2.5 Objectives

The overall objective of this project is to produce universal and functional coated red blood cells, via the LbL deposition technique of polyelectrolytes, for medical transfusion. Three specific objectives have been identified as follows which correspond to the major component of the experimental approach.

Development of two-dimension model and optimization of RBCs coating and immunocamouflage

The first objective consists of developing a protocol for non-fixed and functional RBCs' immunocamouflage in a two dimensional (2-D) model. This model requires the adhesion of a monolayer of RBCs on a silica surface. The characterization of the multilayer shell is investigated by zeta potential measurement and quartz-crystal microbalance with the dissipation factor (QCM-D). The immunocamouflage assays are carried out with the QCM-D and immunofluorescence. A demonstration of the RBCs' viability through hemolysis assays is also assessed.

Development and optimization of RBCs coating in suspension

Once the immunocamouflage optimization is achieved in a 2-D model, the second objective consists of developing a protocol for the coating of RBCs in

suspension. The establishment and optimization of the LbL system using extensive physicochemical characterization is required in order to achieve an effective and uniform coating of the RBCs. The functionality and the viability of coated RBCs will also be assessed.

Assessment of the coated RBCs Immunocamouflage

The final objective is to assess the immunocamouflage of the coated RBCs *in vitro* and the coated RBCs biocompatibility *in vivo*, in order to reach our final goal of demonstrating their potential for application in medical transfusion.

3.1 Red blood cell characteristics

Erythrocytes or red blood cells were described for the first time by the Dutch scientist Lee Van Hock in samples of human blood in 1674. A typical human erythrocyte consists of a simple plasmatic membrane that contains a high quantity of hemoglobin (Figure 3.1). It has a nominally circular shape with a diameter of 6-8 μm and a thickness of 2 μm. Within a certain pH range and salt concentrations, the cell membrane of RBCs is deformable, however, it remains tolerant toward mechanical stress *in vitro* and *in vivo*.[7] In a hypotonic medium, the cell swells and becomes a large sphere before hemolysis occurs. Conversely, the cell shrinks and becomes crenate in a hypertonic medium. However, the cell is stomatocytic at pH 5.5 and crenate at pH 9.5 if the tonicity is not changed.[7]

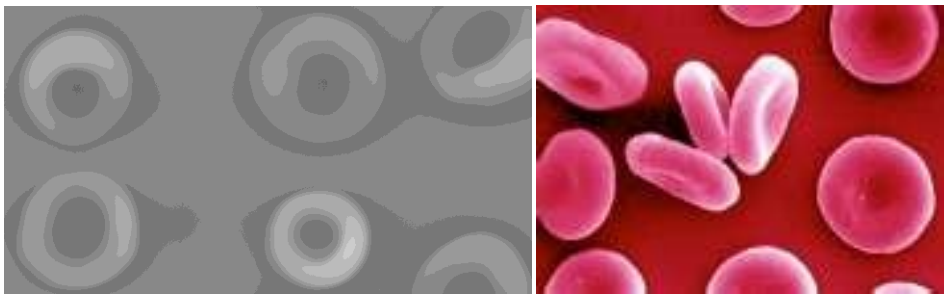

Figure 3.1. Scanning electron microscopy of red blood cells.

Mammalian RBCs are continually produced by the bone marrow. During their maturation and before starting to circulate in blood, they lose their nuclei and the majority of their internal structure.[8] Mature RBCs lack cellular organelles such as mitochondria, golgi apparatus and endoplasmic reticulum. As a result, the

RBCs produce the energy carrier ATP from glucose by a glycolysis pathway. RBCs do not contain deoxyribonucleic acid (DNA) and cannot synthesize ribonucleic acid (RNA). In addition, RBCs cannot divide and have limited repair capabilities.[8] The average life cycle of a red blood cell is 120 days.[9] At the end of their life-span, RBCs become senescent, and are removed from circulation by macrophages and subsequent phagocytosis in the reticuloendothelial system (spleen, liver and bone marrow). This process removes old and defective cells and continually purges the blood.[10]

Hemoglobin, first identified in the 19th century by Hope Seyler, is at the heart of RBCs and plays a crucial role in oxygen delivery to different tissues.[9] The hemoglobin molecule is an assembly of four globular protein subunits. Each subunit is composed of a protein chain tightly associated with a non-protein heme group.[11] Each protein chain arranges into a set of alpha-helix structural segments connected together in a globin fold arrangement. A heme group consists of an iron (Fe) ion (charged atom) held in a heterolytic ring, known as a porphyrin ring which consists of four pyrrole molecules cyclically linked together with the iron ion bound in the centre.[11] Hemoglobin, the main oxygen-carrying molecule in red blood cells, carries both oxygen and carbon dioxide. CO_2 bound to hemoglobin does not bind to the same site as oxygen. Instead, it combines with the N-terminal groups on the four globin chains. However, because of allosteric effects on the hemoglobin molecule, the binding of CO_2 decreases the amount of oxygen that is bound for a given partial pressure of oxygen. The decreased binding to carbon dioxide in the blood due to increased

oxygen levels is known as the Haldane Effect, and is important in the transport of carbon dioxide from the tissues to the lungs.[12] Conversely, a rise in the partial pressure of CO_2 or a lower pH will cause offloading of oxygen from hemoglobin, which is known as the Bohr Effect.[12]

CO_2 is carried in blood in three different ways.[13] About 70% to 80% of the CO_2 is converted to bicarbonate ions HCO_3^- by the enzyme carbonic anhydrase in the red blood cells, by the following reaction:

$$CO_2 + H_2O \rightarrow H_2CO_3 \rightarrow H^+ + HCO_3^- \qquad (3.1)$$

Bicarbonate ions are crucial for regulating the pH of blood. The amount of CO_2 that is dissolved in the plasma corresponds to about 5% – 10% while the remaining 5% – 10% is bound to hemoglobin as carbamino compounds.[13] A person's breathing rate influences the level of CO_2 in their blood. Shallow or low breathing causes respiratory acidosis, while rapid breathing leads to hyperventilation, which can cause respiratory alkalosis.

Upon accidents or during surgical operations with high blood loss, erythrocytes have to be transfused to the patient. To perform transfusion without complications, patients should have the same blood group as the transfused blood. The different blood groups are discussed in the following section.

3.2 Blood groups and red blood cells antigens

To date, 29 blood systems, including the ABO system, have been discovered with approximately 270 different antigens (table 3.1). The ABO system was discovered by Karl Landsteiner.[14] This system offers four possibilities of expression (phenotype): A, B, AB or O (figure 3.2). Each individual possesses one of these four phenotypes [15] and the serum antibodies that are directed against the antigens that are not present in his blood. Specifically, a person with A group has antibodies anti-B; B group has antibodies anti-A; AB group does not have antibodies and finally O group has antibodies anti-A and anti-B. For example, the "A" antigen is present in "A" people, the "B" antigen is present in "B" people and "H" antigen is present in "O" people.[16] Most blood groups antigens are synthesized by the RBCs, but the antigens of the Lewis and Chido/Rodgers systems are adsorbed onto the RBCs membrane from the plasma. Some blood group antigens are detected only on red blood cells; others are found throughout the body.

Biochemical analysis of blood group antigens has shown that they fall into two main types: (i) protein determinants, which represent the primary products of blood group genes and (ii) carbohydrate determinants on glycoproteins and glycolipids, in which the products of the genes controlling antigen expression are glycosyltransferase enzymes. Some antigens are defined by the amino acid sequence of a glycoprotein, but are dependent on the presence of carbohydrate for their recognition serologically.

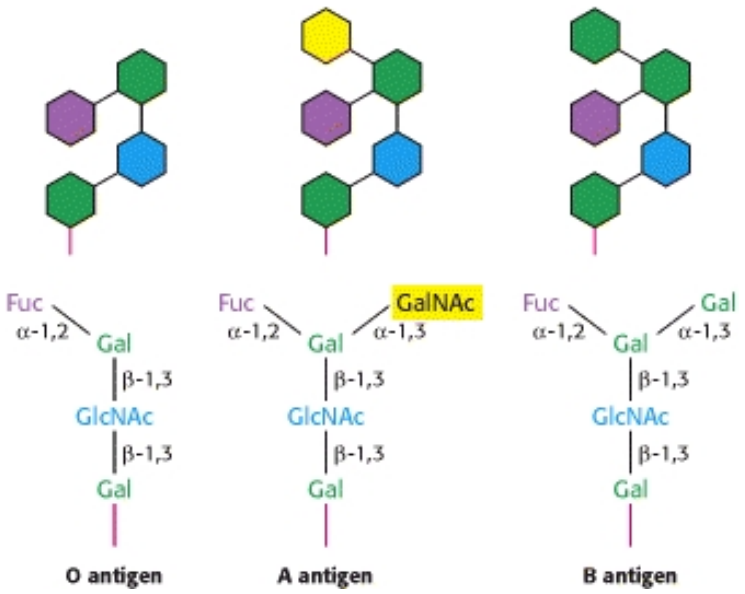

Figure 3.2. Structures of A, B, and O Oligosaccharide Antigens. Abbreviations: Fuc: fucose; Gal:galactose; GalNAc: *N*-acetylgalactosamine; GlcNAc:*N*-acetylglucosamine.[17]

The discovery of the ABO blood groups first made the blood transfusion feasible. The disclosure the Rh antigens led to the understanding and subsequent prevention of hemolytic disease. Transfusion of red blood cells is the most common and tolerated form of tissue transplantation. Normally, simple blood typing ABO/Rh-D is sufficient to identify appropriate donors. Transfusion of ABO-incompatible units is the major cause of transfusion-induced fatalities in the US and the UK.[18] ABO is special in that it is the only histocompatible alloantigen for which pre-existing antibody is present in naive, previously untransplanted (untransfused) recipients. Non-ABO antibodies against the different blood systems listed above are the result of previous transfusions and can also cause hyperacute rejection.

Table 3.1. Human blood groups system [16]

System	Symbol	No of antigens
ABO	ABO	4
MNS	MNS	43
P	P1	1
Rh	RH	46
Lutheran	LU	18
Kell	KEL	24
Lewis	LE	6
Duffy	FY	6
Kidd	JK	3
Diego	DI	21
Yt	YT	2
Xg	XG	2
Scianna	SC	3
Dombrock	DO	5
Colton	CO	3
Landsteiner-Wiener	LW	3
Chido/Rodgers	CH/RG	9
H	H	1
Kx	XK	1
Gerbich	GE	7
Cromer	CROM	10
Knops	KN	7
Indian	IN	2
OK	OK	1
Raph	RAPH	1
JMH	JMH	1

3.3 Red blood cell membrane

The red cell membranes are composed of 19.5% (w/w) water, 39.6% proteins, 35.1% lipids, and 5.8% carbohydrates, the relative contents of which appear to be similar to those in most animal membranes.

3.3.1 Membrane lipid

The content of total lipids is approximately 5.0 x 10^{-10} mg per red blood cell, in which phospholipids are about 60 %, neutral lipids, free cholesterol 30 %, and the rest is glycolipids. In human RBCs, phosphatidylcholine (PC), phosphatidylethanolamine (PE), sphingomyelin (SM), and phosphatidylserine (PS) are predominant, that is, approximately 31% (w/w), 29 %, 26 %, and 13 %, respectively.[19,20] Minor components are phosphatidylinositol (PI), PI-monophosphate (PIP), PI-4,5-bisphosphate (PIP2), phosphatidic acid (PA), lysophosphatidylcholine (L-PC), lysophosphatidylethanolamine (L-PE). At the physiologic pH, PS, PA, and PI have a net negative charge, although the other major phospholipids are electrically neutral.

Table 3.2. Red blood cell membrane lipids

Free cholesterol (FC)	1202 ±103
Total phospholipids (PL)	2604 ± 241
Lysophosphatidylcholine (L-PC)	34 ± 18 (1.3 ± 0.7 %)
Phosphatidylcholine (PC)	747 ± 73 (28.7 ± 2.8 %)
Sphingomyelin (SM)	674 ± 49 (25.9 ± 1.9 %)
Phosphatidylethanolamine (PE)	805 ± 42 (30.9 ± 1.6 %)
Phosphatidylserine (PS) + phosphatidylinositol (PI)	344 ± 34 (13.2 ± 1.3 %)
PC + SM + L-PC/PE + PS + PI	1.27 ± 0.04
FC/PL ratio	0.90 ± 0.04
SM/PC ratio	0.90 ± 0.07

The numbers represent μg per 10^{10} red cells.
The numbers in parentheses represent the percentage of phospholipids (mean value ± 1 SD).

Phospholipids, known as amphipathic lipids, contain aliphatic carbon chains (hydrophobic tails) at one end of the molecule which attach to polar groups (hydrophilic head).[19,20] The hydrophobic tails of these molecules exclude water by associating together and forming a nonaqueous interior while the hydrophilic heads keep contact with the aqueous solution. This molecular mechanism leads to the formation of cell membrane which allows the membrane lipid to exist in the hydrophobic environment of a membrane bilayer. The most amphipathic phospholipids are phosphoglycerides and SM. Most phospholipids have two chains, which are attached to a glycerol backbone. The state of saturation (saturated or unsaturated) of chains, and the length of these acyl chains affect the degree of membrane fluidity significantly. The lysophospholipids have only one fatty acid, and demonstrate strong hemolytic properties, especially on L-PC.

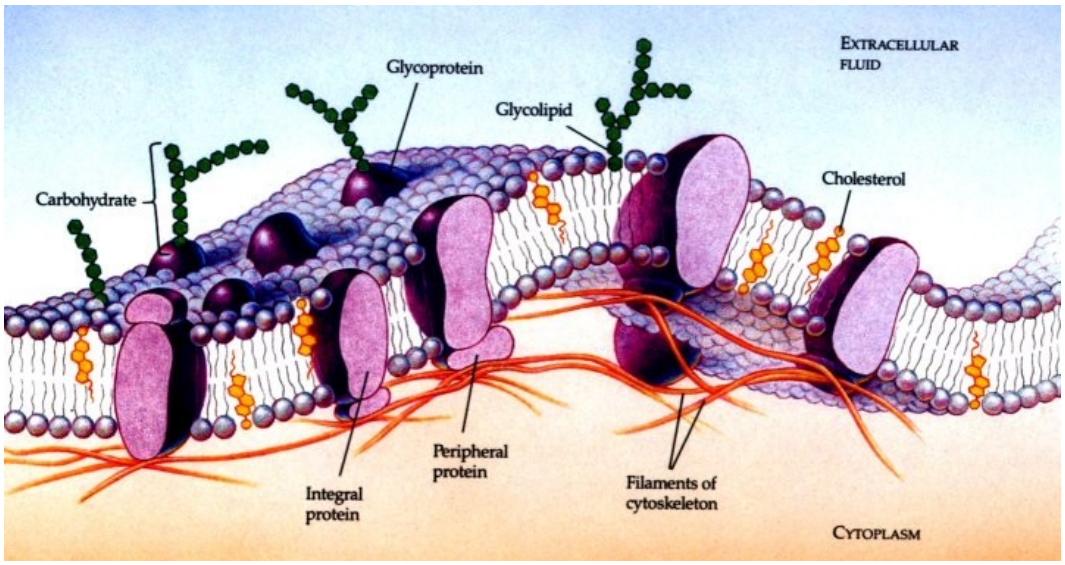

Figure 3.3. Red blood cell membrane.[21]

The glycolipids in human red cells are mostly based on sphingosine, such as glycosphingolipids. Glycolipids are located almost exclusively on the extracellular side of the lipid bilayer, where they carry several important RBC antigens, such as A, B and H.[22] Glycolipids and cholesterol are intercalated between the phospholipids in the bilayer, with their long axes being perpendicular to the lipid bilayer.

In human RBCs, PS and PE are mainly located in the inner monolayer of the lipid bilayer, while PC and SM are predominantly located in the outer monolayer.[19,20] This lipid asymmetry is a widespread property of eukaryotic membranes, and plays a critical role in the normal interaction of the cell with its outer environment.[23,24] The best example is the appearance of PS on the outer surface which leads to a thrombotic diathesis through its binding to prothrombinase, or to apoptosis with the complement activation. The

complement induces apoptosis of the cell by the appearance of PS on the outer surface. This translocation depends on the activity of flippase [25], which actively translocates PS and PE to the inner leaflet, and that of floppase [26,27], which catalyzes translocation to the outer leaflet of the bilayer.

3.3.2 Membrane Proteins

Membrane proteins are categorized into two groups, the peripheral proteins and the integral proteins. The peripheral proteins are loosely associated, and they appear to be associated with only one face (exterior or interior) of the membrane. The integral proteins are extracted only by harsh reagents (chaotropic solvents or detergents), since they are tightly embedded into and throughout the lipid bilayer by hydrophobic domains within their amino acid sequences. The representative peripheral proteins are spectrins (α- and β- chains), and the most typical examples of integral proteins are band 3 and glycophorins.

Membrane proteins are also classified into three categories according to their functional properties in the membrane ultrastructure. The proteins of the first category are cytoskeletal proteins that includes spectrins (α- and β- chains), protein 4.1, and actin. They are associated together to form a cytoskeletal network localized just beneath the lipid bilayer. The second are integral proteins such as band 3 and glycophorins that are embedded into the lipid bilayer. The proteins of the third category are anchoring proteins, such as ankyrin and protein 4.2. These membrane proteins connect with the cytoskeletal network and the integral proteins.

Membrane lipids can interact with membrane proteins within the lipid bilayer. The transmembrane segments of these membrane proteins (especially band 3 protein) maintain multi-component channels and the membrane transport is pumped through stable associations with protein domains within the lipid bilayer. Some membrane proteins, such as glycophorin A (GP-A), bind anionic phospholipids (PS, PI). Positively charged amino acids are predominantly concentrated on the cytoplasmic side of the bilayer-spanning domains of glycophorins and other membrane proteins. Anionic phospholipids (PS, PI) cluster near these regions of positive charge. Spectrin and protein 4.1 bind preferentially to anionic PS and PI, resulting in a nonrandom topography at the inner leaflet of the bilayer.

Negatively charged scialic acid residues are abundant in the RBCs surface. They are present mostly on glycophorin A but also on other glycophorins, band 3 (the anion exchanger), and glycolipids. Integral proteins, glycophorins A, B, C, and D are four sialic acid-rich glycoproteins which constitute approximately 2% of the total human RBCs membrane proteins.[28,29]

Carbohydrates which are located near or at the cell surface, impart a strong net negative charge to the cell surface. The negative charge reduces the interaction of red blood cells with one another, in the same fashion as it does with other blood cells and vascular endothelial cells.

Blood type antigens are also located on the RBC surface. MN blood group antigens reside on the glycophorin A molecule, the Ss antigen on glycophorin B,

and the Gerbich blood group antigen on glycophorin C. The Rh blood group antigens are carried by a family of nonglycosylated but palmitoylated membrane proteins consisting of Rh 30 (RhD and RhCE) polypeptides and the Rh 50 glycoprotein. Other blood type antigens (Duffy, Kell, Kidd, Lutheran, Lewis, and many others) are also known to reside on the surface. Glycosylphosphatidylinositol (GPI)-anchored membrane proteins are embedded in the outer leaflet of the lipid bilayer. A hydrophobic GPI anchor connects externally exposed hydrophilic proteins with the hydrophobic lipid bilayer. Numerous biologically important GPI-linked surface proteins have been identified, including CD59, acetylcholinesterase, leukocyte alkaline phosphatase, the CD4 antigen, and many others.

3.4 Hematopoiesis

Hematopoiesis is a complex developmental process involving the differentiation of 12 distinct cell lineages from a small population of pluripotent stem cells and occurring over many cell generations.[30] In mammals, the sequential sites of hematopoiesis include the yolk sac, an area surrounding the dorsal aorta termed the aorta-gonad mesonephros (AGM) region, the fetal liver, and finally the bone marrow.[31] Hematopoietic stem cells (HSCs) developed in the AGM migrate into fetal liver, where most of the hematopoiesis occurs during mid-gestation and late-gestation.[32,33] Just before birth, hematopoiesis shifts from fetal liver to spleen and finally to the bone marrow, the site that becomes the major hematopoietic organ during adult life.[34-37] During the hematopoiesis primitive pluripotent stem cells give rise to differently regulated, lineage-committed

progenitor cells, which ultimately produce various types of mature end cells that circulate in the peripheral blood. The retention of hematopoietic-committed but lineage-unrestricted state and vast proliferative potential through successive cell divisions is referred to as hematopoietic stem cell self-renewal. However, these terms (self-renewal and differentiation) remain necessarily vague as the nature, multiplicity and potential interrelationships of different mechanisms that may be involved in irreversibly restricting hematopoietic stem cell functions are still largely unknown.[31,38] Under normal conditions the number of differentiated cells in the blood remains relatively constant, however under conditions of stress or increased demand, (e.g., hemorrhage, or following chemotherapy), rapid changes in cell number are observed, which is followed by a return to normal levels when the stress is relieved. These features reflect the existence *in vivo* of complex feedback control mechanisms that operate throughout the hematopoietic hierarchy. Although much progress has been made in identifying a variety of hematopoietic growth factors/cytokines that can singly or in combination influence various properties of primitive hematopoietic stem cells e.g., self-renewal, cell cycle progression or differentiation, the genetic mechanisms that are responsible for stem cell maintenance, activation and lineage commitment are still unknown.

Human erythropoiesis is a dynamic complex multistep process that involves differentiation of early erythroid progenitors to enucleated red blood cells.[31,39] Basically, pluripotent HSCs and early multipotent progenitors (MPP) generate committed erythroid precursors (erythroblasts), which then give birth to mature

erythrocytes (red blood cells; RBCs).[40] In the bone marrow, the HSCs are stimulated by cell-cell interactions and extrinsic factors to begin RBC production.[41,42] The hematopoietic progenitors undergo several transition steps of differentiation and generate the common myeloid progenitor (CMP) and the common lymphoid progenitor (CLP). CLP supplies T and B lymphocytes, natural killer (NK) cells, and maybe dendritic cells (DCs), CMP is converted into megakaryocytic/erythroid (MEP) and granulocyte-myeloid (GMP) progenitors. MEP cells upon the action of growth factors are differentiated into erythropoietin (Epo)-responsive erythroid, burst forming unit-erythroid (BFU-E) and colony forming unit-erythroid (CFU-E). The CFU-Es are then differentiated into orthochromatic normoblasts and finally via enucleation yield reticulocytes first and then RBCs (Figure 3.2).[43]

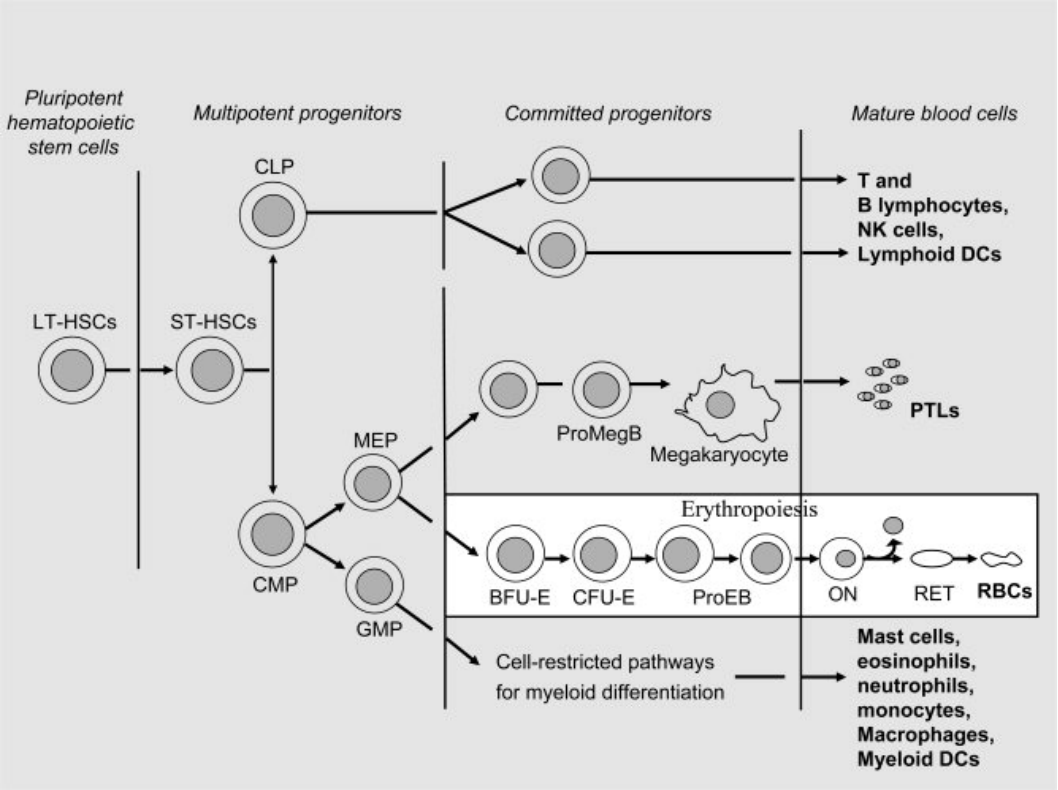

Figure 3.4. Schematic representation of normal hematopoiesis and illustration of the erythrocytic pathway of development. Hematopoiesis in adult life begins in bone marrow at the level of pluripotent long-term HSCs, which then give rise to short-term HSCs and multipotent hematopoietic progenitors. These cell types then yield committed progenitors and finally mature blood cells. Among various hematopoietic cell-restricted pathways illustrated above, erythropoiesis represents a unidirectional pathway of maturation. The erythrocytic pathway of differentiation (highlighted) begins from megakaryocytic/erythroid pluripotent progenitor (MEP) that gives rise to BFU-E, CFU-E, intermediate forms of proerythroblasts (ProEB), and then to orthochromatic normoblasts (ON). Enucleation of ONs leads to birth of reticulocytes (RETs). The latter cells finally yield mature enucleated red blood cells (RBCs). BFU-E, burst forming unit-erythroid; CMP, common myeloid progenitor; CFU-E, colony forming unit-erythroid; CLP, common lymphoid progenitor; DCs, dendritic cells; EB, erythroblast; GMP, granulocyte-myeloid progenitor; MEP, megakaryocytic/erythroid progenitor; MPP, multipotent progenitors; NK, natural killer; ON, orthochromatic normoblast; PLTs, platelets; RBCs, red blood cells; RET, reticulocyte.[43]

Erythropoiesis is a dynamic process regulated by oxygen tension in vertebrates and requires the orchestrated action of specific molecular mechanisms to strictly

regulate cell proliferation, prevent apoptosis, and coordinate cell-cycle arrest with terminal maturation. Although many questions still remain unanswered regarding the underlying molecular mechanisms that govern lineage-determining decisions toward the path of terminal maturation, specific signaling pathways and molecular networks have been identified to control erythropoiesis. The kidneys can detect low levels of oxygen in the blood, which respond by releasing the Epo. Iron homeostasis, hypoxia (low oxygen tension), and stress physiology affecting transcriptional factors and regulators represent key elements contributing to erythropoiesis.[44]

CHAPTER 4: AN OVERVIEW OF THE IMMUNE SYSTEM

The role of the immune system is to defend against infections by providing rapid, specific, protective immune responses to infectious bodies without causing damage to the hosts themselves. In addition, the immune system has the ability to "remember" a pathogen and induce a protective response in the event of subsequent exposure. The immune system consists of two main branches: innate and adaptive immunity.

The innate immunity is older and exists in a primitive form in all multicellular organisms, and is a non-specific approach which distinguishes between self and non-self according to complexes such as carbohydrate signals.[45] The innate system acts by recruiting neutrophil to the site of infection, by activating the complement system (figure 4.1) and by activating eosinophil, mast cells and natural killer cells. This system recruits immune cells to the sites of infection by producing cytokines and remove foreign substances by specialized white cells.[46] The adaptive immunity is an acquired and highly specific immunity and is found in cartilaginous and bony fish, amphibians, reptiles, birds and mammals.[47] This system is induced by lymphocytes, generates a very large repertoire of antigen receptors (either T Cell Antigen Receptor (TCR) or B Cell Antigen Receptor (BCR)) with the potential to recognize different antigens.[46] Adaptive immunity can be further divided into two types. One type is the humoral immunity, which is mediated by antibody molecules secreted by B lymphocytes. The other type is

the cellular immunity, which is mediated by T lymphocytes. An essential difference between these two types of immunity lies in the means by which they recognize pathogens. [46]

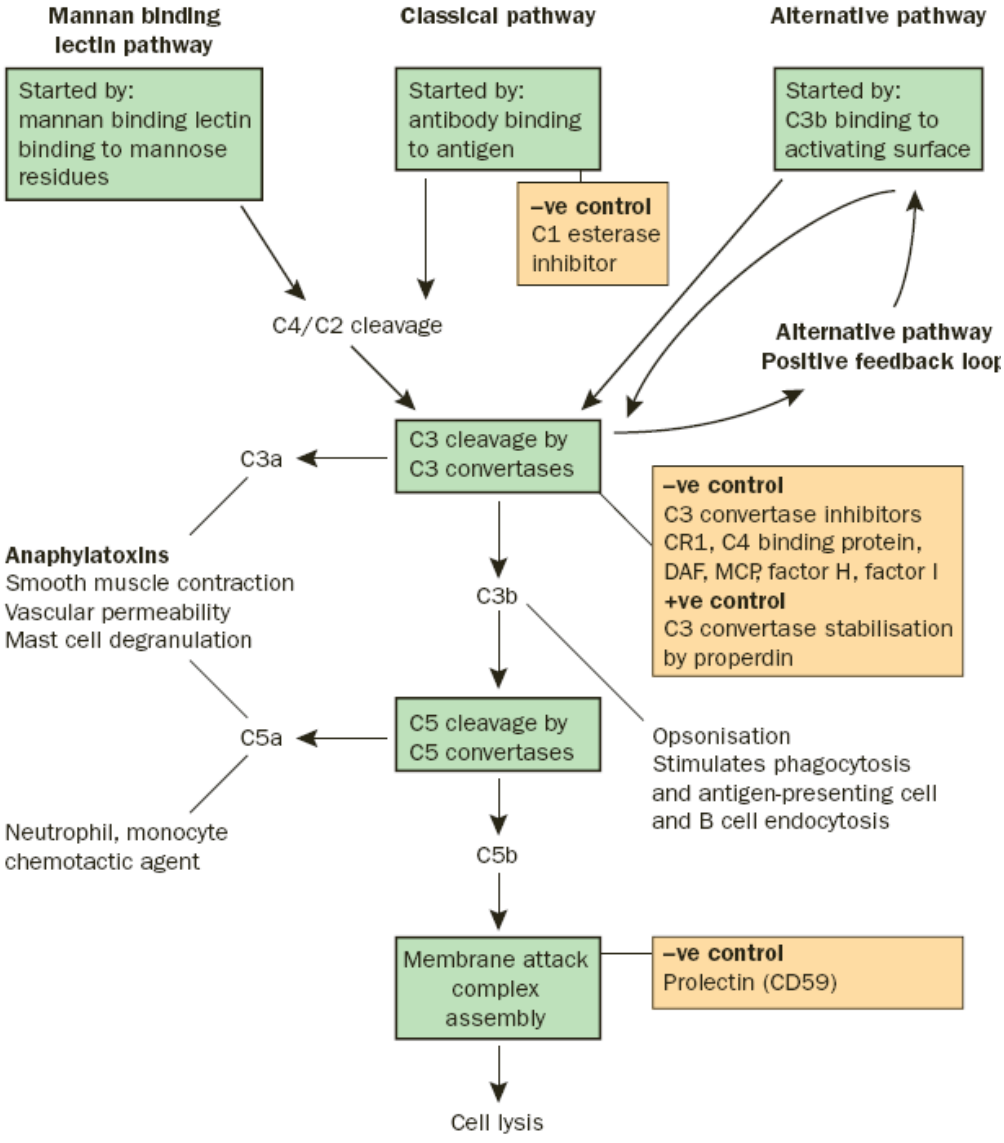

Figure 4.1 : Complement system activation pathway . Regulatory proteins are shown in orange. Components of activation pathways are shown in green.[46]

The main characteristic of the adaptive system is the use of antigen-specific receptors on T and B cells to target two-stage effecter responses. As shown in

Figure 4.2, the antigen is presented in the first stage and it is recognized by the antigen specific T or B cell leading to cell priming, activation and differentiation. These processes usually occur within the specialized environment of lymphoid tissue. In the second stage, the effecter response takes place when the activated T cells leave the lymphoid tissue to go to the infection site, or when the antibodies from activated B cells are released into blood and tissue fluids and forwarded to the infection site. [46]

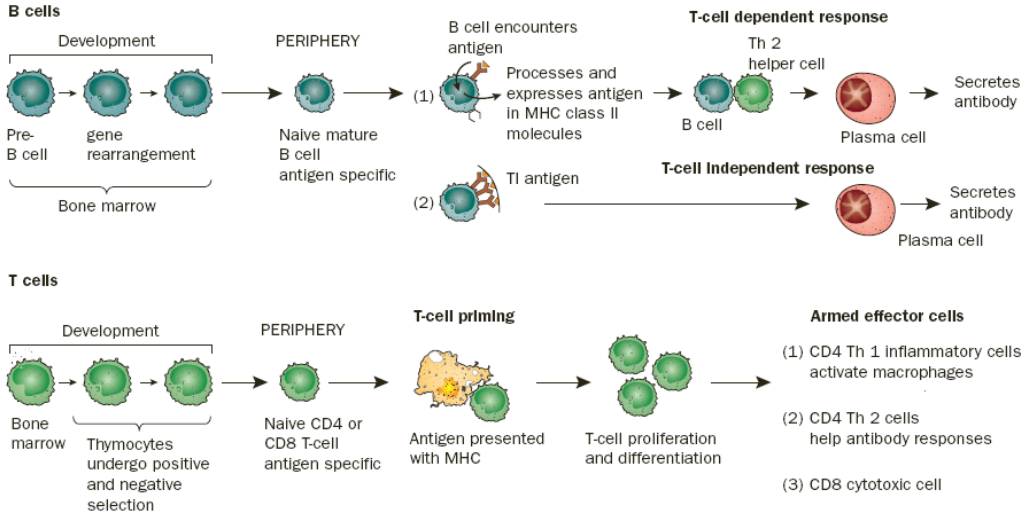

Figure 4.2. The role of T and B lymphocytes in specific immunity. [46]

All the components of an immune system have to work together in order to make efficient and effective defences. For instance, the innate immunity may instruct the adaptive immunity system regarding to what component it responds to.[45] In addition to defence, another important characteristic of the immune system is the tolerance to host self and homeostasis. Host self consists of all the possible peptides that can be generated from the host proteome. Even though self-reactive lymphocytes are created constantly, they are removed within the thymus

gland to prevent auto-immune disease.[46] Homeostasis is the ability or tendency of an organism or a cell to maintain internal equilibrium by adjusting its physiological processes. The immune system maintains such an equilibrium state, whereas the number of the immune cells is roughly the same as it was prior to infection, despite its continuous exposure to self antigens plurality of generated responses to diverse collections of microbes. To maintain this homeostasis, the repertoire of immune cells is altered in a way that ensures a protective response to a particular antigen.

CHAPTER 5: UNIVERSAL RED BLOOD CELLS

5.1 Immunocamouflage

Over the last several years, the prevention of donor tissues' (erythrocytes, lymphocytes, endothelial cells and pancreatic islets) recognition by the immune system has been investigated by the application of cellular "immunocamouflage".[48-52] In general, the immunocamouflage effect relies on the modification of the cell membrane surface with non-immunogenic molecules, creating a barrier that prevents the recognition of allogenic sites by circulating cells and antibodies of the recipient.[53] The main advantage of immunocamouflage is that it can directly modify the inherent immunogenicity of the donor tissue itself, using means that are strictly physicochemical in nature and do not rely on the details of activation pathways, thus leaving fully competent, the immune system of the recipient. The immunocamouflage effect has been mainly induced by modifying the membrane surface with polyethylene glycol (PEG).[48-52,54] Other methods consist of cleaving the antigenic groups from the surface of RBCs using specific enzymes, which will be reviewed in the next section.[55-58]

The immunocamouflage of red blood cells is mediated by the covalent grafting of cell surfaces with polyethylene glycol (PEG). PEG is an hydrophilic polymer composed of repeating ethylene oxide subunits. It has a basic structure of $HO{-}(CH_2CH_2O)_n{-}CH_2CH_2OH$. PEG exists in many molecular weights and configurations (linear, branched, star).[59] PEG contains 2 hydroxyl groups that

can be chemically activated. One of the 2 hydroxyl groups can be converted to methoxy or other alkoxy groups to make PEG unifunctional. To chemically graft the PEG to proteins, a chemical linker compound is attached to one of the terminal hydroxyl residue. The chemical linkers employed include cyanuric chloride (CN) also known as dichlorotriazine, succinimidyl propionate (SP), benzotriazole carbonate (BTC) and N-hydroxylsuccinimide (NHS). The linkers target the terminal amine of lysine. PEGs are uncharged; they are soluble in water by virtue of hydrogen bonding of 3 water molecules per ethylene oxide unit. Thus, in aqueous solution, each PEG molecule is surrounded by a large hydration sphere. Biophysically, the grafted PEG confers its immmunoprotective effects due to the rapid mobility and intramolecular flexibility of the heavily hydrated PEG chains. Because PEG attracts water molecules, PEGylated proteins (eg, on RBC membranes) will be covered with a "shell" of PEG + water molecules, and it has been suggested that this combination should block antibody from reaching its appropriate antigen (Figure 5.1).[59]

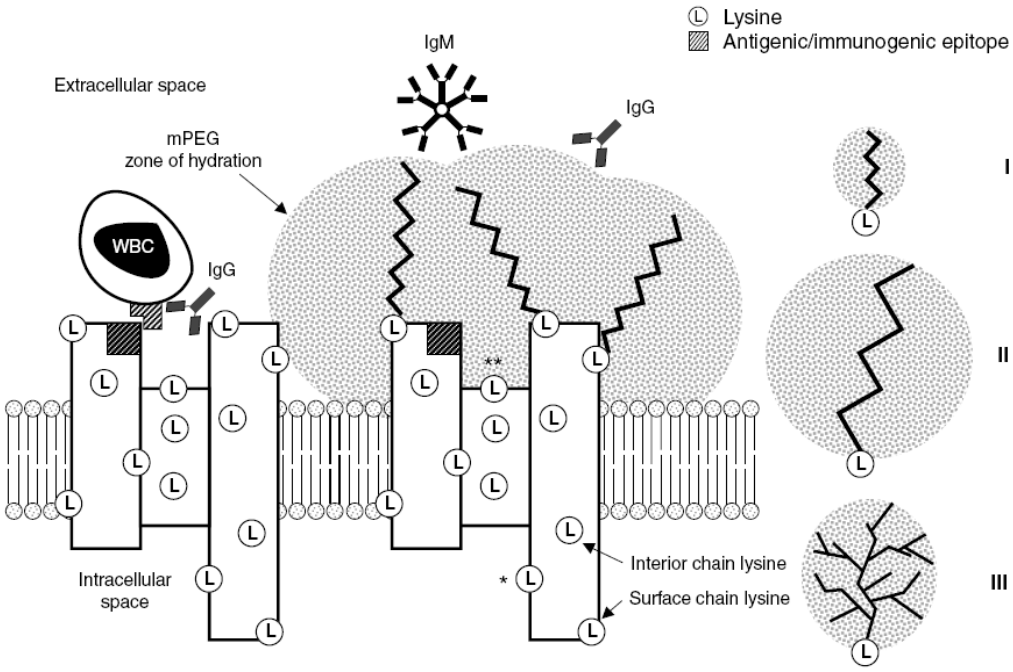

Figure 5.1. Derivatisation of membrane proteins occurs only on the extracellular face. Intracellular lysines, denoted by (*), are not derivatised by the extracellular methoxypoly(ethylene glycol) [mPEG]. Furthermore, some extracellular lysines (**), while potential targets for derivatisation, are unlikely to be derivatised because of the steric interference of the previously grafted mPEG polymers. The immunological camouflage is demonstrated by the inability of white blood cells (WBC) to recognise antigenic determinants because of the mPEG hydration sphere, which sterically hinders the approach and binding of large molecules (e.g. immunoglobulins M and G) and WBC. The efficacy of the immunocamouflaging effect (stippled area) of mPEG polymers of varying molecular size and shape differs significantly: I represents a small (e.g. 5kD) linear molecule; II represents a higher (e.g. 20kD) molecular weight linear compound that more effectively camouflages the cell; III represents a multibranched PEG. As indicated by the zone of hydration and the polymer density, III may be most effective in preventing antigenic recognition.[48]

In 1996, Jeong and Byun reported that RBCs membrane modified with PEG reacted less with anti-A, anti-B and anti-D than virgin RBCs.[60] Since 1996, several groups used PEG to mask RBCs antigens.[48,54,60-65] RBCs covalently bounded to PEG showed greatly diminished reactivity with a range of antibodies to blood group antigens (e.g., ABO and Rh). MD Scott *et al.* produced antigenically silent RBC via the covalent attachment of PEG. This group

injected mPEG (methoxypoly(ethylene glycol)) sheep RBCs into mice which resulted in a "blunted" immune response.[51] Approximately 90% fewer antibodies were produced when mPEG sheep RBCs were injected into mice compared to untreated sheep RBCs. The initial xenogeneic transfusion also showed an increased survival of mPEG-modified RBCs.[48]

This and several other studies have confirmed that covalent grafting of PEG to the membrane does not affect the viability, morphology, deformability, and other membrane functions.[48,49,66] However, there is a concern over the extent to which mPEG is grafted on each RBC (heterogeneity or homogeneity) and over the attachment stability of mPEG with the membrane proteins. Specifically, as PEG was grafted to the specific sites, other non-modified surfaces are still able to interact with the existing antibodies.

For instance, Garratty et al. encountered several problems with a 5-kDa linear PEG. When Pegylated RBCs were incubated (30–60 min) in vitro with normal compatible plasma, non-specific uptake of proteins (e.g. IgG and IgM) onto RBCs was detected.[65] These results suggested that these PEG-grafted RBCs would have reduced survival in humans. To improve the RBCs masking by the PEG system, various modifications of the original procedures were developed. Garratty *et al.* addressed many of the serological problems by crosslinked or branched PEG molecules.[67] Moreover, in 1999[68], a '2nd generation' PEG was used which was cross-linked with albumin. These RBCs reacted weakly with anti-AB. These preliminary studies by the Garratty group and others have

indicated that the non-specific uptake of proteins may be diminished with the use of the "2nd generation" PEG derivatives.[69,62] Later, a higher MW PEG (20 kDa) and SP and BTC were used instead of CN. The BTC 20 kDa PEG RBCs were reported to survive normally in mice.[70]

The "2nd generation" Pegylated RBCs [71] overcame problems related to the partial masking and they no longer reacted with antibodies to Rh and other blood group. Most reactions caused by anti-A and anti-B were prevented, except for in vitro hemolysis of A_1 RBCs by some group O sera.[72] Reactions with normal donor plasma/sera were reduced; non-immunological uptake and subsequent interactions were prevented.[69] While these preliminary studies have shown some promising results for the use of covalently linked PEGs on RBC surface for immunocamouflage, it has also been demonstrated that covalently bound PEG does not prevent the recognition by antibodies of A and B antigens. The antigens A and B on RBC membrane are more extended than other antigens and interact with their respective antibodies in spite of the covalently bound PEG.[48,60,64,72,73]

5.2 In vitro conversion of group A and B red blood cells to group O red blood cells

For incompatible transfusion prevention and creation of a universal blood supply, the idea of converting blood group A and B antigens to H using specific exo-glycosidases capable of removing the immunodominant sugar residues was pioneered by Goldstein and colleagues at the New York Blood Center in the early 1980s.[55] This idea was based on earlier work by other investigators who had shown that small quantities of RBCs could be converted quite easily in the

laboratory. [74-78] The earliest work in this area led to the development of the biochemical and genetic pathways of ABH structure and development.[55] Many authors published methods for converting group B RBCs to group O RBCs using a galactosidase from green coffee beans rather than from bacteria.[76-78]

In 1980 and 1982, Lenny and Goldstein showed that ^{51}Cr-labelled group B gibbon and human RBCs, respectively, treated with coffee bean α-galactosidase to yield group O RBCs survived normally (human recipients were groups A, B and O).[55] These very promising results led Lenny et al. to treat the whole units of group B RBCs with coffee bean enzyme and to transfuse such units to groups A and O healthy volunteers.[56] ^{51}Cr-labelled enzyme-converted group-B-to-group-O (ECO) RBCs survived normally and the recipients had no adverse effects. The results also indicated that some B antigen was still present on the group B ECO RBCs.[79] The results of study in which, multiple and second transfusions of B ECO RBCs have been given to group O volunteers, were published in 1995.[57] The B ECO RBCs were prepared using recombinant coffee bean α-galactosidase. There was normal survival of the B ECO RBCs, no clinical reactions (as compared to appropriate controls), no rise of anti-B titres and negative direct antiglobulin tests (DAT) post-transfusion.

In 2000, Kruskall et al. extended the B ECO RBC trials by enrolling hospitalized patients that possessed the antigen A.[80] One unexpected problem encountered was that 20% of group A and 40% of group O sera from random patients reacted in vitro with the B ECO RBCs. For large scale RBC conversion, the method

suffered two additional limitations: (1) the enzyme catalyses optimally at a pH 5.5 which is not an ideal pH for RBCs; and (2) the large quantities of used enzyme in 80–90% RBC hematocrit make the process exorbitantly expensive.

Enzymatic conversion of group A RBCs has lagged behind due to the lack of appropriate glycosidases and the more complex nature of A antigens. Identification of novel bacterial glycosidases with improved kinetic properties and specificities for the A and B antigens has greatly advanced the field. Goldstein *et al.* screened many microbial and animal sources for a suitable A-zyme, finally selecting an N-acetylgalactosaminase from chicken liver.[81] Using this enzyme, they were able to convert group A_2 RBCs to group O but could not completely convert A_1 RBCs. Another problem was that the enzyme reacted optimally at pH 3·65 and 1–2 g/unit of RBCs were needed at pH 5·5. The method would be impractical for routine use.[81]

For the last few years, ZymeQuest and their collaborators have been searching for new enzymes and the results of their investigation have been recently published.[82] In this study, a large panel of 2500 fungal and bacterial isolates for A- and B-zymes was screened. They used methods that would identify enzymes with selective or exclusive substrate specificities for the more complex branched A and B structures, rather than the previously used monosaccharide p-nitrophenyl substrate. They also selected enzymes that reacted optimally at near neutral pH with increased efficiency. Five of the isolates displayed α-galactosidase activity and two α-N-acetylgalactosaminidase activities. One suitable B-zyme was from Bacteroides fragilis (Frag A) and one A-zyme was

from Elizabethkingia meningosepticum. The latter is similar to an A-zyme from E. meningosepticum that has been cloned; the recombinant A-zyme is a very efficient enzyme working at a neutral pH (approximately 60 mg of enzyme required to convert 200 ml of A_1 RBCs; conversion of A_2 RBCs only required 15 mg). Groups A, B and AB ECO RBCs (more than 200 groups A_1 and A_2 RBCs), prepared using the new enzymes, did not react with the most powerful commercial monoclonal anti-A, anti-B or anti-AB (e.g. ES-15 that detects A_x).[82] Data on the clinical trials using the new ECO RBCs and cross-match results have not yet been presented.

While this method has many advantages, it is still not a universal solution. Specifically, it cannot be applied in the case of patients who suffer from autoimmune hemolytic anemia (AIHA) or sickle cell disease because they have antibodies against antigens other than ABO which limits its use in transfusion medicine.

5.3 Stem cells

In the 1960s, researchers discovered that the bone marrow contains two kinds of stem cells: the hematopoeitic stem cells (HSCs) and the bone stromal cells.[83] HSCs forms all types of blood cells in the body while the bone marrow stromal cells are a mixed cell population that generates bone, cartilage, fat, and fibrous connective tissue.

The usage of human embryonic stem cells (ESCs) as a resource for cell therapeutics presents an intensive field of research. From ethical point of view,

research involving human embryonic cells is highly controversial, and many countries are reviewing their legislation on this subject. The main ethical issues raised are the generation of human ESCs from in vitro fertilized embryos, the moral status of the embryo, and the acceptability of using such derived cells for therapeutic purposes.[83]

Nevertheless, stem cells have been widely employed during the past decade in an attempt to produce universal RBCs. To produce human RBCs from HSC with a transfusion aim, research are facing two main challenges: (1) The first challenge lies in reproducing *in vitro* the same pathway that a simple enucleated RBC undertook to achieve its maturation, while (2) the second challenge resides in maximizing the numerical expansion of RBCs to be sufficient for medical transfusion, since an RBCs' unit contains 2×10^{12} cells. [84] In the next section, these obstacles faced by the researchers are enumerated.

5.3.1 Challenges for in vitro RBCs production

5.3.1.1 Achieve the maturation stage of erythrocytes.

To overcome this obstacle, the experimental conditions in vitro should fulfill three requirements: stimulate the proliferation of the primitives HSC, induce their exclusive engagement towards the erythroid line, and lead at the ultimate stage of maturation, which corresponds to the enucleated RBCs. Neildez-Nguyen described a process of RBCs expansion of HSC of SC in a medium and without stroma, based on sequential addition of growth factors.[85] On the basis of a population enriched in hematopoietic original cells and progenitors, the protocol allowed an important cellular production (up to 200.000 times of

amplification) of pure erythroid precursor cells (95 to 99%) containing foetal hemoglobin (HbF). Not yet mature, these cells have shown to undergo terminal differentiation in a non-obese diabetic/severe combined immunodeficient (NOD/SCID) murine to form enucleated RBCs.[86]

5.3.1.2 Scale-up production *in vitro*

The objective to be reached is the production of units containing 2×10^{12} RBCs. The cellular expansion reached during the first stage of culture is directly correlated to its duration. Thus, by prolonging the culture for three days, the levels of cellular amplification can reach 1×10^{7} and 2×10^{5} times for the cells coming from cord blood and bone marrow respectively. The level of enucleation was preserved during the following phases (70 - 90%).[84,86]

5.3.1.3 Design the tools for industrial developments

An automated production of RBCs is a necessary tool for their clinical application. Indeed, while the production of RBCs starting from peripheral blood or cord blood is easily accomplished at the bench work level, up-to-date, the production of sufficient quantities is not successful. It is also imperative that the produced RBCs have the same functionality as the native RBCs in terms of oxygen transport capacity. This requires an important progress in cellular biology. Considerable progress must be made in the control of the expansion, renewability and the differentiation of the hematopoietic progenitors. Such system should also be automated in order to ensure reproducibility and standardization by limiting human interventions. Other necessary advancements

regarding the automation of cellular selection, culture and packaging are also required. Overall, it is a real challenge to overcome.[84,86]

5.3.1.4 Universal RBCs production

This farming system will potentially give birth to new approaches in the research of the "universal" RBCs which are deprived of the principal systems of blood group ABO/Rh. These new approaches will not attempt to eliminate an antigen already formed, but will be focused on the prevention of their synthesis before the cells reach their maturity. Since the systems ABO or Rh, not expressed on the original cells, are present at the stage of erythroblast, two possible approaches remain: (1) the inhibition of the genes in CD34+ cells, or (2) the biochemical intracellular inhibition of the specific glycosyltransferases of the antigens A and B.[86]

CHAPTER 6: LAYER-BY-LAYER TECHNIQUE

6.1 Layer-by-layer self-assembly principles

The LbL assembly technique was first assessed by Iler in 1966. In 1991, Decher and Hong expanded the technique and brought it to the forefront of materials science and engineering. The basic principle behind this technique of film preparation is the alternate, sequential and repeated electrostatic adsorption of positively and negatively charged polymers onto a charged substrate from dilute polyelectrolyte solutions (Figure 6.1). Multilayer film formation is possible because of charge reversal on the film surface after each polyelectrolyte adsorption step. The process allows a multilayer build-up with an infinite layer number in principle. It is simple and considerably more versatile than other techniques of thin film preparation such as no special apparatus is required for LbL assembly, the multilayer film can be fabricated under mild, physiological conditions. The production is relatively straightforward, and the process is amenable to automation, scalable and it enables control over structure and function at the nanometer scale. A diverse range of materials and surfaces are suitable for deposition, as the only criterion is the net charge of the adsorbing species at the assembly pH. The process is independent of the size, shape, and composition of the surface. The process also allows for numerous control variables, for example polyelectrolyte concentration, solution ionic strength, adsorption time, pH and temperature.[87]

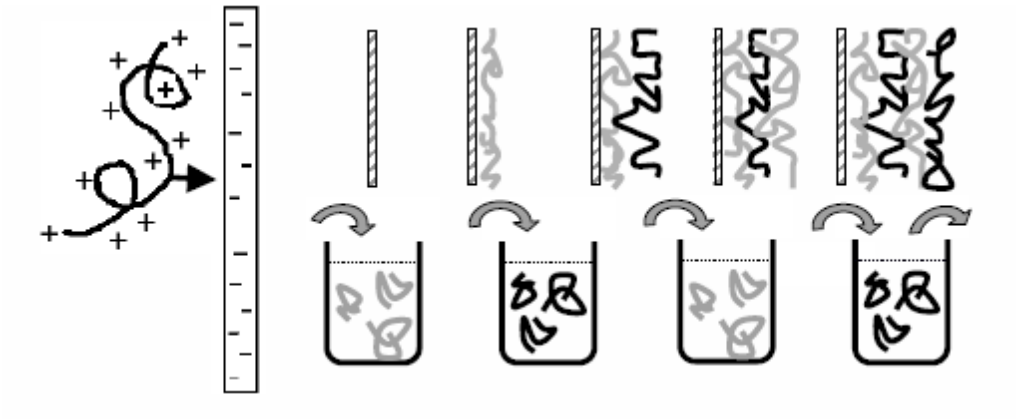

Figure 6.1. The procedure of self-assembly of multilayers on planar substrates.[88]

The principle of assembly is based on coulombic attraction and repulsion. In general, the layer-by-layer assembly technique is based on a sequential adsorption of positive or negative charged species by alternatively dipping into the solutions. The excess or remaining solution after each adsorption step is rinsed with solvent and thus resulting in a thin layer of charged species on the surface ready for next adsorption step. Surface charge depends on the last adsorbed layer, permitting a degree of control over surface and interface properties. The resulting films are stable, uniform, and have an interpenetrated architecture.[87] Each layer has a thickness on the order of nanometers, enabling the design and engineering of surfaces and interfaces at the molecular level. Subtle changes in organization and composition can influence film structure and functionality. The LbL technique has been used on various substrates with bioactive molecules, such as drugs, enzymes, DNA, proteins.[89,90] Such films are being developed for a variety of applications: contact lens coatings, sustained-release drug delivery systems, biosensors etc.

The stepwise assembly technique applied on planar surfaces has been performed also on particle in suspension [91-93] and lately on cells.[94] By using degradable particles, hollow capsules are produced through dissolving the templating core.[91] This thin membrane can allow small polar molecules to diffuse in and out of the capsule.[95,96] The permeability to small molecules can be controlled by modifying the molecular weight of polymers, ionic strength and pH used in the LbL build-up. This matter will be explained more in depth in the next chapter.

6.2 Multilayers growth regimes

There are two multilayer build-up growth regimes depending on the polyelectrolyte properties. In one growth regime, the mass and the thickness of the multilayer film grow linearly with the number of deposition steps. They involve strong polyelectrolytes where their charge remains unchanged through the pH range. It was shown that such films exhibit a "fuzzy" layered structure.[97] There is typically no "communication" between a polyelectrolyte deposited at step i and a polyelectrolyte deposited at step $i \pm p$ with p larger than 2 or 3. It should be emphasized that p depends on the chemical nature of the polyions involved and both larger and smaller values were reported.[98]

In the other growth regime, the mass and the thickness of the multilayer film grow exponentially with the number of deposition steps. There are two mechanisms explaining the exponential build-up regime: surface roughness and diffusion "in" and "out" of the whole film. The nonlinear build-up can be attributed to the continuous increase of surface roughness, which leads to an increase in the physical surface area available for adsorption.[99,100] The diffusion

of polyelectrolytes in and out of the film is achieved if the whole film acts as an active volume in which at least one of the polyions can freely diffuse.[101] The structure of these films is quite different from that of linearly growing films. For example, these films are not as structured but can be more seen as gels of polyanion/polycation complexes.[98]

The growth mechanism involves mainly electrostatic interactions between the polyelectrolytes in solutions and the polyelectrolytes of the opposite charge forming the outer layer of the film.[102] Hyaluronic (HA)/chitosan (CH) multilayers exhibit an exponential increase of film thickness with the number of deposited bilayers.[103] In this case, CH is the diffusing polyelectrolyte and HA is the non diffusing moiety. For CHRichert *et al.* showed that a progressive transition from an exponential to a linear growth regime is observed when the ionic strength decreases from 0.15 M to 10^{-4} M.[104] They showed that it is hard to build an exponential growth film at a very low ionic strength ($<10^{-4}$ M) and found that the alternation of the charge after each CH or HA addition is independent of the ionic strength.[104] Kujawa *et al.* showed that the multilayer thickness at a given stage depends on the size of both CH and HA. They demonstrated that the assemblies of high molecular weight polysaccharides (HA, 360 kDa; CH, 160 kDa) were twice as thick as those obtained with low molecular weight polymers (HA, 30 kDa; CH, 31 kDa); approximately 900 nm and 450 nm, respectively.[102,105] It should be mentioned that the thickness values depends on measurement technique as well.

The experimental data show that alginate (AL)/poly-L-lysine (PLL) multilayers are thicker than those prepared of AL–CH. The apparent thickness of the first polycation layer deposited on a glass substrate was 16 nm and 17 nm for PLL and CH. The observed differences in thickness of the multilayer films are suggested to arise from differences in degree of interpenetration between AL and the respective polycation layers during the deposition leading to different mechanisms of growth where CH diffuses more into the multilayers. The multilayers with PLL are thicker and rougher, and the differences will be amplified with the number of bilayers, enhancing the difference between the two polyanion–polycation pairs.

6.3 Polymers characteristics

A polyelectrolyte is defined as strong if its net charges arise from strongly dissociating groups; they will remain charged throughout the pH range. A polyelectrolyte is "weak" when the net charge arises from reversible proton transfer with the solvent and therefore is pH dependent. The linear charge density of a weak polyelectrolyte is tunable by a simple adjustment of the pH. Such polymers are essentially fully charged at a certain pH. The pKa of ionizable groups in a weak polyelectrolyte will be sensitive to the local environment, and the net charge can shift significantly. In this section, the properties of CH, AL, PLL and HA which are all weak polyelectrolytes, will be described.

6.3.1 ***Chitosan***

CH is a cationic biocompatible polymer made of two repeated units: N-acetyl-D-glucosamine and D-glucosamine. It is derived by partial deacetylation from chitin, a natural polysaccharide extracted from the crustacean shells (Figure 6.2). It is also found in some microorganisms in yeasts and fungi.[106] At low pH and low ionic strength, the intrinsic viscosity of a CH solution increases rapidly with decreasing salt concentration.[107] This reflects the fact that CH, due to strong electrostatic segment-segment repulsion, adopts an extended conformation at low ionic strength.[107]

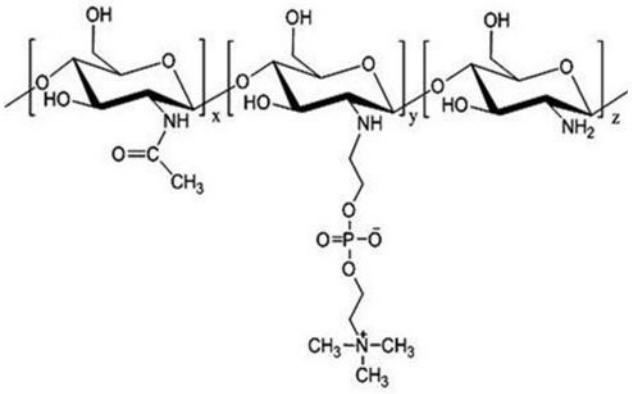

Figure 6.2. Structure of chitosan-*graft*-phosphoryl choline.

The properties of CH in solution depend on CH molecular weight, its degree of deacetylation, the pH, and ionic strength. The pKa value of the glucosamine segments is 6.3-7.[107] CH is a weak base, and a certain amount of acid is required to transform the glucosamine units into the uncoiled and positively charged water-soluble form. At neutral pH values, CH loses its charge and precipitates

from solution. Thus, the potential use of CH in RBC coating for transfusion is limited. The presence of amines and hydroxyl groups make CH a versatile polymer with unique properties and enable the preparation of derivatives with different physico-chemical properties, especially enhanced water solubility at neutral pH. Tiera et al. have shown that a CH partially grafted with phosphoryl-choline (PC) has enhanced water solubility, a direct consequence of the zwitterionic nature of the PC group [108]and shifing the pKa of the amine groups to 7.2. Moreover, PC groups are remarkable in their ability in repelling protein adsorption, their non-toxicity and hemocompatibility.[108-110]

CH has been administered to humans by several routes without toxic effects.[111] It has also been used as a dietary fiber.[111,112] CH represents a new generation system for DNA, proteins, drugs and antigen delivery.[113] Since CH can be hydrolysed by lysozymes, it is also biodegradable in nature. The degradation rate of CH can be controlled by changing the ratio of glucosamine to N-acetylglucosamine or its molecular weight.[114] The degraded products of CH are non-toxic, non-immunogenic and noncarcinogenic.[115] A high deacetylation degree of CH enhances its mechanical strength, decreases the biodegradation rate, reduces the inflammatory tissue reaction and decreases complement activation.[116]

6.3.2 Alginate

Alginates are linear copolymers of a guluronic acid and mannuronic acid (1→4) linked (Figure 6.3).[117] The intrinsic pKa of alginic acid is around 3.[118] Alginates occur as structural components in brown marine algae (*phaeophyceae*) and in

some microorganisms, where they are believed to have many functions, such as capsular polysaccharides in the soil bacteria, *Azotobacter vindenadii*.[119] The proportion of guluronic acid residues and manuronic acid residues determines the chemical and physical properties of alginate.[119] There are different sequences and compositions of these monomers in various types of AL.[120] The monomers occur in the AL chain in the form of blocks. The structural domains are referred to as M blocks for poly (mannuronic acid) and G blocks for poly (guluronic acid).[120] This sectional nature of the alginate polymer confers different backbone chain flexibility to polymers in solution.[120] G-blocks are responsible of ionic interactions, as in the presence of multivalent cations (Ca, Sr, Ba, Fe(III) and Al) they can associate to form aggregates of the "egg-box" type. The term ''Egg Box'' arises from a similitude model in which the cation fits into electronegative cavities like eggs in an egg-box.[121] The selective binding of divalent metal ions and the corresponding gel strength were found to increase in the order: MM block<MG block<GG block.[122]

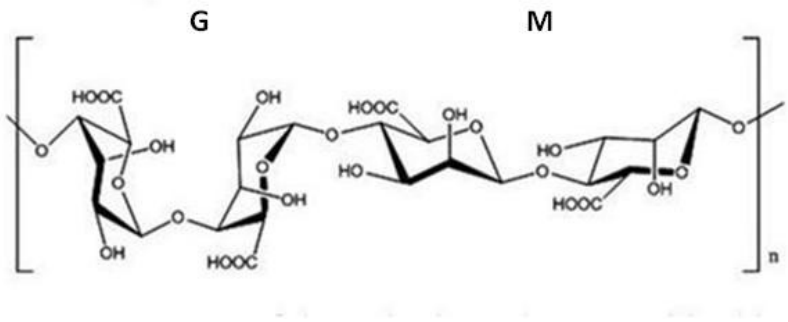

Figure 6.3. Structure of Alginate

The most important properties of AL in term of application are their thickening character, their ionic exchange properties, and their gel forming ability in

presence of multivalent counterions. Because of their linear structure and high molecular weight, alginates form strong films and fibers in the solid state. Alginates are food additives for thickening soups and jellies.[123] They are used in anti-acid preparations, in mold-making material for dentistry (in the presence of slow release calcium salt to control the delay of gelation), pharmaceutical or textile applications.[118] AL can be processed into fibres or films and are commercialized as hemostatic material but also wound dressing.[124] Calcium alginate gels are often used in the form of beads as an immobilization matrix for animal cells. Moreover, alginate is widely use in cell encapsulation [125-127] drug [128-130] and DNA delivery.[131]

6.3.3 Poly-L-lysine

Poly-L-lysine (PLL) is a homo-poly-(amino acid). Its solubility in water is high and its pKa is ~ 9.0. When the ε-amino groups are protonated at low pH, the molecule is randomly coiled and is a typical example of the soluble synthetic polyelectrolytes.[132] At physiological pH, the positively charged amine groups on the PLL side chain can electrostatically bind with negatively charged substrates.[133] At high pH and low concentration where the ε-amino groups are neutral, the polymer tends to form an α-helix at low concentration.[132] PLL shows a wide range of antimicrobial activity. The mechanism of the inhibitory effect of PLL on microbial growth involves the electrostatically driven adsorption to the surface of microorganisms. PLL produced by a fermentation process using *Streptomyces albulus*.[134]

PLL grafted with PEG, consists of PEG chains grafted to a fraction of the side chain amino groups of a PLL backbone (Figure 6.4). At physiological pH, the positive charge of the remaining free amino groups adsorbs spontaneously onto negatively charged surfaces through electrostatic interactions, leading to a monolayer with the PEG chains stretched out perpendicularly to the surface.[135] Such coated surfaces are protein repellent even in the presence of full human serum.[135,136] A PLL-PEG of 20 kDa backbone, 2 kDa PEG side chains, and a grafting ratio of 3.5, was found to efficiently minimize opsonisation and recognition by phagocytes.[137]

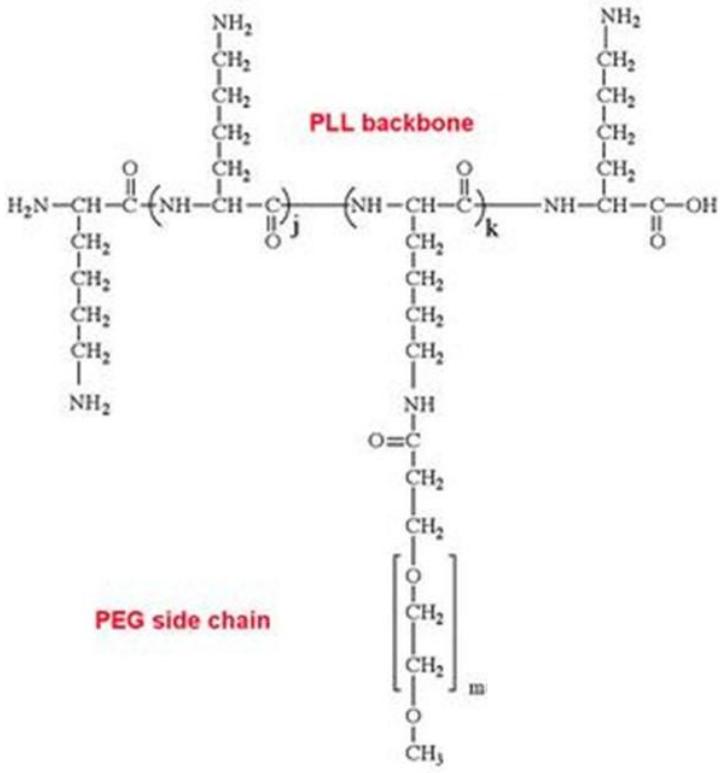

Figure 6.4. Structure of Poly-L-Lysine-graft-poly(ethylene glycol) (PLL-g-PEG)

6.3.4 Hyaluronic acid

Hyaluronic acid (HA) is a negatively charged polymer. It is a naturally occurring linear polysaccharide. The repeat disaccharide unit consists of N-acetylglucosamine and glucuronic acid linked via a β-(1→4)-linkage (Figure 6.5).

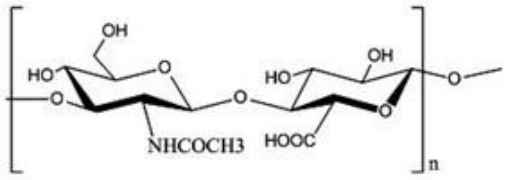

Figure 6.5. Structure of Hyaluronic acid.

The chain is rather stiff and the molecule behaves in solution as an extended, random coil. [138] Hyaluronan chains start to entangle at concentrations of less than 1 g/L and form a continuous polymer network. [138] It is ubiquitously distributed in the organism but is found in the highest concentrations in soft connective tissues.[139] In the liver, high-molecular weight hyaluronan is rapidly degraded in the lysosomes to low-molecular weight products, lactate and acetate.[140] HA has been assigned a variety of important physiological functions. As a component of the extracellular matrix, it maintains water balance and is important in cellular interactions. HA is known to exert a protective effect against oxidative cells damage.[141]

HA polymers have an opposing biological function depending on the size of the molecule. Large matrix polymers of HA are space-filling, anti-angiogenic, and immunosuppressive, whereas the small-sized polymers comprising 25–50

disaccharides are inflammatory, immunostimulatory, and highly angiogenic. Smaller oligosaccharides are anti-apoptotic and induce heat shock proteins.[142]

6.4 Film characterization techniques

The characterisation methods, often employed UV/Vis spectroscopy and X-ray reflectometry, require one to interrupt the deposition process to take the measurement. They also have to be taken in dry conditions, which may not be desirable in LbL deposition on cells. In this case, in-situ "wet" methods are necessary in order to characterize the multilayer build-up. Such methods also allow one to follow the kinetics of adsorption and/or multilayer reorganisation. Besides measurements of the zeta potential and results obtained by quartz crystal microbalance, typical methods include surface plasmon spectroscopy, atomic force microscopy (AFM), ellipsometry, optical waveguide lightmode spectroscopy (OWLS), optical reflectometry in stagnation point flow cells, scanning angle reflectometry (SAR) and attenuated total reflection Fourier transform infrared spectroscopy (ATR-FTIR).[143]

6.4.1 Quartz crystal microbalance

The Quartz Crystal Microbalance (QCM) is a sensitive mass sensor, capable of measuring mass changes in the nanogram range. QCMs are piezoelectric devices consisting of a thin plate of quartz with electrodes affixed to each side of the plate. A QCM consists of a thin quartz disc sandwiched between a pair of electrodes. By applying an AC voltage across these electrodes, the quartz crystal oscillates due to its piezoelectric properties. The quartz crystal microbalance is ideally suited for screening the adsorption kinetics and for optimizing the

adsorption conditions. The adsorption kinetics, the thickness of each monolayer can be calculated using several mathematical models depending on the films characteristics.

Assuming a rigid film, the mass of the adhering layer is calculated by using the Sauerbrey relation[144]:

—— (6.1)

Where C = 17.7 ng Hz^{-1} cm^{-2} for a 5 MHz quartz crystal and n = 1,3,5,7 is the overtone number.It is also possible to get an estimation of the thickness (d) of the adhering layer:

—— (6.2)

where ρ_{eff} is the effective density of the adhering layer

In most situations the adsorbed film is not rigid and the Sauerbrey relation becomes invalid. A film that is "soft" and viscoelastic is fully couple to the oscillation of the crystal; hence the Sauerbrey relation will *underestimate* the mass at the surface.[145,146]

A soft film dampens the crystal's oscillation. The damping or, dissipation (D), of the crystal's oscillation reveals the film's viscoelasticity, D is defined as:

——— (6.3)

where E_{lost} is the energy lost (dissipated) during one oscillation cycle and E_{stored} is the total energy stored in the oscillator.

The dissipation of the crystal is measured by recording the response of the oscillating crystal that has been vibrated at its resonance frequency. By measuring at multiple frequencies and applying a viscoelastic model (the so called Voigt model), the adhering film can be characterized in detail; viscosity, elasticity and correct thickness may be extracted even for soft films when certain assumptions are made.[146]

6.4.2 Zeta potential

Layer buildup driven by electrostatics can be followed by measuring the surface potential of polyelectrolyte covered surfaces. This can be achieved on flat films and on colloids. It demonstrates that the adsorption of each polyelectrolyte layer leads to an overcompensation of the previous surface charge. Such measurements only show that there is a contribution of electrostatics in the case of multilayer buildup using positively and negatively charged components. Depending on the chemical nature of the polyions and/or colloids employed for deposition, the importance of the electrostatic contribution should vary and other interactions such as van der Waals, hydrogen bonding or charge transfer may more or less be involved as well.[143]

CHAPTER 7: LITERATURE REVIEW

This chapter presents the scientific contribution that has been made in the LbL self-assembly field in coating flat surfaces and colloidal surfaces as well as their biomedical applications. Several parameters such as the effect of the ionic strength, the pH, the layer number and the crosslinking on the two-dimensional and three-dimensional films permeability are overviewed. The loading and release of biologically active molecules from multilayers are also reviewed.

The following manuscript entitled "**Modulating the release kinetics through the control of the permeability of the LbL assembly: A review**" presents an overview of the background of LbL self-assembly on surface and colloids and it has been published in Expert Opinion on Drug Delivery, June 2009 (ISSN: 1742-5247).

Modulating the release kinetics through the control of the permeability of the LbL assembly: A review

Sania Mansouri[†], Françoise M. Winnik[‡], Maryam Tabrizian[†,♦]

[†]Department of Biomedical Engineering, [♦]Faculty of Dentistry, McGill University, H3A 2B, [‡]Faculté de Pharmacie and Département de Chimie, Université de Montréal, H3C 3J7

*Corresponding author: Maryam Tabrizian: PhD, MBA; Associate Professor
Phone: +1- 514-398-8129
Fax: +1-514-398-7461
Email: maryam.tabrizian@mcgill.ca

7.1 Abstract

The layer-by-layer (LbL) self-assembly technique has emerged as a simple and versatile method for coating biological and non-biological templates for various biomedical applications. A promising avenue of this technique lies in the encapsulation of drugs and other biological substances for controlled release. Fundamental studies of LbL assembly on flat surfaces have provided a sound understanding of film deposition theory and its pertinence to ionic and molecular transport and diffusion through polyelectrolyte multilayer (PEM) films. However, there is a lack of information on the permeability of three-dimensional PEM shell systems. In either PEM films or shells, it has been shown that drug release is a function of the ionic strength, pH and/or multilayer thickness. This report aims to provide an overview of the physicochemical parameters affecting the permeability of two and three-dimensional multilayer shells including ionic strength, layer number and pH. Furthermore, their synergic effect on loading and release of biologically active molecules from LbL multilayers are discussed.

Keywords: Layer-by-Layer assembly, polyelectrolyte multilayer film and shell, tuned permeability, controlled release of biomolecules

7.2 Introduction

Surface modification can modulate and improve material surface properties required for a given application. These modification techniques include chemical grafting, non-specific adsorption and chemisorption through electrostatic interactions. Over the last two decades, Decher *et al.* have significantly contributed to the latter field with the development of Layer-by-Layer (LbL) electrostatic self-assembly techniques using polyelectrolytes for the preparation of ultrathin films on surfaces of both 2-D and 3-D templates.[147,148] Potential applications for such films cover a broad range including biosensing [149], membrane separations [150] and controlled release [151].

The LbL approach involves polyelectrolyte multilayer (PEM) preparation through the sequential adsorption of oppositely charged polyelectrolytes from dilute aqueous solutions onto charged solid substrates. [148,152-155] A crucial step in this LbL build-up involves the removal of free polyelectrolytes after the layer deposition, which is commonly accomplished by means of centrifugation and membrane filtration.[156]

The LbL method is versatile as it does not impose restrictions on the type of polymers employed. A wide variety of materials, including synthetic polyelectrolytes [157], proteins [158], DNA [159], clay materials[160], dendrimers[161],

colloidal particles[162] and redox systems [163] are used as polyelectrolytes on various templating supports, namely latex, inorganic crystals, proteins aggregates, organic particles, oil droplets and cells. Hollow capsules are also produced after core material removal by dissolution or by calcinations.[164,165] The potential applications of LbL coating are determined by the properties of the employed polyelectrolytes.

Polyelectrolytes belong to the category of *smart* polymers. This is due to the fact that their permeability can be controlled through their response to a stimulus.[166] For instance, their molecular structures can be triggered to expand or contract in a controlled fashion by varying conditions such as temperature, pH, ionic strength, and the solvent nature. These stimuli-responsive phenomena are attributed to backbone-interactions between the polyelectrolyte molecules within the multilayer. Decreasing the number of interactions between oppositely charged species leads to the loosening of the layer structure and thus promotes enhanced permeability. This behavior is frequently induced to modulate the permeability of PEM/LbL coating materials to ions and other species. There is a great body of literature that investigates permeability behavior, particularly for hollow capsules [164,165], as well as its relevance to drug delivery carriers, microreactors and catalytic systems. By varying the deposition conditions and polyelectrolyte composition, authors have reported achieving highly permeable, semi-permeable, or nearly impermeable PEM films. The permeability requirement varies according to specific applications. For surface protection, an ideal film should be impermeable; while for drug release, the films should

exhibit adequate permeability in order to attain the proper therapeutic dose release over a given period of time.

Permeability is particularly important when working with cell templates. Previous studies involving the coating of *E. Coli* have shown that cells remained viable and metabolically active following LbL polyelectrolyte deposition using either chitosan (CH)/alginate (AL) or CH/hyaluronic acid (HA) films.[167] Moreover, Mills *et al.* employed a poly-L-lysine (PLL)/HA shell that successfully encapsulated stem cells while preserving their morphology and viability for 7 days.[168] These results mainly indicate that cells remain viable because of the films' characteristic permeability which promotes nutrient and waste exchange.

The permeability of the LbL films assembly on flat surfaces has been extensively studied by electrochemical methods in order to assess factors affecting molecular transport and diffusion through the PEM film. Characterization of PEM permeability in three dimensional colloidal and particulate templates has however proved significantly more challenging for both loading and release behaviors of compounds from PEM shells. Therefore, it is beneficial to first critically analyze the effects of experimental parameters on the permeability of two-dimensional films in order to conduct more comprehensive analyses of three-dimensional PEM shells. Major factors influencing the structure of multilayers, and in turn their permeability, include ionic strength, wall/film thickness, pH value and charge balance. This review aims to discuss the aforementioned parameters and their respective effects on the permeability of

PEMs deposited on various surfaces and particles, with a focus on drug release modulation and release kinetics, as well as their underlying collective and synergistic relationships.

7.3 Permeability

For many polymers, the capacity of PEMs to be permeable to a fluid, molecules or ions strongly depends on the pH, polarity and ionic strength of the solution. A change in any of these parameters affects the backbone-interactions between the polyelectrolyte molecules within the multilayer and leads to the alteration of the layer structure and overall permeability. Other important factors affecting PEM permeability include the layer number, multilayer porosity and the size of the permeable compound.

For two-dimensional constructs, total internal reflection fluorescence (TIRF) spectroscopy, electrochemistry and *in situ* ellipsometry are the main techniques used to study PEM permeability.[169,170] While for three-dimensional constructs, the main approach consists of encapsulating soluble materials, measuring and analyzing the release profile from the capsule interior. The main disadvantage of this method is that the capsules are prepared at different equilibrium conditions in relation to the release study. Mohwald *et al.* determined the permeability of PEM shells by encapsulating fluorescent crystals and analyzing their subsequent dissolution.[171] The fluorescein dye employed does not interfere with multilayer properties and is used in the initial solution without altering the pH. More recently, the molecular beacon (MB) technique was applied in measuring the permeability of PEM capsules.[172] The MB technique employs a molecular probe

consisting of a single-stranded DNA molecule with a fluorophore and a quencher at opposite ends.[173] This method involves first immobilizing MBs inside particles, followed by encapsulating the MB-loaded particles within the LbL film to be probed. The encapsulated MB-loaded particles are then incubated with DNA target sequences of different lengths. Permeation of the DNA targets through the capsule shell causes hybridization of the DNA targets with the MB complementary loop region resulting in an increase in MB fluorescence.[173]

A typical dissolution curve of covered particles (figure 7.1) consists of a linear and an exponential phase. During the first phase of dissolution, the core particle is immersed in a saturated solution within the shell. It is then possible to calculate the permeability coefficient using the readily available variables of particle radii and density in lieu of variables such as solution volume and number of particles.[171] Other essential parameters required to calculate the permeability coefficient are the time of dissolution, which can be measured experimentally, and the saturation concentration.[171] The permeability coefficient P is given by:

$$P = \frac{C_m V_0}{t_m C_s S} = \frac{2}{3}\frac{\rho}{C_s t_{\max}}\frac{ab}{b + \frac{a}{\varepsilon}\arcsin\varepsilon} \qquad \text{Where } \varepsilon = \sqrt{1 - \frac{b^2}{a^2}} \qquad (7.1)$$

and C_m is the external concentration of the material, V_0 is the volume of the solution, t_m is the time of dissolution, C_s is the saturation concentration, S is the total polyelectrolyte wall surface, ρ is particle material density, t_{max} is the time of dissolution when the external concentration of the material is maximal, a and b are the particle radii in the case of ellipsoidal particles.

During the second step of the dissolution process, when the solid core is dissolved, the release process is determined by Fick's law[171]:

$$\frac{\partial}{\partial} V = - \; 'S\Delta \; ' \tag{7.2}$$

Where the concentration gradient, $\Delta C = C_i - C_e$, consists of C_i and Ce, the concentrations in the interior and exterior of the capsule, respectively. It is important to conduct experiments under a uniform mixing regime in order to obtain a consistent solubility of the core.

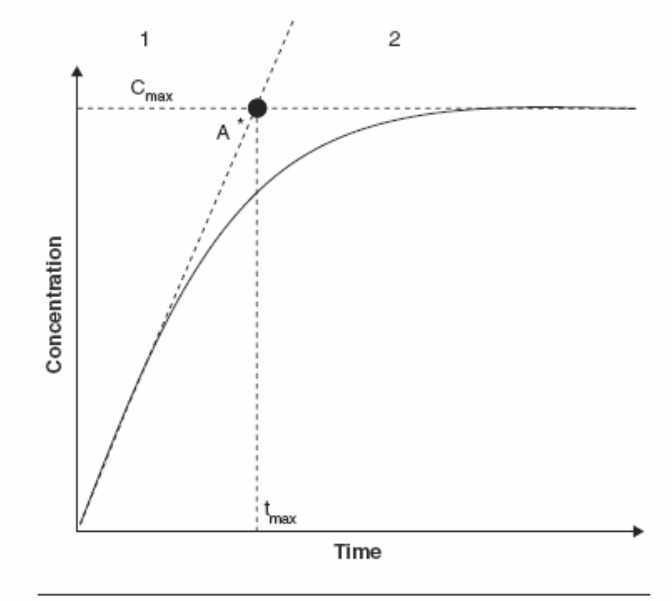

Figure 7.1. Linear (1) and exponential (2) stages of release in a typical release curve**.** The extrapolated point A* determines the characteristic time of dissolution t_{max}. Adapted from[171] .

7.4 Permeability of PEMs in two-dimensional structures

7.4.1 Effect of ionic strength on permeability of PEM films

The ionic strength of the polymer solutions and the washing buffer are of critical importance. The salt concentration during the build-up process dictates the

multilayer thickness and film structure. Von Klitzing *et al.* [174] found that the thickness of LbL poly(allylamine hydrochloride) (PAH)/ poly(sodium-4-styrene sulfonate) (PSS) (Figure 7.2) is directly proportional to the square root of the salt concentration. Furthermore, it was reported that the addition of more salt to the system after completion of the polyelectrolyte built-up process did not affect the final film thickness.[174] Similarly, Harris and Bruening[170] demonstrated that 20 bilayers of PAH/PSS prepared in the absence of salt had the same thickness as 4 bilayers prepared in the presence of salt. It is also interesting to note that a greater film permeability is observed with the addition of salt.[170] With respect to film structure, Caruso *et al.* observed, using atomic force microscopy (AFM), considerable structural changes to the surface of a PAH/ poly(acrylic acid) (PAA) (Figure 7.2) film when the ionic strength of the deposition solution is altered through the washing buffer. Moreover, the produced films exhibited considerable surface roughness.[175] However, relatively smooth multilayer films were formed when the salt concentration was maintained constant during the assembly process and the washing step. For such smooth films, subsequent exposure to pure water led to the introduction of regular, discrete and nanometer-sized pores.[175]

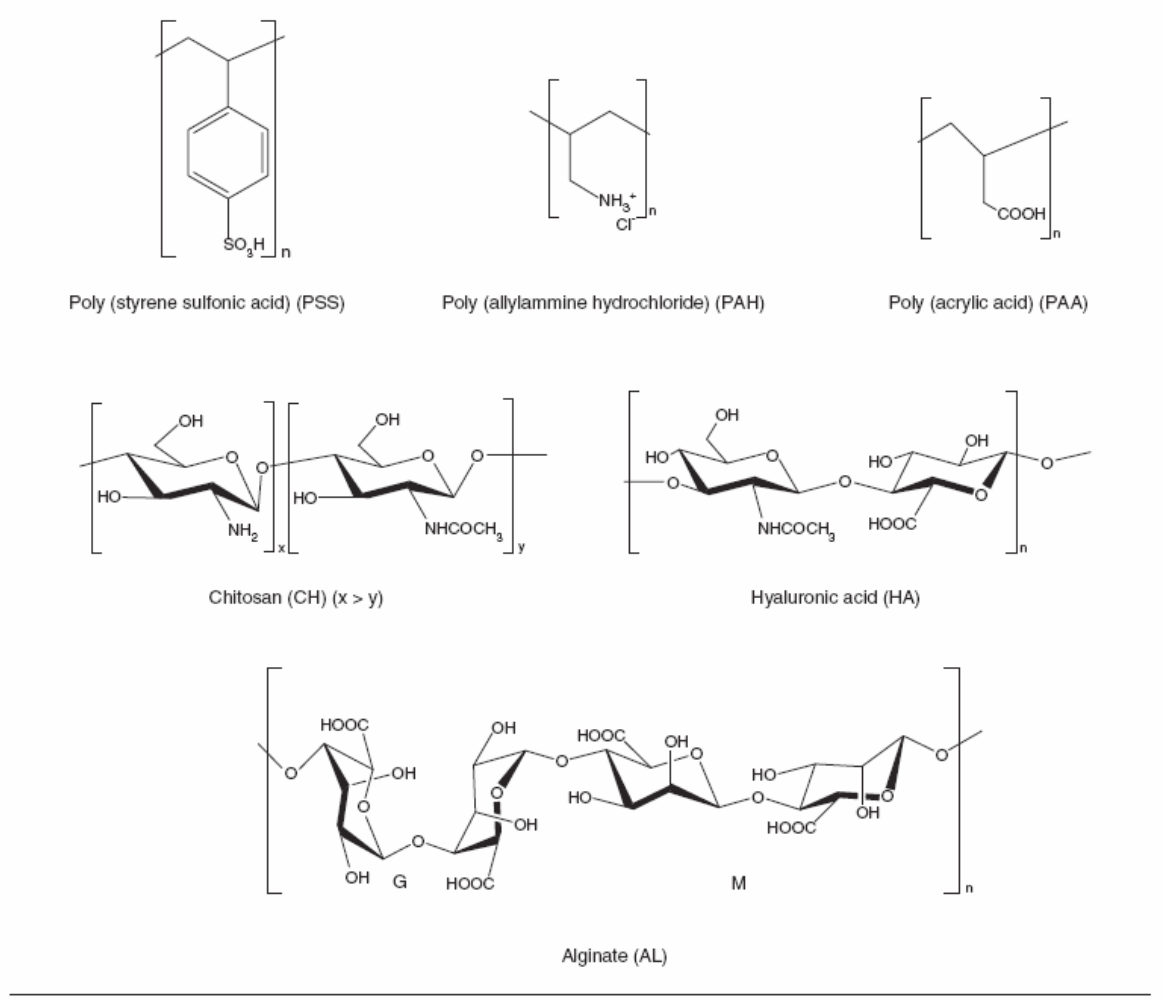

Figure 7.2. Polyelectrolyte structures.

When LbL films assembled primarily through electrostatic interactions are incubated in a salt solution, counter-ions and accompanying water molecules are usually incorporated into the films, causing swelling. A higher salt concentration causes a greater degree of swelling, which leads to a change in film morphology and an enhanced film permeability [176], while also contributing to multilayer film decomposition. The resulting dissolution is caused by the competition between polymer-to-polymer interactions, which hold the films together, as well as the polymer interactions with external salt ions.[177] Winnik *et al.* showed that the

ionic strength alters film morphology. Increasing the ionic strength induces the reorganization of the surface topography from isolated spherical islets to elongated worm-like features.[178] Therefore, the ionic strength influences not only the range of the electrostatic forces but also their intensities. In many cases, a large increase in ionic strength can lead to dramatic weakening of interactions between polyelectrolyte layers, resulting in the destruction of the inter-polyelectrolyte complex.

With respect to the individual layer thickness, at low ionic strengths, the polymers are elongated at the surface and form thin films; whereas at high ionic strengths, they predominantly form loops and thicker films. It is interesting to note that the transport of rhodamine molecules through layers formed of flat polyelectrolytes, prepared without salt, was reported to be 3 times faster as compared to those composed of looped polymers.[169] The difference in permeability in this case is attributed to the size distribution of defects in the multilayers, from a few large defects at low ionic strengths to many small pores at high ionic strengths.

7.4.2 Effect of film thickness on the permeability of the PEM films

Lynn *et al.* [179] investigated layer growth in poly(*β*-aminoesters) and DNA on surfaces modified with 10 bilayers of polyethyleneimine (PEI) and PSS. The results showed that films prepared using plasmid concentrations of 1 mg/mL were thicker than those prepared using concentrations of 0.5 and 0.25 mg/mL. Film thickness was thus modified through DNA concentration and controlled by varying the number of polyelectrolyte layers. The permeability decreases with

increasing layer number at a much faster rate than that achieved linearly by an increase in thickness. The growth mechanism involves mainly electrostatic interactions between the polyelectrolytes from the solution and the outer layer of the film.[102,104] For an HA/CH multilayer system, an exponential increase of the optical film thickness is measured as the number of deposited bilayers increases.[103] The exponential growth of the HA/CH system relies on the diffusion of polyelectrolytes in and out of the film during each bilayer step. In this system, chitosan is the diffusing polyelectrolyte while HA is the non-diffusing species. Furthermore, it is demonstrated that the multilayer thickness at a given stage depends on the sizes of both CH and HA. The assemblies of high molecular weight polysaccharides (HA, 360,000; CH, 160,000) were twice thicker than those obtained with their low molecular weight counterparts (HA, 30,000; CH, 31,000), giving rise to thicknesses of approximately 900 nm and 450 nm, respectively.[105] Film thickness and thus permeability are affected by polymer concentration and molecular weight as well as by the constituent number of layers.

7.4.3 Effect of pH and charge on the permeability of PEM films

pH-responsive or pH-switchable membranes are currently applied in filtration systems, membrane-based separations, bio-separations, and sensors. pH has a direct effect on the ionization degree of the polyelectrolyte. Each dissociable polyelectrolyte is considered a potential vehicle for a charged ion, as they act in the dissociated state. The diffusion of charged ions through the multilayer is a result of site to site hopping on the dissociated polyelectrolytes. Therefore, the

ions' permeability is dependent on their respective charges.[171] Moreover, the permeation rates of amino acids [180,181] and ionic drugs [182] through membranes with pH-sensitive chemical groups are greatly influenced by local pH and electrolyte concentration. The ionization state of the chemical groups can either generate an excess of positive or negative charges, giving rise to anion or cation-permselective membranes, respectively. Several research groups [182-184] have conducted theoretical and experimental studies of these ion-permselective membranes. Martin *et al.*[185-189] reported a pH-responsive transport membrane system consisting of gold nanotubules capable of altering between cation-transporting, non-ion-permselective, and anion-transporting states. This multi-bipolar architecture makes polyelectrolyte multilayer membranes especially suitable for ion separations. Krasemann and Tieke[150] showed that polyelectrolyte multilayer membranes composed of 10 to 60 bilayers of PAH/PSS exhibit $Cl^-/SO4^{2-}$ selectivity factors as high as 45 in diffusion dialysis experiments. They suggested that Donnan exclusion resulting from fixed charges in the membrane is responsible for this selectivity. The strength of interactions is proportional to the charge density of the permeating ions and of the polyelectrolytes constituting the membrane. Warzynski et al. studied the permeability of electroactive molecules (1,2-Naphthoquinone 4-sulfonic acid sodium salt and 9,10-antraquinone-2,6-disulfonic acid disodium salt) to PEI/PSS films formed at pH 6 and pH 10.5 using electrochemical technique.[190] At pH 10.5, PEI is weakly charged and is strongly charged at pH 6. They concluded that permeability of the film formed

with strongly charged PEI is lower than that built with weakly charged polycation.[190]

7.4.4 Effect of cross-linking on the permeability of PEM films

In order to control permeability through ion-transport selectivity in multilayered polyelectrolyte films, Bruening and coworkers [191-194] investigated the combined effect of cross-linking, hydrophobicity and charge density modification. Cross-linking was achieved via heat-induced amidation followed by hydrolysis of PAH and PAA polymers. Both the hydrophobicity and charge density of PAH/d-PAA films were controlled by partial esterification of PAA (d-PAA).[195] The authors showed that the variation of the ester functionalities in PAH/d-PAA films, along with subsequent cross-linking and hydrolysis, yielded stable and highly dense $-COO^-$ groups in the films. As a result, a higher permeability for positively charged $Ru(NH_3)_6^{3+}$ ions was obtained than for $Fe(CN)_6^{3-}$ ions. They also studied controlled ion transport through PEM membranes by increasing the net fixed-charge density in the films.[196] Advincula and coworkers studied the effects of pH and cross-linking [197] on pH-responsive membranes and successfully induced film permselectivity by varying the pH of either the solution or the film itself (*ex situ*) following cross-linking. The cross-linking serves to stabilize the structure while responsiveness to pH variation could be maintained. This approach is particularly versatile, since it allows for the preparation of weak polyelectrolyte capsules with stable structures for use in various applications including microcontainers, delivery vehicles, biosensors, and bioreactors.

7.5 Permeability of PEM shells built within three-dimensional templates

7.5.1 Effect of ionic strength on the permeability of PEM shells

As previously discussed, the increase in salt concentration results in the weakening of electrostatic interactions between polyelectrolytes due to the competing salt ions.[198] In three-dimensional constructs, the intercalation of salt ions promotes swelling of the capsule wall through the osmotic storage of water. The wall structure and interconnectivity is rendered loose while the mesh widths become larger, thus resulting in an increased diffusion rate of the encapsulated molecules. However, this effect is reversible. After the removal of salts, the capsules become impermeable to the probe macromolecules. This reversible permeability switch, induced by modifying salt concentrations, has been exploited to achieve capsule loading with macromolecules.[198]

In other studies, the release of encapsulated fluorescein microcrystals from PSS/PAH capsules was strongly enhanced by increasing salt concentration.[171] Additional measurements at low concentrations of different salts showed that this effect could be purely attributed to electrostatic effects, but may also depend on additional specific interactions of the salts with the capsule wall. However, in a different study, the release of ibuprofen (IB) from PEI/PSS and PAH/PSS multilayers decreases with higher salt concentrations.[199] In this case, as the IB solubility is reduced in salt solutions, a progressive and controlled release rate is observed as salt concentration is increased.

Generally, for PEM systems in which the pH is maintained, it has been suggested that the permeability obeys a power law $P \sim k\ [salt]^n$ where n is the ion charge. The ionic strength in the capsule wall may in principle be the sum of ionic strengths of the component parts: the buffer and the permeate.[200] Moreover, it is believed that permeation through polyelectrolyte multilayers is a function of the free energy of the interpolyelectrolyte interactions and can be controlled by parameters responsible for the interpolyelectrolyte complex formation. In a system with variable pH, it has been shown that the permeability coefficient has a non-linear dependence on the salt concentration. A pH shift changes the ratio between positive and negative charges within the multilayer and therefore loosens the PEM structure.

7.5.2 Effect of film thickness on permeability of PEM shells

Drug encapsulation with the LbL is conducted in conditions where the drug is not soluble. The encapsulated drugs are then subjected to appropriate soluble conditions that allow for their controlled release. Drugs are generally encapsulated within the outer layers and their release rate is a function of the encapsulating shell thickness. An increased number of layers in the LbL shell serves to increase the bioavailability of the poorly soluble drugs and maintain a sustained release in host system.[201]

Table 7.1. Loading methods of drugs and molecules in a polymer multilayer by means of LbL self-assembly technique.

Method of loading	Drugs/Molecules	Polymers	Ref
Core for LbL coating	Ibuprofen	(PEI/PSS), (PAH/PSS) (CH/DEXs)	199 202
	Furosemide	(PSS/PDDA)+(PSS/Gelatin)	201
	Dexamethasone	(PDDA/PSS) (PDDA/Gelatin)	203
	Indomethacin	(PSS/PDDA)	204
Chemical attachment to polymer before coating	Paclitaxel	(HA-paclitaxel/CH)	205
Within nanoparticles	DNA/PEI nanoparticle	Poly(L-glutamic acid)	206
Embedding	BSA	(CH/AL)	207

Several studies have reported on the controlled drug release from LbL/PEM shells (table 7.1). In one study, fluorescein dye microcrystals coated with PSS and PAH were used as a model system. Mohwald *et al.* showed that increasing the layer number resulted in decreased shell permeability and prolonged microcrystal dissolution.[208] Similar trends were observed with furosemide [201], dexamethasone [203] and IB[209]microcrystals encapsulated within a multilayered film (table 7.2). In the case of the furosemide microcrystals, the reported release rate was 300 fold slower compared to the uncoated system.[201] For encapsulation, both shell thickness and diameter can be controlled with high precision, within a few nanometers, by varying the polyelectrolytes used in the assembly process.[203] The diffusion-controlled release mechanism of the microcrystals is a two-step process: first, diffusion of the bulk solution into the capsules to dissolve the drug

crystals; and second, diffusion of the dissolved drug molecules out of the capsules (Figure 7.3).[202] It is important to note that the core, or drug, dissolution is accompanied by an increase in osmotic pressure that alters polyelectrolyte multilayer shell properties.[204]

Table7.2: Half time release of several drugs encapsulated in polymers multilayer via LbL self-assembly technique.

Encapsulated	Conditions/Polymer	drugs release ($t_{1/2}$)	[Ref]
Ibuprofen	pH1.4/$(CH/DEXs)_{10}$	8 min	202
	$(CH/DEXs)_{20}$	18 min	
	$(CH/DEXs)_{30}$	30 min	
	pH 7.4/$(CH/DEXs)_{10}$	4.5 sec	202
	$(CH/DEXs)_{20}$	7 sec	
	$(CH/DEXs)_{30}$	9 sec	
	$(PEI/PSS)_5$	8-9sec	199
	$(PAH/PSS)_5$	36 sec	199
Furosemide	pH 1.4/$(PSS/PDDA)_2$+$(PSS/Gelatin)_6$	3.3 min	201
	$(PSS/PDDA)_2$+$(PSS/Gelatin)_4$	1.8 min	
	pH 7.4/$(PSS/PDDA)_2$+$(PSS/Gelatin)_6$	12 min	
	$(PSS/PDDA)_2$+$(PSS/Gelatin)_4$	1.2 min	
Dexamethasone	PBS, pH 7.2,/$(PDDA/PSS)_4$/PDDA	3.3 min	203
	$(PDDA/Gelatin\ B)_4$/PDDA	45 min	
Indomethacin	PBS, pH 6.8 /$(PSS/PDDA)_4$	2h	204
	$(PSS/PDDA)_8$	5h	
Insulin	pH 7.4/ $(PMA/WSC)_8$	1h	210

Studies have also demonstrated the ability to design systems with multiple release kinetics. This has recently been shown by Tabrizian *et al.* using bovine serum albumin protein (BSA) encapsulated in liposomes coated with CH and AL.[207] As expected, the LbL structure retards the release rate of the protein. Furthermore, BSA is found to be encapsulated between the layers and inside the

liposomes (figure 7.4). As a result, the rate of release showed two distinct phases: an initial release from the shell, lasting 0 to 7 days; and a terminal phase with a core release of over 11–30 days.[207] Similar release trends were achieved with bone morphogenetic protein-7 (BMP-7).[211]

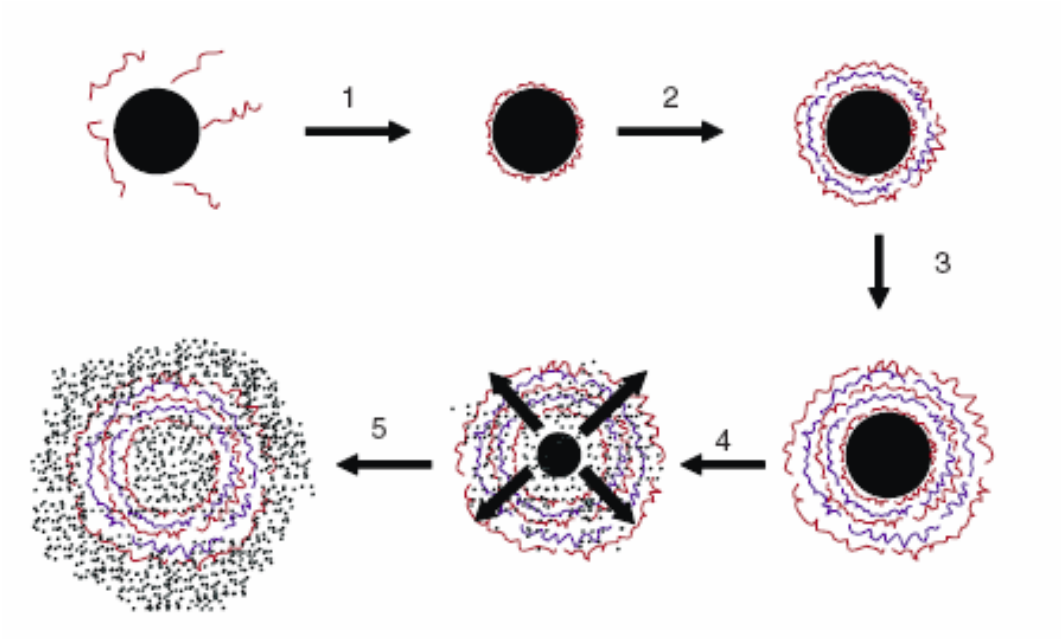

Figure 7.3. Scheme of the polyelectrolyte multilayer assembly and of the subsequent core dissolution. The initial steps (1 – 3) involve stepwise shell formation on a microcrystal core. After the desired number of polyelectrolyte layers is deposited, the coated particles are exposed to conditions where the core is dissolved (4), resulting finally in fully dissolved cores and remaining hollow capsules (5). Adapted from[209]

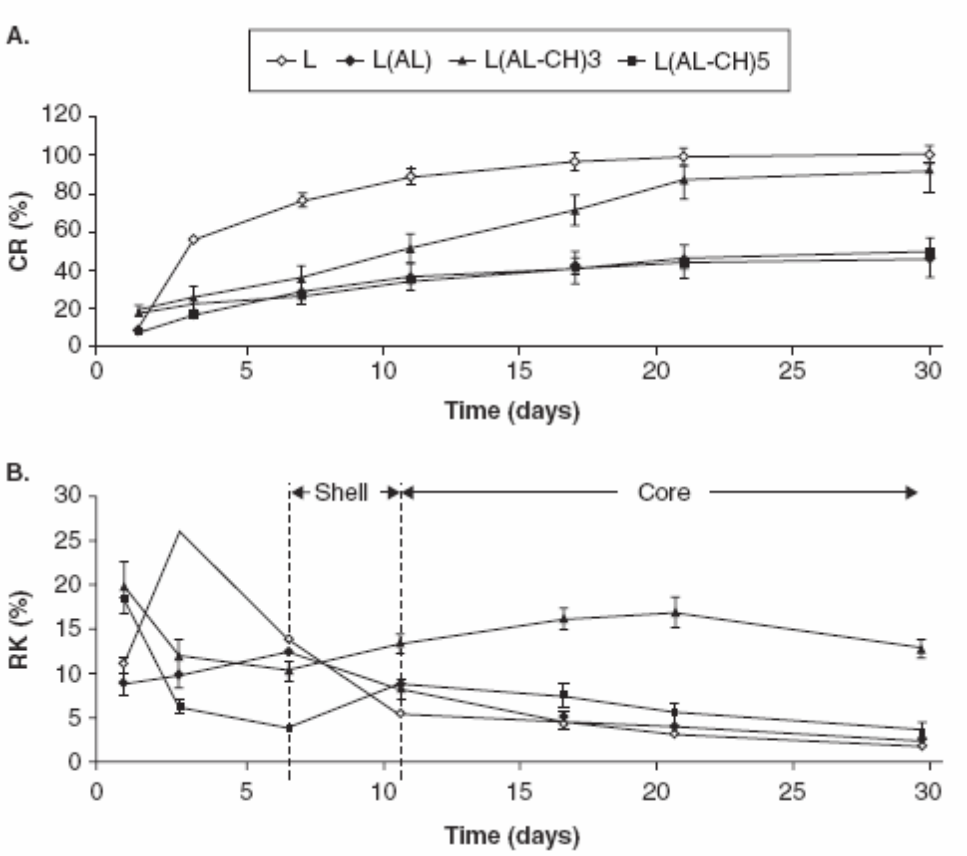

Figure 7.4. A. Cumulative percentage in vitro release profile (CR) of BSA-loaded uncoated and coated liposomes. **B.** Absolute percentage in vitro release (RK) of BSA-loaded uncoated and coated liposomes at each time point in UPW. Data represent mean plus or minus standard error of the mean[202]
By permission of Science Direct.

7.5.3 Effect of pH and charge on permeability of PEM shells

Li *et al.* showed that the permeability of L-R-dimyristoylphosphatidic acid (DMPA)/human serum albumin (HSA) microcapsules can be tuned by changing the pH value of the media.[212] In this system, HSA molecules take a different conformation and charge at low pHs of 2.5- 4.5 and at higher pHs ranging from 5 to 7.[212,213] At lower pHs, positively charged HSA is more likely to be exposed to the outside of the capsules and interact with the DMPA solution. At pHs above 5, HSA is negatively charged and the interaction between HSA and DMPA is

mainly repulsive. The latter less ordered structure exhibits an increase in permeability.

The use of pH changes to modify the charge of a molecule is generally applicable to both small and large molecules. A small change in pH for a molecule bearing multiple weak acid functionalities may have a significant impact on the diffusion of this molecule through PEMs. PEM shell systems can thus be designed to target the release of bioactive agents transported in this manner for targeted release in either an acidic or a basic environment.[151] For example, an amine-bearing drug molecule should be released more quickly in the host's intestine (higher pH) than in the stomach (lower pH) since it is neutral in the former and charged (protonated) in the latter. Chen and Lin showed that indomethacin crystals (figure 7.5) encapsulated with PDDA and PSS displayed slower release in simulated gastric fluid (pH 1.4) compared to simulated intestinal fluid (pH 6.8) [204] (table 7.2). Zeng et al. demonstrated that PEM coating of $CaCO_3$ microparticles loaded with IB have a higher release at acidic pH where IB is not soluble.[214] At a neutral pH, these coated microparticles with 5 bilayers of PRO/PSS possess a slower release when compared to uncoated IB crystals.[214]

Mohwald and coworkers[202] exploited the pH-dependent solubility of IB encapsultated with CH/AL, CH/dextran sulphate (DEXs) or CH/carboxymethyl cellulose (CMC) shell to vary concentration gradient. By raising the bulk solution pH, the release rate of IB increased with the solubility of IB. At pH 7.4, the solubility of the drug was very high and IB was released very rapidly (table 7.2). At pH 1.4, where the IB solubility was very low, the release of the drug

was prolonged (table 7.2). This supports a model consisting of two release channels in this system; one by diffusion at pH 1.4 and the other by pressure through pore-like structures at pH 7.4. Such pores were observed for thin, flat PAA/PAH films. Furthermore, at the molecular scale, it can be concluded that polyelectrolyte films are not smooth and may contain pores that are influenced by changes in pH or salt content.[157,169] Although pH plays a key role, it is important to note that drug release behavior is primarily governed by shell thickness.

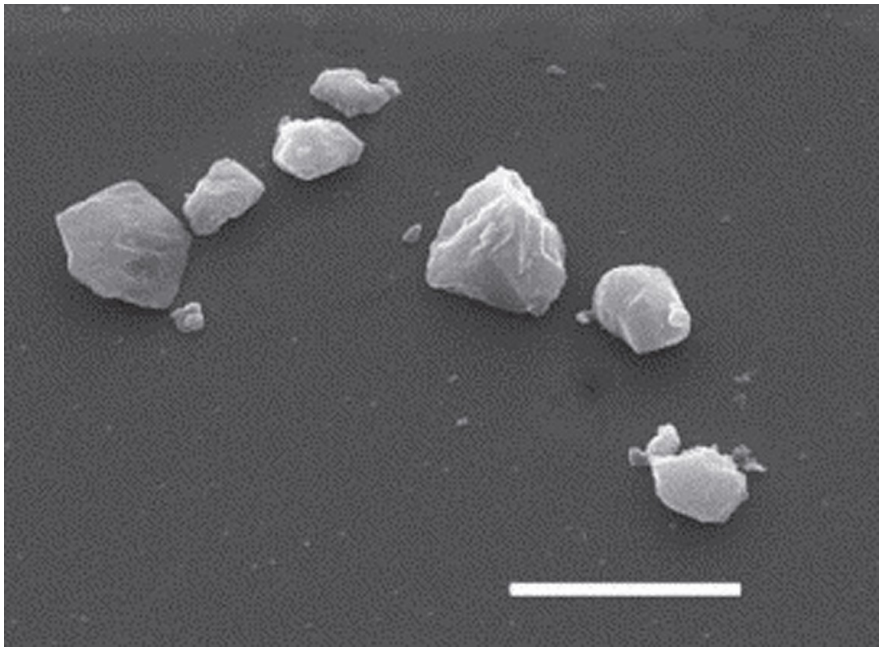

Figure 7.5. Scanning electron microscope image of indomethacin microcrystals. The scale bar corresponds to 10 μm.[215] By permission of Science Direct.

Moreover, variation in pH was used to control the permeability of the weak polyelectrolyte (PAH), in PSS/PAH capsule walls in order to encapsulate macromolecules. PSS/PAH capsules were prepared at neutral pH.[216] Capsules could then be switched between open and closed states by varying the pH value;

this influenced the interactions in the PAH/PSS wall and created local charges and defects in the film. Macromolecules could penetrate into the capsules at low pHs but are excluded at pHs over 7. This reversible switching behavior, attributed to the protonization/deprotonization of the weak PAH, provides the opportunity to encapsulate different substances under mild conditions.

7.5.4 Effect of temperature and cross-linking on permeability of PEM shells

In drug delivery applications, LbL multilayer capsules are required to provide protection to the encapsulated drug from enzymatic decomposition in the human body while reducing drug toxicity to the non-targeted human organs.[217,218] Critically, drug activity must remain intact before reaching the target tissue. So far, few reviews have presented an overview of the development of new multilayer films and an understanding of their physical and chemical properties [148,219-221]. However, most of the polyelectrolytes used for drug delivery systems are biodegradable. This biodegradability damages the PEM multilayer and affects their permeability, and consequently the drug release kinetics.[215,222]

To enhance the stability of AL/CH multilayer films, it is important to limit enzymatic desorption. This was accomplished by raising the deposition temperature in order to effectively slow enzymatic activity and in turn desorption and release rate. It was shown that increasing the deposition temperature from 20 ºC to 60 ºC efficiently reduced the release rate of encapsulated indomethacin microcrystals (Figure 7.5 and 7.6) due to the increase in the thickness and a better organization of the AL/CH multilayer film.[223] Moreover, cross-linking the

AL/CH multilayer film with 1-Ethyl-3-[3-dimethylaminopropyl]carbodiimide hydrochloride (EDC) significantly reduced the enzymatic desorption and the drug release rate.[224] Therefore, increasing deposition temperature and cross-linking neighbouring layers are effective methods by which to protect LbL assembled multilayer films from enzymatic erosion, as well as to prolong the release of the encapsulated drug.

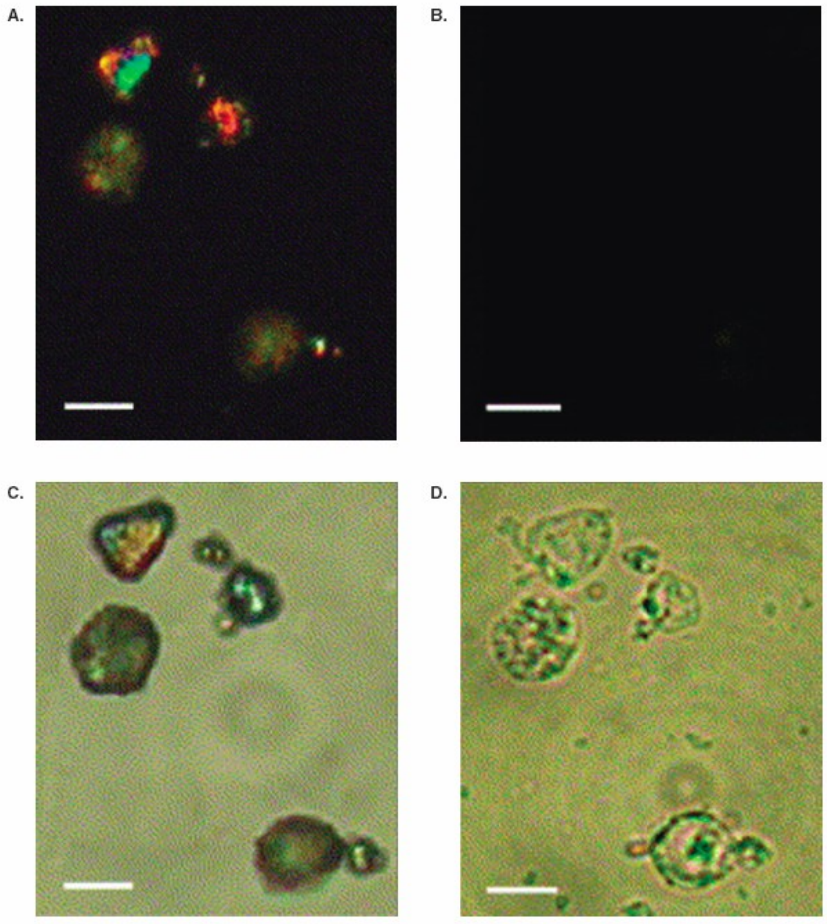

Figure 7.6. Optical microscope images following dissolution of the encapsulated indomethacin (IDM). Encapsulated IDM microcrystals (**A**) and hollow capsules (**B**) observed with crossed polarizer and analyzer. Encapsulated IDM microcrystals (**C**) and hollow capsules (**D**) observed under the normal light. All the scale bars correspond to 5 µm.[215] By permission of Science Direct.

7.6 Discussion and conclusion

Among the features governing PEM film characteristics, permeability plays a key role in drug release applications. However, due to the lack of techniques to study the shell permeability of three-dimensional systems, investigations are mostly oriented towards understanding the parameters which affect the permeability of PEM films in two-dimensional systems. Ionic strength seems to be the most important parameters affecting directly and by various manners, the LbL structure and morphology. A high ionic strength enhances the PEM permeability to molecules, whereas a low salt concentration decreases the permeability.[200] Films thickness can also be controlled by varying the ionic strength of the solution and as well by the number of layers of polyelectrolyte deposited.[169] At low ionic strength, the polymers are elongated at the surface forming a thinner individual layer thickness and thereby a thinner film, whereas at high ionic strength they predominantly form loops and consequently a thicker PEM film.[225] There is also a linear increase of film thickness with the square root of salt concentration depending on the nature of polymers [226] at a given pH.

By modifying the pH and the ionisation degree of polyelectrolytes, interactions inside the multilayered shell are altered, affecting the permeability. Strong polyelectrolytes possess more charge and in turn form stable multilayers. Weak polyelectrolytes, on the other hand, can be treated by means of high temperature or crosslinking in order to arrive at a functional stability.

The collective outcome of parameters affecting the permeability and controlled release of drugs is much more complex for polyelectrolyte LbL build-up on

particulate templates. The drug release rate from these stable nanoshells is dependent on the solubility and the size of the drug, the number of layers and thickness of the shell, as well as on the type of polyion employed in the LbL assembling process.[199 201]

To discuss effectively the parameters influencing the permeability, one should also consider other factors such as the nature of polyelectrolytes. As demonstrated by Lvov *et al.*, the use of gelating/polyelectrolyte bilayers displayed better sustained and controlled release of furosemide when compared with shells constructed from PSS/PDDA (Poly(diallyl dimethylammonium) chloride).[201]

Filled capsules can serve not only in controlled drug release vehicles but also as bioreactors and biosensors.[227 228] Furthermore, the encapsulation of enzymes and proteins provides protection from inhibitors, proteases and bacteria which are unable to permeate the capsule wall. Encapsulated enzymes have also demonstrated higher activity when compared to their chemically immobilized counterparts, which only retain 50% or less of their optimal activity. Encapsulated glucose oxidase enzymes were able to maintain 60% of their activity as well as retain their native protein conformation.[229]

7.7 Expert opinion

The controlled modification of permeability through LbL build-up of polyelectrolyte multilayers can be effectively employed in applications within diverse areas, including drug delivery systems, biosensors, catalyst research and

biotechnology. By adjusting the permeability through parameters such as ionic strength, pH, cross-linking, thickness, nature and molecular weight of polyelectrolytes, many issues associated with drug formulation and release could be addressed.

LbL assembly has the ability to modify a large range of surfaces at the nanometer scale, as well as the capacity to incorporate a wide array of macromolecules. This characteristic allows the LbL technique to be extended to biomaterials and biomedical device design. Current research interests involve surface modifications of stents and hip implants through the coupling of LbL techniques with biocompatible polymers in order to enhance implant biocompatibility and limit side effects. Ongoing research is predominately focused on the investigation of coated endovascular devices by drugs, growth factors and bioreceptors embedded into multilayer films for site-specific release of drugs. For such an application, a sound understanding of PEM/LbL permeability, and in turn macromolecule release, is very critical. In three dimensional systems, PEM shell development is extensively directed towards drug encapsulation and controlled release via infrared, ultrasound or magnetic field activation. By using these external stimuli, the permeability of the PEM/LbL can be modified to hold or release the encapsulated drug or molecule.

Another application that exploits the adaptability of PEM permeability is the development of selective permeability which acts to exclude large macromolecules from interaction with a given template while permitting smaller molecules. This is particularity interesting and beneficial when living cells are

used as templates. A potential application of this property is the immunocamouflage of red blood cells or encapsulation of pancreatic cells for insulin production. For instance, live red blood cells can be encapsulated within a natural and biocompatible shell where immune system molecules are excluded while nutrient and ions permeate freely. The multilayered shell provides crucial immuno-protection which serves to prolong survival and functionality.

These are few examples of the many applications of LbL assembly which holds great potential in the biomedical and biological fields of research. The versatile, biocompatible, and controllable nature of LbL coating techniques and the underlying permeability in both two and three-dimensional systems is undoubtedly a great asset for future development and optimization of a variety of biomedical devices.

7.8 Acknowledgment

This work is supported by Canadian Institutes for Health Research-regenerative medicine-Nanomedicine grants and the Fonds Québécois de la recherche sur la nature et les technologies in the framework a grant to Centre for Biorecognition and Biosensors (CBB). Sania Mansouri acknowledges the post-graduate scholarship from the Fonds de la Recherche de la Santé du Québec.

CHAPTER 8: IMMUNOCAMOUFLAGE OF RBCS IN A 2-D MODEL BY MEANS OF LBL ASSEMBLY

This chapter presents a proof of concept of the ability of biocompatible and non-toxic polymeric multilayer built on a monolayer of RBCs in a two-dimensional model to induce the immunocamouflage.

The results are presented in a December 2009 article entitled “Silencing red blood cells recognition towards antibody-Anti A by mean of polyelectrolytes LbL assembly in a 2-D model system” This paper presents a first step towards meeting the first objective outlined in this thesis. The work has been published in Langmuir and is reprinted with permission. Copyright American Chemistry Society.

Silencing Red blood cells recognition towards antibody-Anti A by mean of polyelectrolytes LbL assembly in a 2-D model system

Sania Mansouri[†], Julien Fatisson[†], Zhimei Miao[‡], Yahye Merhi[§], Françoise M. Winnik[‡], Maryam Tabrizian[†,♦]

[†]Department of Biomedical Engineering, [♦]Faculty of Dentistry, McGill University, H3A 2B, [‡]Faculté de Pharmacie and Département de Chimie, Université de Montréal, H3C 3J7, and [§] Montreal Heart Institute, H1T 1C8, Montreal, Canada

*Corresponding author: Maryam Tabrizian: PhD, MBA; Associate Professor
Phone: +1- 514-398-8129
Fax: +1-514-398-7461
Email: maryam.tabrizian@mcgill.ca

8.1 Abstract

Silencing the antigenic response of red blood cells (RBC) is a prerequisite towards the development of universal blood transfusion. Using a 2D-model whereby non-fixed RBCs are adsorbed on a human fibronectin (HFN) coated surface, we demonstrate that the layer-by-layer (LbL) assembly technique of biocompatible polyelectrolytes can be employed to achieve the immunocamouflage of RBCs against the Anti-A antibody while maintaining the integrity and viability of the cells. The multilayered film consisted of a protecting shell (P-shell), containing 5 bilayers of chitosan-graft-phosphorylcholine (CH-PC) and sodium hyaluronate (HA), covered by a camouflage shell (C-shell) made up of 5 bilayers of poly-(L-lysine)-graft-poly(ethylene glycol) (PLL-PEG) and alginate (AL). Control experiments in which RBCs were coated by $(CH\text{-}PC/HA)_{10}$ bilayers indicated that the two polyelectrolytes alone did not prevent immunorecognition. The LbL film

formation on RBCs and model substrates was monitored by quartz crystal microbalance with dissipation factor (QCM-D) and analyzed through ζ-potential measurements, atomic force microscopy (AFM), and optical microscopy. Antibody interaction with the coated RBCs was investigated by QCM-D, fluorescence microscopy, and hemolysis assays. Results from these measurements demonstrated that the hybrid LbL system built-up with different sets of polyelectrolytes was able to protect the RBCs from hemolysis and recognition by the Anti-A antibody.

Keywords: Layer-by-layer assembly, chitosan-*graft*-phosphorylcholine, hyaluronic acid, poly-L-lysine-*graft*-polyethylene glycol, alginate, non-fixed RBCs, quartz crystal microbalance, fluorescence microscopy, antibody recognition, immunocamouflage

8.2 Introduction

Blood transfusion is the most widely used cell transplantation procedure in clinical practice. ABO blood-matching tests are carried out routinely prior to blood transfusion in order to avoid incompatibilities and immunological reactions on the part of the patients. In some cases, after the transfusion, patients develop alloantibodies against antigens of several blood group systems, resulting in an increased risk of blood incompatibility in the event of future transfusions. This problem and, more generally, the worldwide difficulty to secure reliable and suitable donors have prompted research towards the production of a "universal blood" in which the antigens are silenced. Currently, two approaches seem quite promising, although neither of them is devoid of limitations, as they often induce

complications in case of repeated transfusions. One method consists of cleaving the antigenic groups from the surface of red blood cells (RBCs) using specific enzymes.[55-58] The other involves the chemical modification of the RBC surface by covalent linkage of non-antigenic groups, mostly poly(ethylene glycol).[48,54,230] A benchmark study in the field is attributed to Mohwald *et al.* who used RBCs as templates for the layer-by-layer (LbL) construction of a polyelectrolyte shell.[94,231] The RBCs were first "fixed", i.e. inactivated via crosslinking with agents such as gluteraldehyde as to strengthen the RBCs and facilitate their manipulation during the multilayer construction. The RBCs were consequently digested upon completion of the multilayer build-up, leaving behind hollow microcapsules with the potential of being used as carriers for controlled drug release. These findings demonstrated the feasibility of modifying the RBCs surface with various polyelectrolytes and provided evidence of the multilayered film permeability via the diffusion of fluorescent probes through the shell. [200] Although the authors worked with fixed RBCs, this seminal work put forth the principles for the build-up of multilayer films on biological templates and settled the design guidelines for the modulation of the film permeability.

This principle has been applied more recently to coat living cells with a polyelectrolyte multilayer.[167] *E-Coli* cells coated with a shell of either chitosan/alginate or chitosan/hyaluronate remained viable, metabolically active, and able to divide after polyelectrolyte deposition. Similarly, stem cells encapsulated in poly-L-lysine/hyaluronate LbL assemblies preserved their

morphology and viability for up to 7 days, [168] confirming that nutrients and waste material were able to diffuse in and out of the LbL membrane.

Studies performed on living cells, coupled with the knowledge obtained from working on fixed RBCs, encouraged us to investigate polyelectrolyte multilayer construct to camouflage RBCs so that they evade the autoimmune system of blood recipients. However, compared to *E-Coli*, RBCs are more fragile. *E-Coli* possess a cell wall that contributes to their rigidity during encapsulation. Other particularities of RBCs include their lack of a cell nucleus as well as their negative surface charge included by the presence of N-acetylneuraminic acid (sialic acid) groups. Furthermore, they can bend and pass through blood vessels and their main function is to carry oxygen. These features collectively introduce tremendous challenges towards achieving our goal of immunocamouflage. The RBCs must be wrapped in a multilayer shell that is able to withstand the harsh conditions of the bloodstream, maintain the vital functions of the RBCs, and prevent specific blood group antibodies from reaching the antigens on the cell surface. These stringent requirements drastically limit the number of acceptable polyelectrolyte building blocks and in turn circumscribe the design of an efficient polyelectrolyte system to insure the desired permeability. Among the biocompatible, biodegradable, and non-toxic polymers known to form well characterized multilayers, two polyanions, sodium hyaluronate (HA) and sodium alginate (AL), stand out as acceptable candidates. HA is a linear polyanion ($pK_a \approx 3.0$) consisting of alternating *N*-acetyl-β-D-glucosamine and β-D-glucuronic acid residues linked (1→3) and (1→4), respectively. It is produced commercially

by bacterial fermentation and has found numerous applications in drug delivery systems, synovial fluid replacement therapies, in neutraceuticals, and cosmetics formulations.[232] It has been employed as a multilayer component together with polyanions, such as chitosan (CH)[103,207], poly-L-lysine (PLL)[233] and poly(allylamine).[234] Alginate, which is extracted from seaweed, is a block copolymer of two monosaccharides linked (1→4), β-D mannuronic acid and its C-5 epimer α-L-guluronic acid. Matrices formed from alginate are employed for pancreatic islet encapsulation.[235] They exhibit extended longevity within the body and do not provoke immunogenic responses.[236,237] AL is polyanionic polyelectrolyte and mainly used with CH and poly-L-lysine, both polycationic polyelectrolytes, to form multilayers. CH is a linear polysaccharide composed of β-D-glucosamine and β-D-*N*-acetylglucosamine linked (1→4) obtained by deacetylation of chitin, a natural polysaccharide. It is under consideration for several biomedical applications, such as matrices for tissue engineering and gene therapy formulations.[238] The use of CH as biomaterial suffers from one drawback: the polymer is poorly soluble in aqueous media of pH > 6.2. Although, in some instances, this problem can be circumvented, RBCs cannot withstand conditions of pH < 6. This limits the use of CH in LbL construct. We selected instead to work with a derivative of CH grafted with phosphorylcholine group (CH-PC), known for its solubility in aqueous media of neutral pH. Like CH itself, CH-PC is able to form multilayers with HA, as long as the degree of PC incorporation remains low (~ 30 % mol PC groups/glucosamine units).[108] PLL, the second polycation under consideration in view of its biocompatibility,

was dismissed after initial measurements since it induced lysis of RBCs. PLL was consequently grafted with poly(ethylene glycol) (PEG) chains to yield grafted PLL-PEG. This approach was based on the previous reports regarding the propensity of PLL-PEG to adsorb spontaneously from aqueous solution onto negatively charged surfaces, resulting in a stable polymeric monolayer that renders the surfaces protein-resistant.[136] The structures of the four polyelectrolytes employed are presented in Figure 8.1.

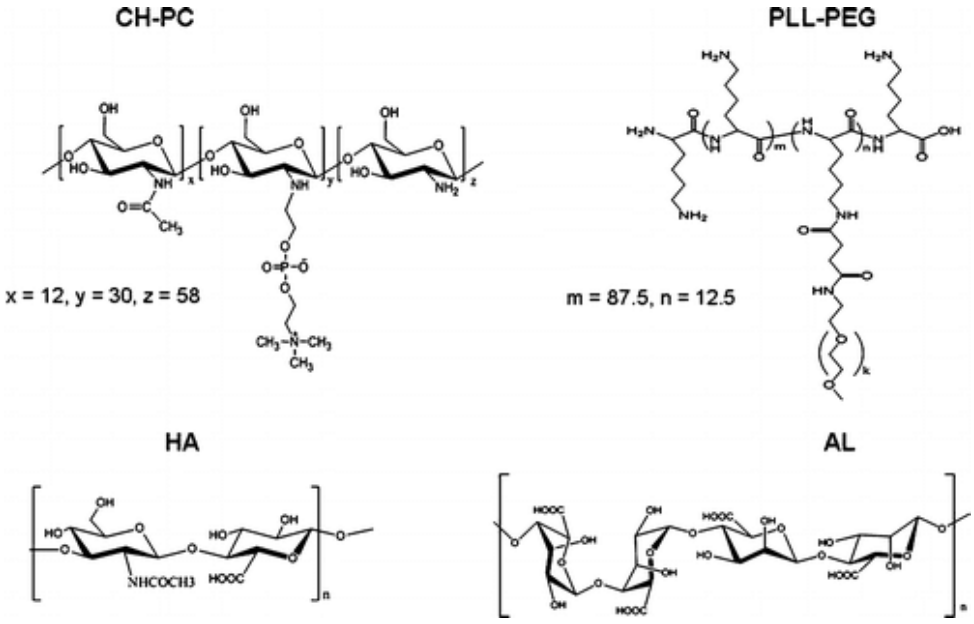

Figure 8.1. Structure of the polyelectrolytes used in this study.

In order to also achieve the membrane permeability required for cell nutrient and waste material exchanges, as well as to retain essential properties against blood group antibodies, a modular approach was adopted during the LbL assembly of the four polyelectrolytes as depicted in Figure 8.2 in the case of the 2-dimension (2-D) system used here. Since the main objective of the study was to fine-tune

the LbL construction on RBCs for immunocamouflage, non-fixed RBCs were deposited as a monolayer on a pre-treated substrate to induce cell adhesion. This allowed us to focus on the properties of the multilayer itself, without encountering aggregation difficulties associated with handling fragile RBCs in colloidal suspensions. Quartz crystal microbalance with the energy dissipation factor (QCM-D) was used to monitor in real time, each step of the multilayer build-up onto the non-fixed RBC monolayer and to assess the interactions of antibodies with coated cells. The QCM-D is frequently used as an immunoassay where antibodies were immobilized on the crystal for the detection of certain antigens.[239,240] Control experiments were carried out to characterize the build-up of the same multilayer on a solid substrate, in the absence of RBCs. ζ-potential measurements, atomic force microscopy (AFM) and Variable pressure scanning electron microscopy (VP-SEM) imaging were used for further physicochemical characterization of the 2-D system construct. The successful camouflage of the RBCs was shown by fluorescence microscopy using a fluorescently-labeled antibody. A hemolysis assay was then employed to compare the hemolytic effect of the antibody towards naked and coated RBCs and to determine the viability and integrity of coated RBCs.

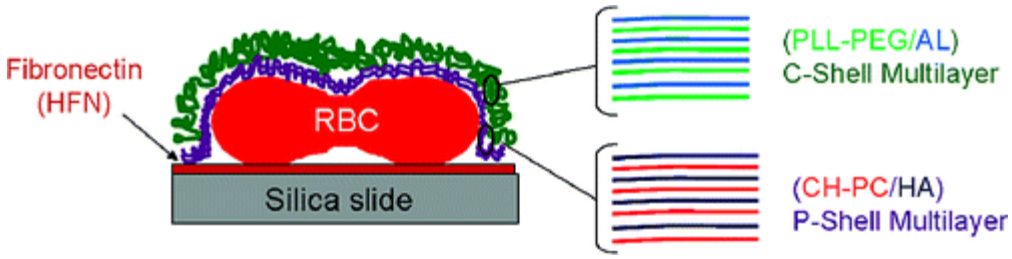

Figure 8.2. Schematic representation of the LbL build-up of P-shell (CH-PC/HA) and C-shell (PLL-PEG/AL) layers on RBC deposited on a HFN-silica surface.

8.3 Materials and Methods

8.3.1 Materials

All solutions were prepared using deionized water (ρ = 18 MΩ cm, Nanopure Diamond system, Barnstead International, Iowa, USA). The pH was maintained at 6.2 with a phosphate buffer saline (PBS) (0.01 M phosphate, 0.137 M NaCl, 0.027 M KCl) (Sigma-Aldrich, Oakville, Canada). Alginate (sodium salt, 250 cP), bovine serum albumin (BSA), Drabkin's reagent, glutaraldehyde, NaCl and sodium dodecyl sulfate (SDS) were purchased from Sigma-Aldrich (Oakville, Canada). Acid citrate dextrose was obtained from Baxter Corporation (Mississauga, Canada). Sodium hyaluronate (HA, MW = 235,000 g mol^{-1} as stated by the supplier) was purchased from Lifecore (Chaska, USA). Human fibronectin (HFN) was provided by Chemicon International (Temecula, USA). Poly-L-lysine (PLL) in the hydrobromide form, (MW 15,000 to 30,000 g mol^{-1}, polydispersity index; 1.1 to 1.5, as stated by the supplier) was purchased from Sigma-Aldrich. PLL-PEG was prepared using methoxy-terminated poly(ethylene glycol) (PEG, MW 2,000 g mol^{-1}) purchased from RAPP Polymere, (Germany). CH (degree of deacetylation (DDA) 88%, Mn = 75,000 g mol^{-1}, determined by gel permeation chromatography (GPC)[108] was

purchased from Fisher Scientific Inc (Pittsburgh, Canada). Phosphorylcholine modified CH (CH-PC) was prepared by reaction of CH with phosphorylcholine glyceraldehyde. The synthesis and characterization of the modified polyelectrolytes (PLL-PEG and CH-PC) are detailed in the supporting information. The grafting ratio (GR) is defined as the percentage of amine functions of PLL or CH modified by PEG and PC, respectively. It was 12.5 mol % for PLL-PEG and 30 mol % for CH-PC, as determined by ^{1}H NMR spectroscopy (see SI). Antibody anti-blood group A-FITC (fluorescein isothiocyanate) was provided by BD Biosciences (Mississauga, Canada). Hellmanex was purchased from Fisher Scientific Inc (Pittsburgh, Canada).

8.3.2 Red blood cell isolation

Blood samples were collected from healthy volunteers in accordance with the guidelines of the ethical committee of the Montreal Heart Institute. The blood withdrawn from the antecubital vein through a 19-gauge butterfly needle was collected in syringes containing acid citrate dextrose acting as an anticoagulant. The blood/acid citrate dextrose part ratio was 5/1. The collected blood was centrifuged at 3,000 rpm with the Beckmann Coulter centrifuge (Mississauga, Canada) for 15 min at room temperature. The plasma and the buffy coat were removed by aspiration. The RBCs were washed three times with a PBS buffer pH 7.4.

8.3.3 Polyelectrolytes multilayer assembly

Solutions for multilayer assembly (1.0 mg mL^{-1}) were prepared by dissolution of the polyelectrolytes, HA, AL, PLL-PEG and CH-PC, in aqueous PBS at pH 6.2.

They were filtered through 0.45 μm Millipore PVDF filters prior to use. A pH of 6.2 was used to increase the polymer charged amine group number of CH-PC. For all measurements the silica slides were cleaned by 30 min immersion, first in a Hellmanex solution (2%), second in aqueous sodium dodecyl sulfate (2%), followed by extensive rinses with deionised water. Before the addition of RBC suspension, the surfaces were treated with an HFN solution (50 μg mL^{-1}) that was left in contact with the substrate for 30 min.[241] After a rinsing step with PBS (pH 7.4), a suspension of RBCs (10 millions cells/mL) was placed in contact with the substrate cell for 2 hours. Silica wafers, or silica-coated quartz crystals for QCM-D measurements, were coated prior to RBCs monolayer deposition with HFN, a protein known to interact with RBCs via RGD moieties.[242] After the deposition, the substrates were rinsed with PBS buffer (pH 6.2). The first layer of positively charged CH-PC was assembled for 20 min and then rinsed extensively with PBS solution (pH 6.2). The resulting surface was left in contact with an aqueous solution of negatively charged HA for 20 min, followed by a rinsing step. After the deposition of $(CH\text{-}PC/HA)_5$ bilayers (refers here as P-shell which stand for permeable layer), $(PLL\text{-}PEG/AL)_5$ bilayers (refers here as C-shell which stand for camouflage layer) were assembled following the same protocol.

8.3.4 Zeta-potential measurements

The ξ-potential of the multilayers was determined with a Electrokinetic analyzer (Anton Paar, Austria) using HFN modified silica surfaces fitted onto a poly(methyl methacrylate) (PMMA) plate used as a support in the asymmetric

clamping cell. The clamping cell included Ag/AgCl electrodes and inlet/outlet tubing to introduce 10 mM NaCl solution into the rectangular channels of the PMMA plate. Prior to measurement, the system was flushed for 10 min with deionised water, after which the electrolyte (10 mM NaCl) was introduced in the cell and circulated for 20 min. Multilayer assembly was performed by sequential deposition of the polyelectrolytes following the protocol described above, starting with CH-PC. The ξ-potential of each layer was measured after rinsing with10 mM NaCl.

8.3.5 VP-SEM analyses

RBCs were deposited from a 10 million cells/mL suspension onto HFN-coated silica wafers as described above. The cells were left in contact with the substrate for 2 hrs at room temperature. After several rinsing step with PBS (pH 7.4), the RBCs were fixed by treatment with a solution of glutaraldehyde (1% w/w in PBS, pH 7.4) for 30 min. A multilayer assembly was performed onto fixed RBCs following the protocol described above. A Variable Pressure Scanning Electron Microscopy (VP-SEM) (Hitachi S-3000N, Schaumburg, USA) operated at 30 Pa, 15.0 kV and a magnification of 500x was used to image RBCs before and after polyelectrolyte self-assembly.

8.3.6 QCM-D measurements

A QCM-D D300 device (Q-Sense AB, Västra Frölunda, Sweden) at the fundamental resonance frequency of 5 MHz is employed. The changes in frequency (Δf) and energy dissipation factors (D) of the 3^{rd}, 5^{th}, and 7^{th} harmonics was recorded on silica-covered quartz crystals (QSX-303) at 24.00 ±

0.02 °C. The Q-Sense software (QSoft) was used to acquire the dissipation factor, *D*, via eq 8.1:

$$D = \frac{1}{\pi f \tau_0} = \frac{2}{\omega \tau} \qquad (8.1)$$

Where f is the resonance frequency, ω is the angular frequency, and τ_0 is the relaxation time constant. The data provided us with the information on the adsorption process as well as on the viscoelastic properties of the adsorbed film. In the case of homogeneous, very thin or quasi-rigid films, the frequency shift is proportional to the mass uptake per unit area, Δm_f, deduced from the Sauerbrey [144] equation (eq 8.2):

$$-\Delta f_{Sauerbrey} = \frac{1}{nC}\Delta m_f \qquad (8.2)$$

Where the mass sensitivity, C, is equal to 17.7 ng cm^{-2} Hz^{-1} at f = 5 MHz. In order to extend the Sauerbrey approximation, the f and D experimental data were analyzed by Voivona *et al* [145,146] model. In this model, it is hypothesized that the film is a homogeneous and isotropic viscoelastic layer. The Q-sense software (QTools) was then programmed to model the raw data.

For in-situ monitoring of the multilayer assembly onto non-fixed RBC, a silica-covered quartz crystal, cleaned in a UV-ozone chamber (Biofore Nanosciences, Inc, Ames, USA) during 10 min, was mounted in the QCM-D measurement chamber stabilized at 24.00 ± 0.02°C. It was then modified following the general protocol described above. For in-situ monitoring of the interaction of the antibody interaction with coated RBCs, an RBC-coated crystal prepared in-situ as described above was covered with the desired number of bilayers. A solution

of BSA (2% in PBS pH 7.4) was injected in the cell and left in contact with the coated RBCs for 30 min. The substrate was rinsed with PBS pH 7.4, after which an anti-A antibody solution was injected in the cell and the frequency and dissipation shifts were recorded during the adsorption steps. Control experiments carried out under identical conditions include: (a) treatment of uncoated RBCs with the anti-A antibody solution; (b) treatment of multilayers constructed onto an HFN-coated crystal in the absence of RBCs; in this case, the build-up was initiated with CH-PC.

8.3.7 AFM measurements

AFM measurements were performed in the tapping mode at ambient temperature with a Nanoscope IIIa (Veeco Instruments Ltd, Plainview, USA). Measurement were performed in a fluid cell filled with PBS buffer (pH 6.2) using 200 µm cantilevers having a spring constant of 0.06 N m^{-1} (NP, Veeco Instruments Ltd.). Areas of about 50 x 50 µm were scanned with a scan rate of 0.5 Hz (drive amplitude of 1−1.2 V). Holes were deliberately created in the films by repeatedly scanning a 10 μm^2 area of the film kept under the buffer solution after lowering the set point to nearly its minimum value (drive amplitude of 1−1.2 V) and increasing the scan speed to 30 Hz in the contact mode. The newly exposed area was then imaged by increasing the scan size to 225 μm^2 and returning to the normal imaging parameters. The thickness of the following assemblies was assessed: P-shell, P-shell + $(PLL\text{-}PEG/AL)_2$-PLL-PEG, and P-shell + C-shell.

8.3.8 Fluorescence microscopy imaging

Following the treatment of cleaned silica surfaces with a HFN solution for 30 min, the surfaces were placed in contact for 2 hr with a RBC suspension. Multilayer assembly was performed on the cell-coated slides at room temperature following the protocol described above in order to prepare the following samples: $(CH\text{-}PC/HA)_2$-CH-PC, P-shell, P-shell + $(PLL\text{-}PEG/AL)_2$-PLL-PEG and P-shell + C-shell. The samples were incubated with BSA (2% in PBS pH 7.4) for 30 min. Subsequently they were incubated for 1 hr with FITC-anti-A antibody (1 $\mu g\ mL^{-1}$ of BSA 2%) and washed with a PBS buffer pH 7.4 prior to imaging by fluorescence microscopy using a Nikon Eclipse TE2000U microscope (Melville, USA).

8.3.9 Antibody permeability assay

The following surfaces were prepared onto HFN coated clean silica slides following the procedure described above: uncoated RBC, RBC coated with: $(CH\text{-}PC/HA)_2$-CH-PC, P-shell, $(P\text{-}shell)_2$, P-shell + $(PLL\text{-}PEG/AL)_2$-PLL-PEG, and P-shell + C-shell. The substrates were incubated for 30 min with a solution of the anti-A antibody in PBS pH 7.4 (10 $\mu g\ mL^{-1}$). The solution was recovered delicately. It was centrifuged for 30 s at 11.750 g (Eppendorf, Mississauga, Canada) to remove any RBCs left in the solution. The supernatant (50 µL) was mixed with 1 mL of Drabkin's reagent for 15 min. The concentration of hemoglobin in the solution was determined by UV-Vis spectroscopy based on the solution absorbance at 540 nm with a µQuant spectrophotometer (Bio-Tek Instruments, Winooski, USA). To validate the results, the hemoglobin quantity

inside the remaining cells was also measured. After coating and washing steps with 5, 10, 15 and 20 layers, cells were lysed by dropping the pH to 5. The released hemoglobin was quantified by the Drabkin's reagent as mentioned above. The results were reported as the percentage of lysis as follow:

$$\frac{\text{Released hemoglobin in supernatant} \times 00}{\text{Total hemoglobin}} = \text{Percentage of lysis} \qquad (8.3)$$

8.3.10 Cell hemolysis assay

The uncoated RBCs, RBCs coated with $(CH\text{-}PC/HA)_2$-CH-PC, P-shell, P-shell + $(PLL\text{-}PEG/AL)_2$-PLL-PEG, or P-shell + C-shell were prepared onto HFN coated clean silica slides as described above. The released hemoglobin was quantified by the Drabkin's reagent as mentioned above. The results were reported as the percentage of lysis (eq. 8.3).

8.3.11 Statistical analysis

All experiments were carried out in triplicate and were repeated 3 times. Results are reported as the mean ± standard deviation.

8.4 Results and Discussion

8.4.1 Multilayer construction and characterization

The premise of this study was that immunocamouflage of RBCs is in effect when antibody recognition is prevented in cells having retained their integrity and functionality.[52,73,243] Before demonstrating the immunocamouflage of RBCs, it was important to characterize the multilayer growth mechanism, surface charge

and thickness. The multilayer build-up started with the deposition of positively charged CH-PC due to the surface pre-treatment with HFN. This protein, which has an isoelectric point (IEP) of 5, takes a negative charge at pH 6.2. ζ-potential measurements confirmed charge reversal upon sequential polyelectrolyte deposition (see supporting information). During the multilayer growth, the ξ-potential varied between +30 mV and -60 mV for the P-shell (5 CH-PC/HA bilayers), and between +50 mV and -50 mV for the C-shell (5 PLL-PEG/AL bilayers). The amplitude of the charge alternation indicated the stability of both LbL constructs. Next, the evolution of the surface coverage was recorded by QCM-D which showed the changes in frequency (3^{rd} overtone) and dissipation during the multilayer film (Figure 8.3).

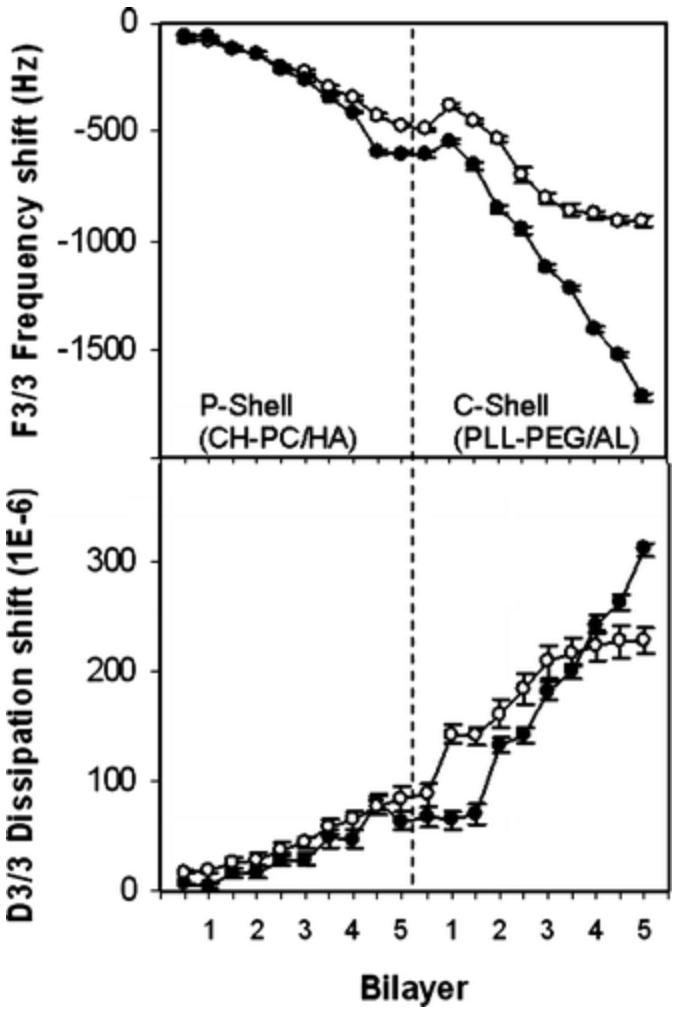

Figure 8.3. Evolution of frequency (a) and dissipation (b) shift of the LbL build-up of CH-PC, HA for bilayer 1 to bilayer 5 (P-shell) followed by the addition of PLL-PEG and AL from bilayer 1 to 5 (C-shell) on a RBC monolayer (open circle) and on a HFN-silica surface (full circle).

For QCM-D analysis, the identical procedure was performed on a HFN-coated substrate covered with a monolayer of non-fixed RBCs. The entire build-up process could be monitored *in-situ,* since the technique was sufficiently gentle to follow changes in frequency and dissipation during the multilayer construction onto RBCs (Figure 8.3). To facilitate comparison of data recorded in the absence and presence of RBCs, the frequency and dissipation shifts generated by the RBC monolayer were subtracted from the data. The presence of RBCs did not

affect markedly the changes in the frequency and dissipation upon construction of the P-shell. The growth of the C-shell on RBCs was, however, characterized by weaker changes in frequency and in dissipation, compared to their evolution on the flat and rigid HFN coated silica substrate. The decrease in adsorbed mass observed at the start of the C-shell assembly is due a very viscoelastic film that is taking place.

Frequency and dissipation shift values presented in Figure 8.3 have been modeled with QTools software in order to obtain the cumulative surface mass. This is accomplished by considering each polyelectrolyte layer as a separate homogeneous layer and by knowing cell number on the surface. The surface coverage by cells was analyzed using VP-SEM (Figure 8.5). After 2 hours, 10^7 RBCs/mL were adhered onto a surface area of 0.427 cm^2 out of a total 1 cm^2. By regarding each RBC as a disc with a mean diameter of 5 μm, the cell density on the surface was calculated to be 2.17×10^6 cells/cm^2. This allowed us to calculate the mass of hydrated polyelectrolytes for the P-shell and C-shell adsorbed on the RBCs (Figure 8.4). The cumulative mass of the P-shell and C-shell was in the order of 7090 ng.cm^2 and 8500 ng.cm^2, respectively. The CH-PC/HA layers are known to possess an exponential growth regime which cannot be detected here due to the low layer number.[244] This behavior was also correlated to the increase of deposited LbL film viscoelasticity. The addition of a viscoelastic mass often leads to increase in dissipation factor. The changes in frequency and dissipation were more pronounced during construction of the PLL-PEG/Al multilayer (C-shell), as compared to the CH-PC/HA construct (P-

shell).[245] As demonstrated in Figure 8.3, when AL is deposited as the first layer of C-shell (shown by charge reverse in the ζ-potential measurement as well, SI-Figure 8.5), an increase in both frequency and dissipation was observed, suggesting that the AL layer is more viscoelastic, thus giving rise to a more viscoelastic C-shell.

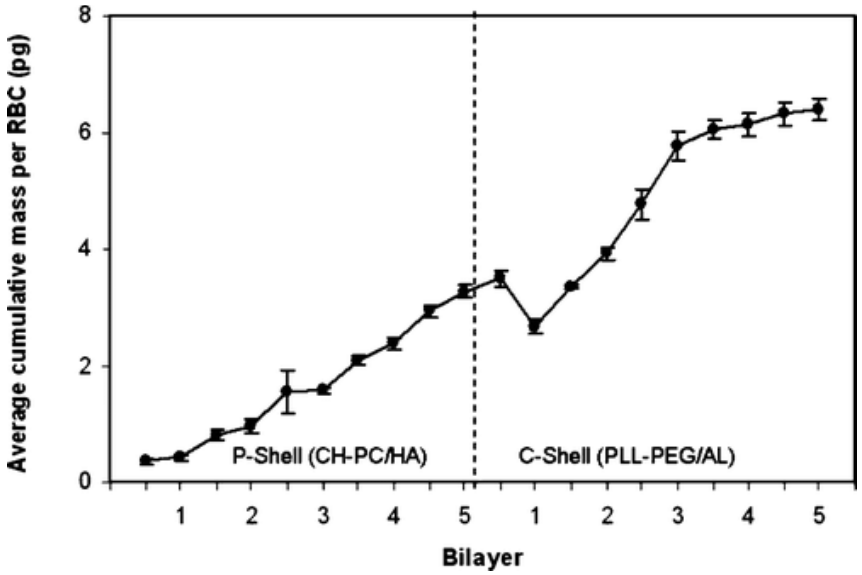

Figure 8.4. Average of the cumulative mass per RBC after the addition of CH-PC, HA, PLL-PEG and AL layers.

The thickness of the 5 $(CH\text{-}PC/HA)_5$ bilayers of the P-shell was 116 ± 47 nm, as measured by an AFM scratch test carried out on hydrated films. The thickness of the complete construct (P-shell + C-shell) reached a value of 1270 ± 344 nm, while an intermediate multilayer consisting of the P-shell + $(PLL\text{-}PEG/AL)_2$-PLL-PEG had a thickness of 574 ± 247 nm. One should notice that the values reported here for the film thickness are for the LbL construct without underneath RBCs monolayer due to the fragility of the RBCs. However, it is assumed that the growth regime and film thickness are not affected too much in the presence of underneath cell layer.[36] It is noticeable that the layer thickness measured by

AFM results is bigger than the one that can be calculated from QCM-D results. This resides in the limitations of these 2 techniques. Since the AFM measures the film roughness and will overestimate the film thickness especially in the case of viscoelastic films. Contrary to the AFM technique, the QCM-D is mainly based on mathematical models to calculate the films thickness and doesn't take into account the film roughness. In this case, the films thickness is underestimated.

8.4.2 Effect of multilayer permeability on viability and integrity of coated RBCs

The percentage of lysis was determined by measuring the hemoglobin released upon construction of the film bilayer on RBCs spectrophotometrically at 540 nm. The release of hemoglobin is recognized as indicative of hemolysis and cell death, since RBCs possess no nucleus and no organs and standard cell viability assays cannot be applied to them.[246] The ratio of released hemoglobin to total hemoglobin concentration indicated only 3% to 6% cells were lysed (Figure 8.6). The incubation of RBCs with PLL-PEG results in 67% of cell lysis. The use of CH-PC/HA as first ten layers is primordial for the protection of the RBC integrity. In addition, SEM imaging of an RBC monolayer before and after coating with the P-shell and C-shell showed that the cells had maintained their typical toroidal morphology during the entire treatment (Figure 8.5). More than 90% of the cells were intact and there was no significant difference in the percentage of cell lysis for cells coated with varying number of layers compared to uncoated cells. This demonstrates that LbL assembly did not interfere with the

viability and the integrity of RBCs. To test the assay' reliability, the pH is decreased to 5 to alter the multilayer permeability and force cell hemolysis. The permeability of the multilayer film was also assessed with a similar procedure through the diffusion of an anti-A antibody protein (150 kDa and ~ 14 nm in size), and then measuring the hemoglobin release. The concentration of anti-A antibody to induce hemolysis has to be higher than the concentration used for fluorescence microscopy. Otherwise with low antibody concentrations, hemolysis will not occur. As such, the hemolytic effect of the anti-A antibody on naked RBCs was 78%. It decreased to 20% for RBCs covered with a P-shell ((CH-PC /HA)$_5$ bilayers) and to 3% for RBCs covered with both the P-shell and the C-shell. Other cell lysis values, for intermediate number of layers are presented in Figure 8.6.

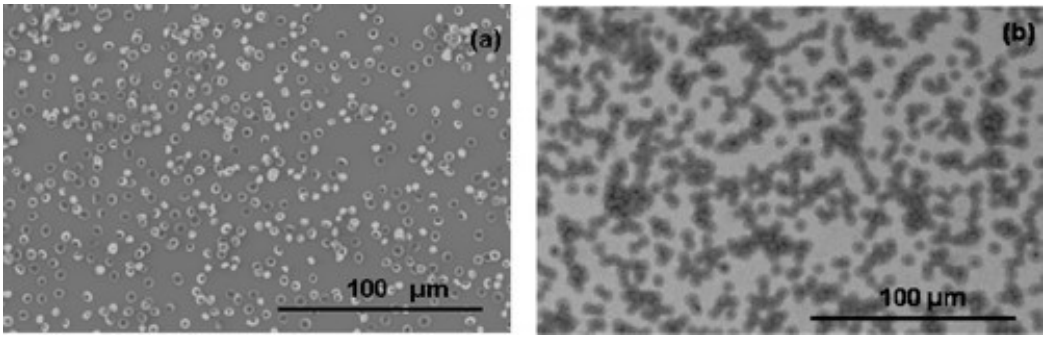

Figure 8.5. VP-SEM microphotographs of RBC on a HFN-silica surfaces (a) and coated RBCs with P-shell + C-shell on a HFN-silica surface (b). Conditions: 30 Pa, 15 kV, and magnification of 500×.

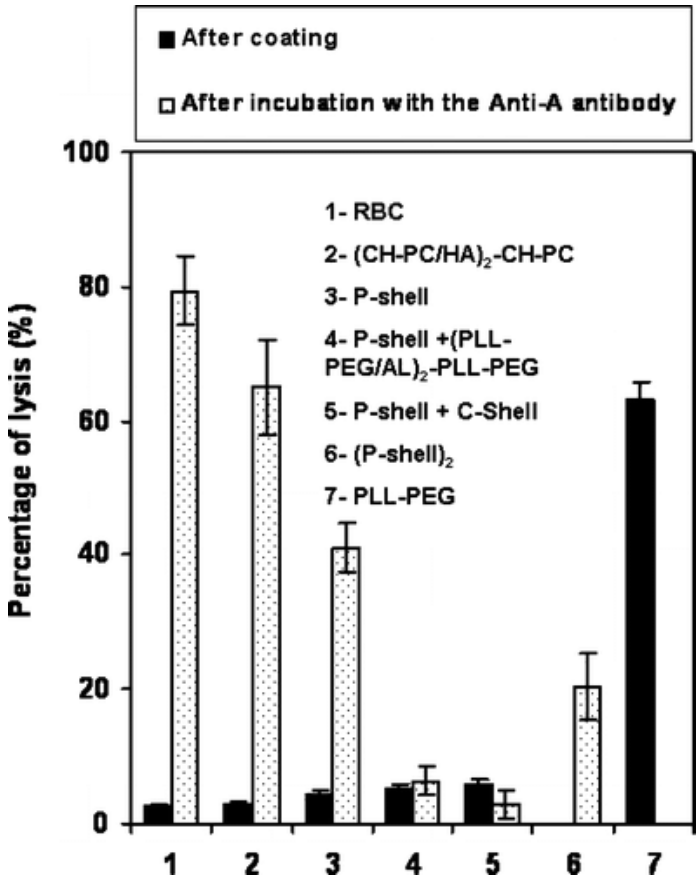

Figure 8.6. Percentage of lysis after coating and after incubation with anti-A antibody of the uncoated RBC (1) and coated RBC with (CH-PC/HA)2-CH-PC (2), P-Shell (3), P-shell + (PLL-PEG/AL)2-PLL-PEG (4), P-Shell+ C-Shell (5) (P-Shell)2 (6); after coating and after incubation with antibody anti-A. Values represent the mean ± SD of 3 experiments.

8.4.3 Kinetics of the interactions between anti-A antibody-coated RBCs and immunocamouflage

The *in situ* deposition of RBC monolayer on a HFN-modified quartz chip was monitored in the QCM-D flow chamber followed by the deposition of P-shell, and of P-shell + C-shell. Then, a buffered solution containing optimal anti-A antibody concentration flowed through the chamber after the desired number of polyelectrolyte layers, and the changes of frequency with time were monitored for 30 min (Figure 8.7). The optimal concentration of anti-A antibody has been predetermined as such to avoid cells lysis. Adsorption of anti-A antibody on

naked RBCs occurred very rapidly, as detected by an immediate increase in frequency which reached saturation level within 2 min. This behavior is typical of antigen/antibody recognition event. The kinetics of anti-A antibody adsorption onto coated RBCs were quite different. The protein/polyelectrolyte multilayer interaction was characterized by rapid adsorption followed by a slow equilibrium stage. This was multilayer composition- and surface charge-dependent.[247] Among the tested surfaces, the highest level of anti-A antibody sorption took place for RBCs covered with (CH-PC /HA)$_2$-CH-PC (5 layers). This was not expected, since anti-A antibody adsorption should be minimized on a surface of like-charge. Non-electrostatic interactions, referred to non specific adsorption, coupled to incomplete coverage of the RBC surface may be the driving forces of the protein sorption in this case. This is in agreement with previous report showing that a film with 5 layers of CH/HA forms small islets and do not have an uniform coverage of the surface.[105] The addition of more layers led to further decrease of frequency shift when anti-A antibody flows into the QCM chamber. Finally, no change in frequency can be detected upon injection of the anti-A antibody once the RBC monolayer coated with the complete P-shell + C-shell construct. These results indicated that this film effectively camouflages the RBC surface antigens from their environment.

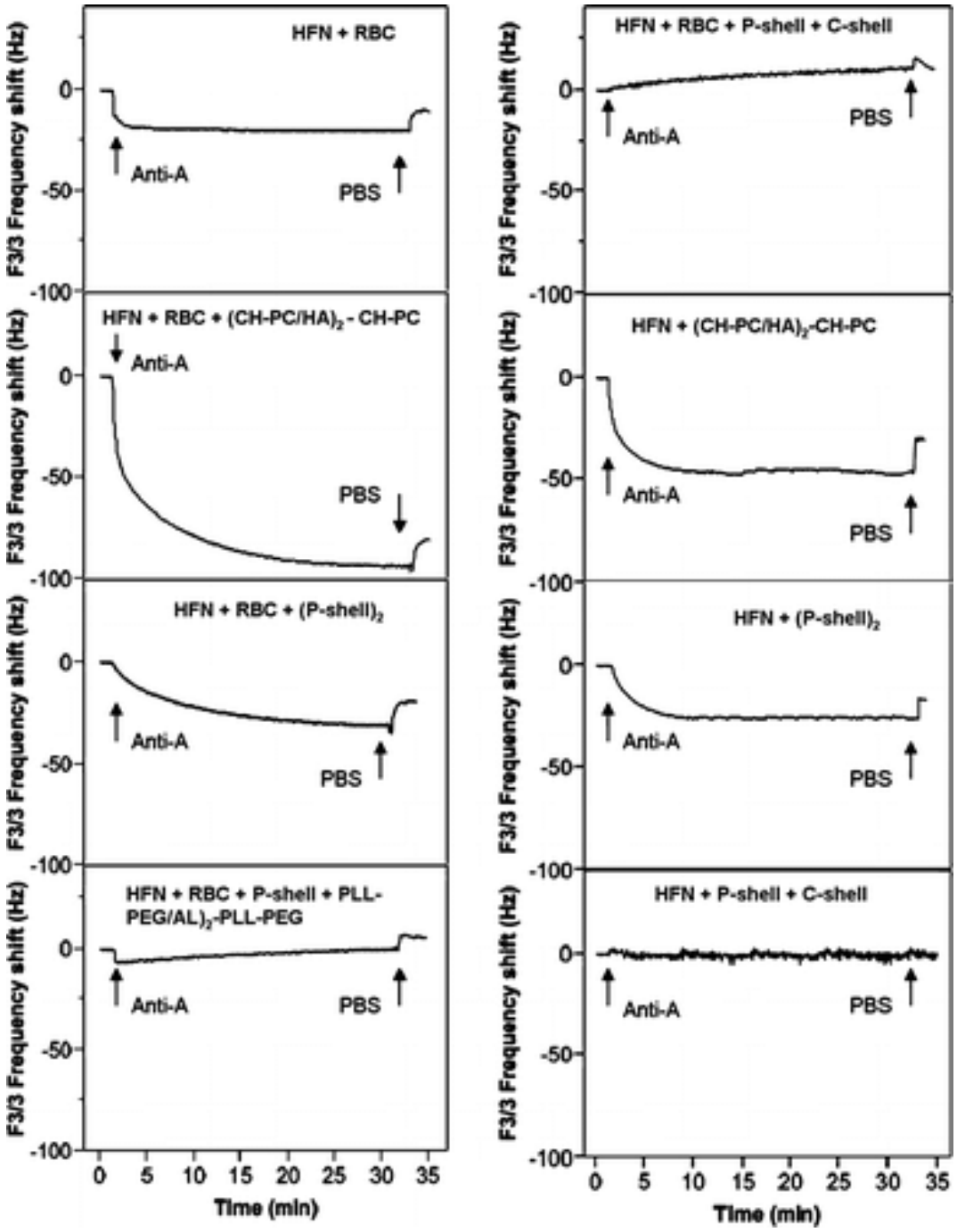

Figure 8.7. Frequency shift following the addition of antibody anti-A on RBCs monolayer; coated RBCs with $(CH\text{-}PC/HA)_2$-CH-PC; coated RBC with $(P\text{-}Shell)_2$; coated RBC with P-Shell + $(PLL\text{-}PEG/AL)_2$-PLL-PEG, coated RBC with P-Shell + C-shell; and on HFN-silica surface coated with $(CH\text{-}PC/HA)_2$-CH-PC, $(P\text{-}shell)_2$ and P-shell + C-shell.

Control experiments were conducted using HFN-coated crystal modified either with P-shell or C-shell in the absence of RBCs (Figure 8.7). The addition of the anti-A antibody to a P-shell construct triggered an increase in frequency. The increase in the signal can be due to non- specific interaction of the antibody and the multilayer on silica surface pre-treated with HFN. However, the signal increase was less important compared to the multilayer that is placed onto a RBC monolayer (see Figure 8.7). No protein adsorption was detected onto the C-shell construct indication no non-specific interactions took place between the anti-A antibody and C-shell.

The fluorescence intensity emission of FITC-anti-A antibody once coupled to antigens of RBC monolayer, compared to controls, was used to visually confirm the immunocamouflage event (Figure 8.8). In agreement with the QCM-D results, there was no detectable emission from the RBC monolayer coated with a P-shell + C-shell film (Figure 8.8b). Figures 8c, 8d and 8e present micrographs recorded upon treatment with FITC-anti-A antibody of an RBC monolayer coated with the $(P\text{-shell})_2$ and with intermediate layers construct. In these cases, the FITC green emission is observed, indicating that the antibody has interacted with antigens on the RBC surface. When the AL is replaced by HA (Figure 8.8f), interaction of the anti-A antibody with RBC antigens occurs indicating that the AL is a contributing factor in the camouflaging effect. It should be noted that this experiment could not be conducted with C-shell alone due to cell lysis with film composition (see Figure 8.6). However, to protect RBCs from antibody recognition, at least 10 layers of PLL-PEG/AL were necessary to tune the LbL

assembled shell permeability.[220,229] To be able to maintain the cell viability while having the desired permeability, in our design ten layers of CH-PC/HA (P-shell) formed the first shell and ten layers of PLL-PEG/AL (C-shell) formed the external shell. Several publications reported the same trends with different polyelectrolytes where the layer number and polyelectrolyte nature could modulate film permeability.[173,208,209,220,248] The polymer nature and layer number affect the multilayer thickness and thus the permeability.[199,208] These findings together with QCM-D measurements and AFM analyses showed that the antibody recognition by RBC antigens could successfully be prevented after the build-up of adequate combination of polyelectrolyte layers.

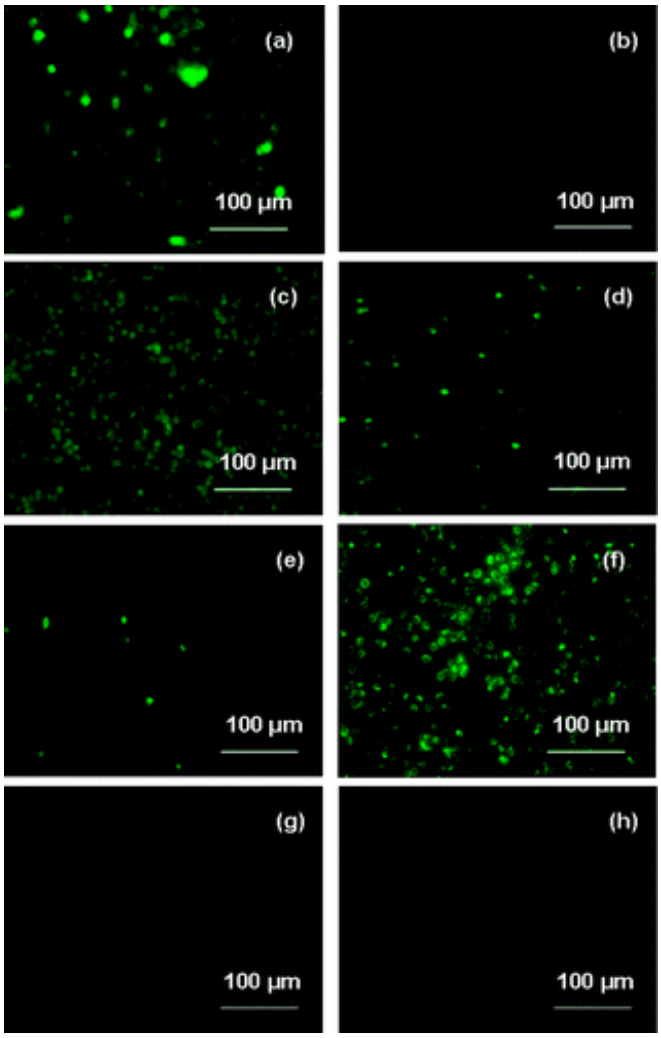

Figure 8.8. Fluorescence microscopy images. Uncoated and coated RBCs with different set of polymers were incubated with FITC-anti A antibody. Uncoated RBCs (a); RBCs coated with P-shell + C-shell (b); P-Shell (c); $(P\text{-shell})_2$ (d); P-shell + $(PLL\text{-}PEG\text{-}AL)_2$-PLL-PEG (e); $(CH\text{-}PC/HA)_5/(PLL\text{-}PEG\text{-}HA)_5$ (f); Positive control (RBC and no antibody) (g); negative control (P-shell+C-shell with no RBC and with addition of antibody anti-A) (h).

8.5 Conclusion

This research has demonstrated that LbL assembly of polyelectrolytes can be used as a mean to induce immunocamouflage of RBC antigens. The natural polyelectrolytes, CH-PC, HA, PLL-PEG and AL were successfully assembled in a well-designed multilayer system on non-fixed RBCs in a 2-D model through

the electrostatic LbL assembly technique. A systematic study of constructs formed by two pairs of oppositely charged biocompatible polyelectrolytes has been performed. The antibody recognition of the coated RBCs was assessed by QCM-D and fluorescence microscopy. By modulation of the LbL film composition and build-up conditions, such as incorporating the protein-repulsive polyelectrolyte PLL-PEG, adjusting the film thickness and the multilayer permeability, we successfully prevented cell recognition of the anti-A antibody, a particularly challenging task as it has been reported that A antigens are more difficult to mask than other minor groups.[48,60,64] The ABH system antigens possess variable length and are more extended than other antigen systems which increase their interactions with antibodies. It is expected that if the antigen A can be masked, the biorecognition of other antigens will be prevented as well. This approach may provide a low cost and effective technique towards the production of universal RBCs.

8.6 Acknowledgments

The authors thank Dr. Jean-François Théorêt for red blood cell purification, Dr. Nathalie Tufenkji for access to the electrokinetic analyzer for ζ-potential measurement and J. Daoud for editing this manuscript. This work is supported by Natural Sciences and Engineering Research Council of Canada-Discovery grant, the Canadian Institutes of Health Research-Regenerative Medicine and Nanomedicine grant and Fonds de la Recherche en Santé du Québec scholarship.

8.7 Supporting information

8.7.1 Polymer synthesis and characterization

8.7.1.1 Preparation of poly(L-lysine)-g-PEG (PLL-PEG)

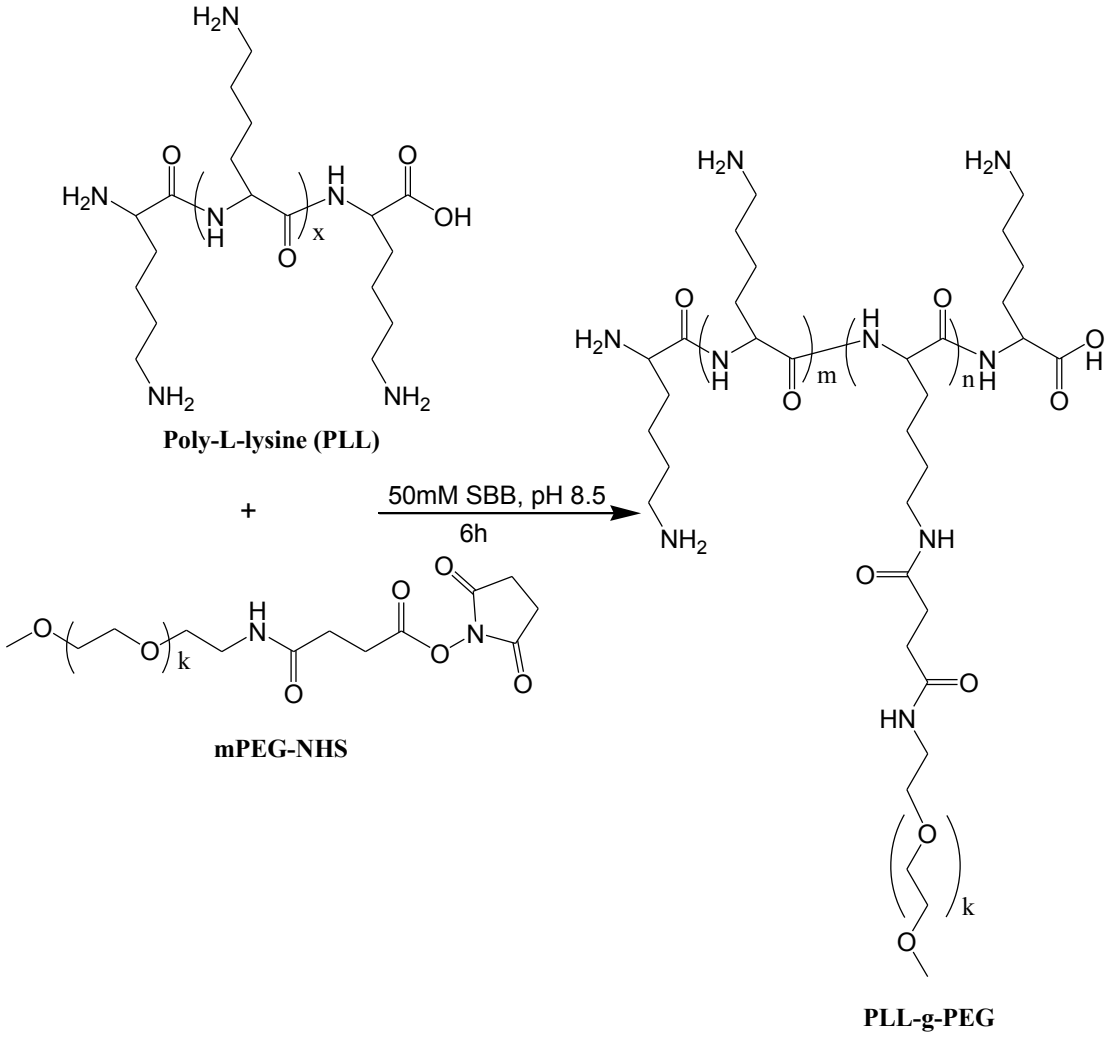

Figure 8.9. Synthesis procedure of PLL-g-PEG

PLL-PEG was synthesized from poly(L-lysine) hydrobromide (PLL-HBr) (Sigma, USA, molecular weight 15-30 kDa, polydispersity 1.1-1.5) and an *N*-hydroxysuccinimidyl ester of methoxy-terminated poly(ethylene glycol) (mPEG-NHS) (RAPP Polymere, Germany, molecular weight 2 kDa) following with

some modifications a reported procedure.[136] Poly(L-lysine) was dissolved in a 50 mM sodium borate buffer solution (pH 8.5) to get a polymer solution of 20 mg/mL. The solution was sterilized by filtration (0.22 μm pore size filter, Millex-GP). mPEG-NHS (1/4 eq. of lysine monomer units in PLL) was added to the solution. The reaction mixture was stirred for 6 h at room temperature. Subsequently, the reaction solution was dialyzed (Membrane of molecular weight cutoff size 6-8 kDa) against deionized water for 48 h, changing the water frequently. The product was freeze-dried and stored at -20 °C before use. The structure of PLL-PEG was confirmed by ^{1}H-NMR spectroscopy, using D_2O as a solvent on a 400-MHz Bruker instrument (ppm): 1.2-1.8 (-(CH_2)$_3$-, PLL side chain); 2.92 (-CH_2-NH_2, PLL side chain); 3.07 (-CH_2-NHCO-PEGm, 3.29 (-O-CH_3, end group of PEG); 3.4-3.8 (-O-CH_2-CH_2-O-, PEG); 4.24 (-NH-C*H*R-CO-, PLL backbone). The average grafting ratio (12.5 mol%, PEG : Lysine = 1 : 8) of the copolymer was calculated from the polymer ^{1}H NMR spectrum, taking the integration ratios of the peaks at 3.07 ppm, 2.92 ppm and 4.24 ppm.

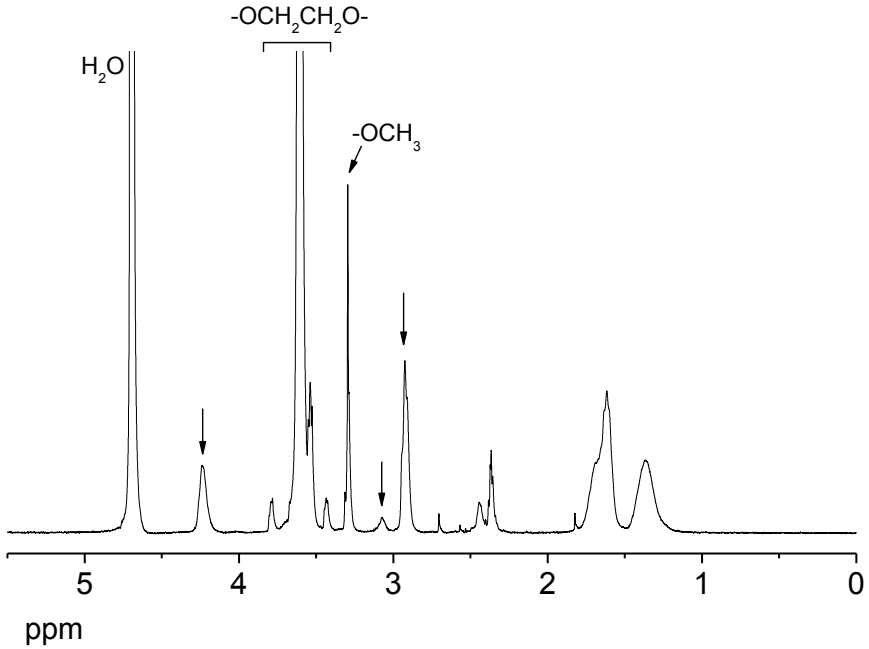

Figure 8.10. H NMR spectrum of PLL-g-PEG in D_2O at 25°C.

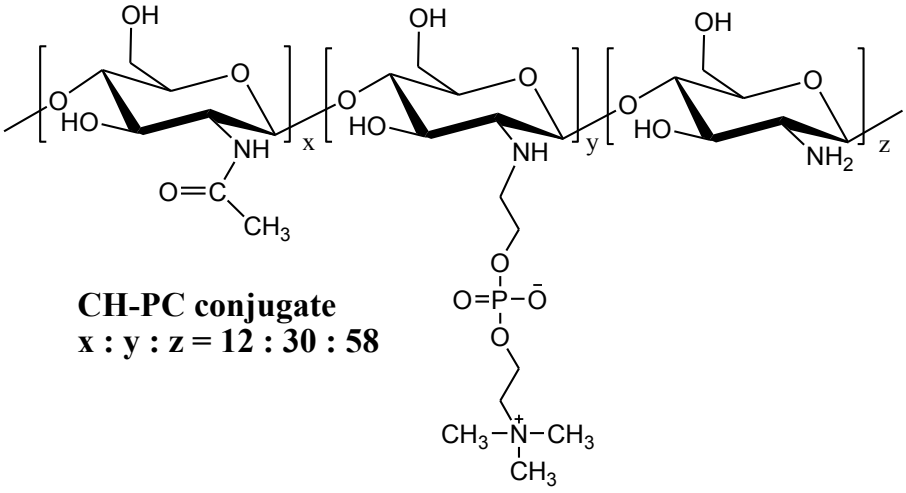

Figure 8.11. Structure of CH-PC conjugate.

8.7.1.2 Preparation of CH-PC conjugate

Chitosan with 30 mol% of grafted PC groups (PC : monosaccharide = 30 : 100) was prepared according to the previously reported procedure.[108] A solution of

PC-CHO (0.2 g, prepared according to the previously reported procedure[249]) in methanol (10 mL) was added dropwise to a solution of chitosan (0.5 g, DDA 88%, Mn 75,000 determined by GPC, MFisher scientific Inc) in aqueous acetic acid (25 mL, 1 wt %) kept at 0 °C. At the end of the addition, the solution was stirred for 30 min at 0 °C. The pH of the reaction mixture was then adjusted to 6.5 by adding aqueous NaOH (1.0 M). The reaction mixture was stirred for 1 h at room temperature, and then cooled to 0 °C, and a solution of sodium cyanoborohydride (0.4 g) in water (10 mL) was added dropwise under stirring. Thereafter, the reaction mixture was warmed to room temperature and stirred for 20 h. The reaction mixture was dialyzed (membrane of MWCO 12000-14000) first against water for 2 days, then against aqueous NaOH (0.05 M) for 1 day, and finally against water for 2 days again. The polymer CH-PC was isolated by lyophilization. The successful conjugation of PC groups to CH was confirmed by ^{1}H NMR spectroscopy (as shown in figure 4), in particular the shifts of the signals of the protons, which linked to C1 and C2 of CH monosaccharide, from 5.36 ppm (H1) to 5.50 ppm (H1s) and from 3.67 ppm (H2) to 3.80 ppm (H2s) respectively after the amine groups, which linked to C2, were substituted by PC groups, and the appearance of the typical signals from PC groups at 3.67 ppm (–$N(CH_3)_3$, overlapped with H2). PC content (30 mol%) was calculated from the integration ratios of the peaks at 5.50 ppm, 5.36 ppm and 2.51 ppm (Hac, -$CONHCH_3$): PC mol% = $I_{H1s}/(I_{H1s} + I_{H1} + I_{Hac}/3)$.

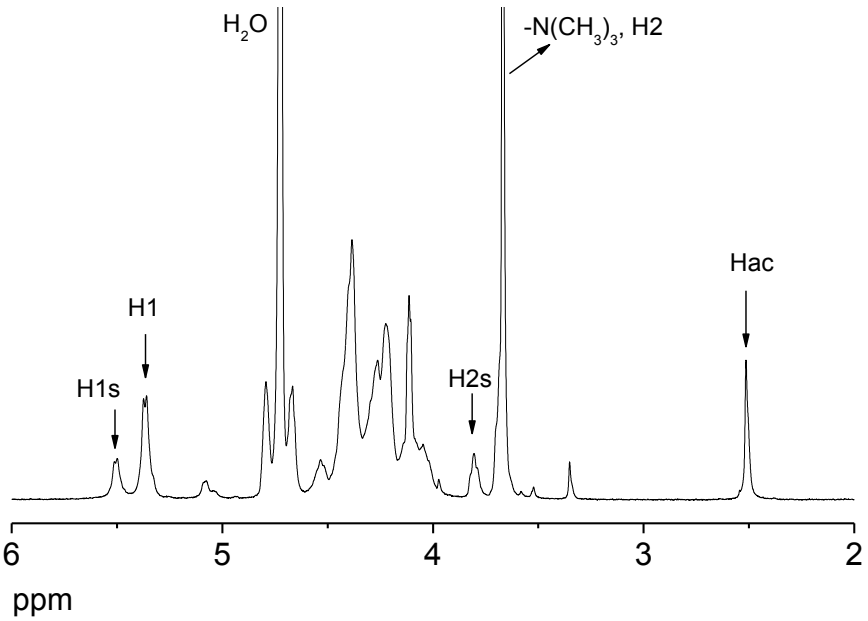

Figure 8.12. ^{1}H NMR spectrum of CH-PC conjugate in D_2O/35 wt% DCl (100/1, v/v) at 70 °C.

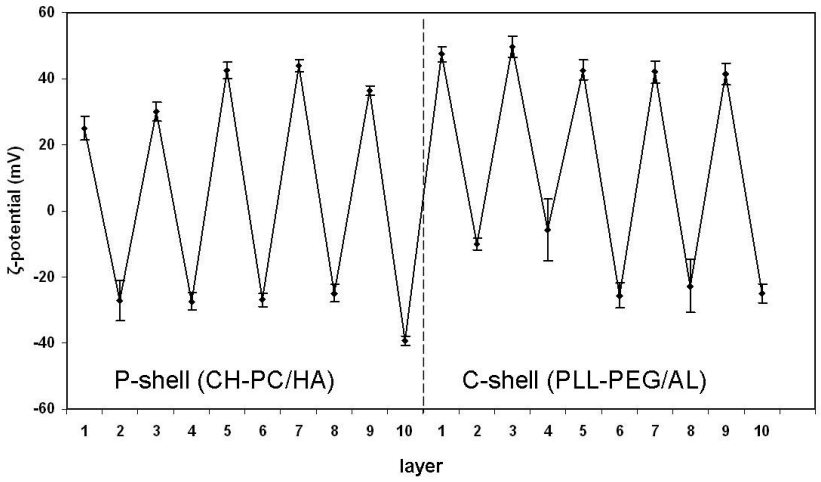

Figure 8.13. Zeta-potential as a function of layer number of the alternation between CH-PC, HA for layer 1 to layer 10 followed by the alternation between PLL-PEG and AL from layer 1 to 10 deposited on a HFN-silica surface.

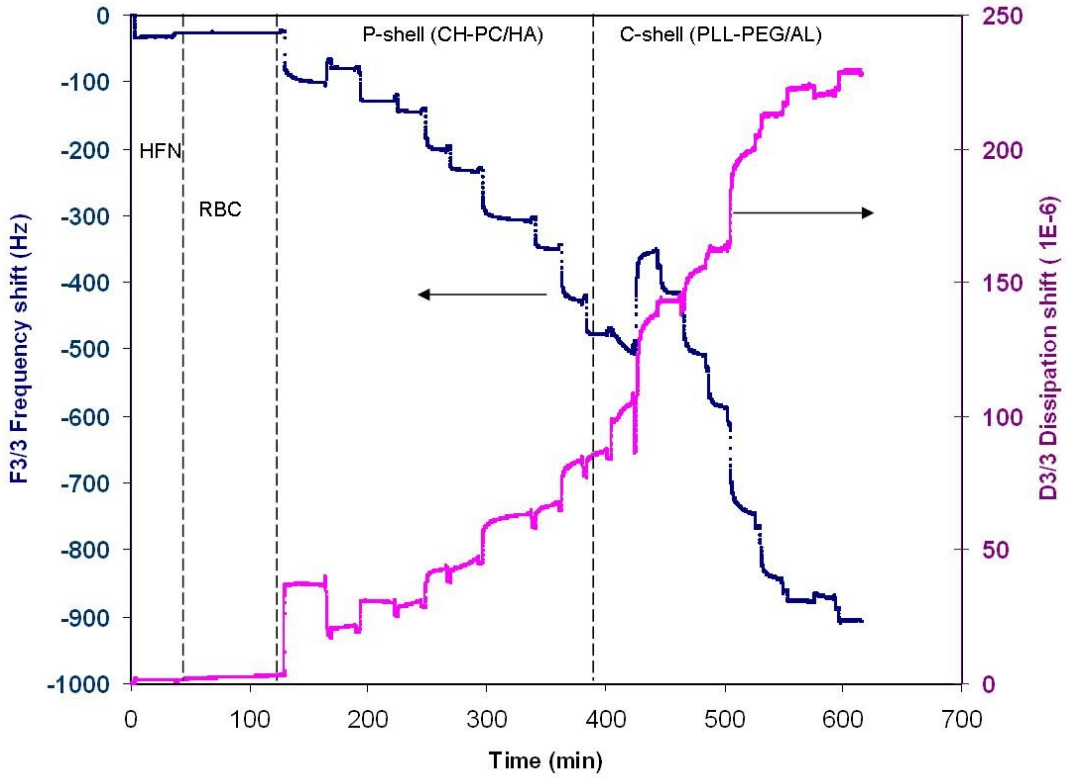

Figure 8.14. Evolution of frequency and dissipation shift of the LbL build-up of CH-PC/HA from bilayer 1 to bilayer 5 (P-shell) followed by the addition of PLL-PEG/AL from bilayer 1 to 5 (C-shell) on a RBC monolayer deposited on a HFN-silica surface.

CHAPTER 9: OPTIMIZATION AND CHARACTERIZATION OF COATED FUNCTIONAL RBCS IN SUSPENSION

Following the proof of concept of the immunocamouflage of coated RBCs in a two-dimensional model, this chapter presents the optimization and characterization of the LbL coating technique on RBCs maintained in a suspension. The results show that the functionality and viability as well as the immunocamouflage of the coated RBCs were maintained.

The results are presented in an article entitled "An Investigation of Layer-by-Layer Assembly of Polyelectrolytes on Fully Functional Human Red Blood Cells in Suspension for Attenuated Immune Response" presents the fulfillment of the second objective outlined in this theses and it has been accepted for publication in Biomacromolecules journal. (Manuscript ID: bm-2010-01200c.R1)

An Investigation of Layer-by-Layer Assembly of Polyelectrolytes on Fully Functional Human Red Blood Cells in Suspension for Attenuated Immune Response

Sania Mansouri[†], Yahye Merhi[§], Françoise M. Winnik[‡], Maryam Tabrizian[†,*]

[†]Department of Biomedical Engineering, [*]Faculty of Dentistry, McGill University, H3A 2B, [‡]Faculté de Pharmacie and Département de Chimie, Université de Montréal, H3C 3J7, and [§] Montreal Heart Institute, H1T 1C8, Montreal, Canada

*Corresponding author: Maryam Tabrizian: PhD, MBA; Associate Professor
Phone: +1- 514-398-8129
Fax: +1-514-398-7461
Email: maryam.tabrizian@mcgill.ca

9.1 Abstract

The encapsulation of live cells with polymeric coatings is a versatile approach to modulate or control the response cells to their environment. The layer-by-layer (LbL) self-assembly of non-immunogenic polyelectrolytes is employed here in order to attenuate or suppress the binding of antibodies to live red blood cells (RBCs) and, consequently, decrease their inherent immunogenicity towards foreign RBCs. The optimized shell was composed of 4 bilayers of alginate (AL) and chitosan-graft-phosphorylcholine (CH-PC) surrounded by 2 bilayers of AL and poly-L-lysine-graft-polyethylene glycol (PLL-PEG). Experimental parameters, including the polyelectrolytes and RBCs concentrations and the cell handling and purification protocols, were optimized to achieve effective encapsulation of live and functional RBCs in suspension. The viability and functionality of coated RBCs were confirmed by a hemolysis assay and by their ability to take up oxygen. The successful immunocamouflage of RBCs was

confirmed by observing that the recognition of the ABO/D (Rh) blood group antigens present on the surface of RBCs by their respective antibodies was muted in the case of coated RBCs. The results of this studies mark an important step towards the production of universal red blood cells.

Keywords: Layer-by-layer self-assembly technique, polyelectrolyte multilayer, coating of functionalized red blood cells, oxygen uptake and transport, immunocamouflage.

9.2 Introduction

Hemolysis and cross-type agglutination reactions caused by blood group mismatch during blood transfusion may lead to organs failure and patient death. The prevention of immunological rejection is performed by ABO/D (Rh) typing, since, among the 29 different antigenic systems on red blood cells (RBCs), the ABO group is the only system that possesses pre-existing antibodies.[16] Antibodies to the other antigen systems are developed after previous blood transfusion. RBC antigens A, B and H are located exclusively on the extracellular side of the lipid RBCs membrane, where they are carried on glycolipids which are intercalated between the phospholipids in the bilayer, with their long axes being perpendicular to the lipid bilayer[22] (Figure 9.1). Negatively charged scialic acid residues are present on glycolipids and are abundant on the RBCs outer surface.[9,34] Thus imparting a strong net negative charge to the cell surface. The negative charge reduces the interaction of the red blood cells with one another. RBCs lack nucleus, cellular organelles such as mitochondria, the

golgi apparatus and the endoplasmic reticulum. They cannot divide and have limited repair capabilities.[8] The ability to carry oxygen is one of the main functions of RBCs, in particular in case of medical transfusion.[9]

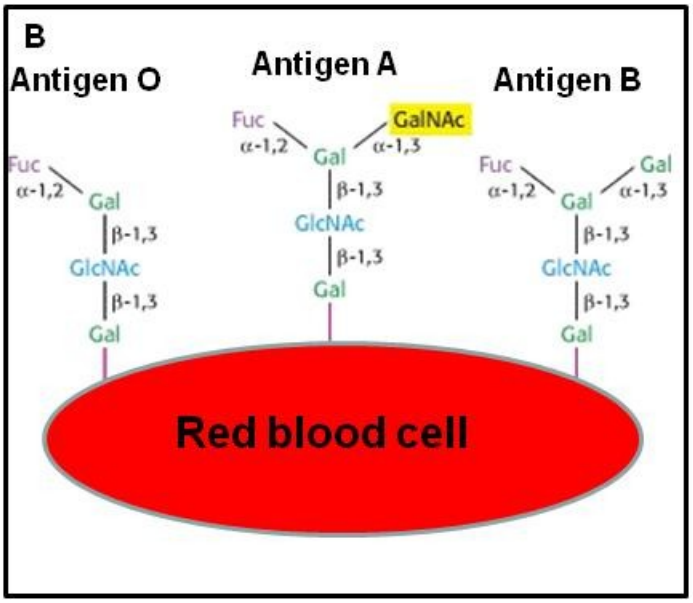

Figure 9.1. Structures of the ABO blood group Antigens. Abbreviations: Fuc: fucose; Gal:galactose; GalNAc: *N*-acetylgalactosamine.

Approaches for the production of a universal blood production, which would bypass tedious blood typing analysis and cross-matching, fall into three main categories: (1) the harvest and differentiation of stem cells, (2) the immunocamouflage of RBCs, and (3) the enzymatic removal of blood group antigens on live RBCs. The first strategy, which has been developed recently, relies on harvesting stem cells *ex-vivo* for universal blood production. The challenge here resides in the large scale production of the wanted blood cell line.[84,250] Cell immunocamouflage has been achieved by manipulating the cell membrane to prevent antibody recognition by concealing the antigenic epitopes

via membrane-grafted non-immunogenic molecules that are not recognized by the immune system.[48,73] This approach suppresses the inherent immunogenicity of the donor tissue itself, using means that are strictly physicochemical in nature and which do not rely on the details of the activation pathways, leaving the immune system of the recipient intact and fully competent. Partial immunocamouflage of RBCs has been achieved by grafting poly(ethylene glycol) on the RBCs' membrane.[54] Historically, the first technique explored for the production of universal RBCs involved the removal of the antigenic groups from the surface of RBCs using specific enzymes.[55,57] This required the use of hundreds of different enzymes specific to each antigen. While successful to a larger extent, the two last methods are not devoid of complications in patients who had previous transfusions.

We report here a new strategy for the immunocamouflage of RBCs that is based on the polyelectrolyte layer-by-layer (LbL) self-assembly technique.[148] This technique involves sequential adsorption of oppositely charged polyelectrolytes from dilute aqueous solutions onto RBCs suspended in aqueous suspension. The challenge resides in the encapsulation of functional and viable cells, which are fragile and very sensitive to their microenvironment. Several studies have demonstrated that it is possible to encapsulate viable cells by means of the LbL self-assembly technique. Yeast cells were encapsulated with poly(styrene sulfonate)/poly(allylamine) shells. *E-coli* were coated with sodium alginate and hyaluronic acid. Both cell types maintained their viability, functionality, and normal exchange of nutrient and waste.[167,251] Mouse mesenchymal stem cells

were encapsulated within polymeric shells consisting of hyaluronic acid and poly(L-lysine).[252] Platelet surfaces were also modified with LbL in order to decorate them with antibodies.[253] Pancreatic islets were coated with multilayers of poly(L-lysine)-*g*-poly(ethylene glycol)(biotin) and streptavidin without loss of viability nor function.[254] Mohwald *et al.* have exploited this technique to coat fixed RBCs as sacrificial template for the production of hollow capsules.[94] The fixation step was necessary to rigidify the cell membrane and maintain its integrity during the multilayer build-up under harsh conditions.

In a two-dimensional (2-D) model, we coated fully functionalized RBCs with a multilayered shell and demonstrated that the antigenic determinant recognition of coated RBCs was prevented by antibody anti-A. The multilayered shell was composed of a protecting shell (P-shell), containing five bilayers of chitosan-graft-phosphorylcholine (CH-PC) and hyaluronan (HA), covered by a camouflage shell (C-shell) made up of five bilayers of poly-L-lysine-graft-polyethylene glycol (PLL-PEG) and alginate (AL).[255] The present study reports the coating of non-fixed RBCs in suspension for the production of RBCs capable of maintaining their functionality and for which the antigenic determinants are camouflaged to prevent the immune system recognition. The polyelectrolytes sets were made of three non-toxic and biodegradable polyelectrolytes: AL, CH-PC and PLL-PEG (Figure 9.2). The anionic polymer AL, extracted from seaweed, is a copolymer consisting of β-D mannuronic acid and its C-5 epimer α-L-guluronic acid linked (1→4). Matrices formed from alginate were previously employed for pancreatic islet encapsulation.[235] They exhibited

extended longevity within the body and did not provoke immunogenic responses.[237,238] CH is obtained by deacetylation of chitin. It is a linear polysaccharide composed of β-D-glucosamine and β-D-*N*-acetylglucosamine linked (1→4). CH is not soluble under physiological conditions and cannot be used to camouflage the RBCs, we employed a derivative of CH grafted with a phosphorylcholine group (CH-PC), which is soluble in aqueous media of neutral pH.[108] Like CH itself, CH-PC with ~ 30 % mol PC groups/glucosamine units is able to form multilayers with AL.[244] In view of its biocompatibility, the second polycation was PLL grafted with poly(ethylene glycol) (PEG) to provide protein repulsive properties to the coating.[136]

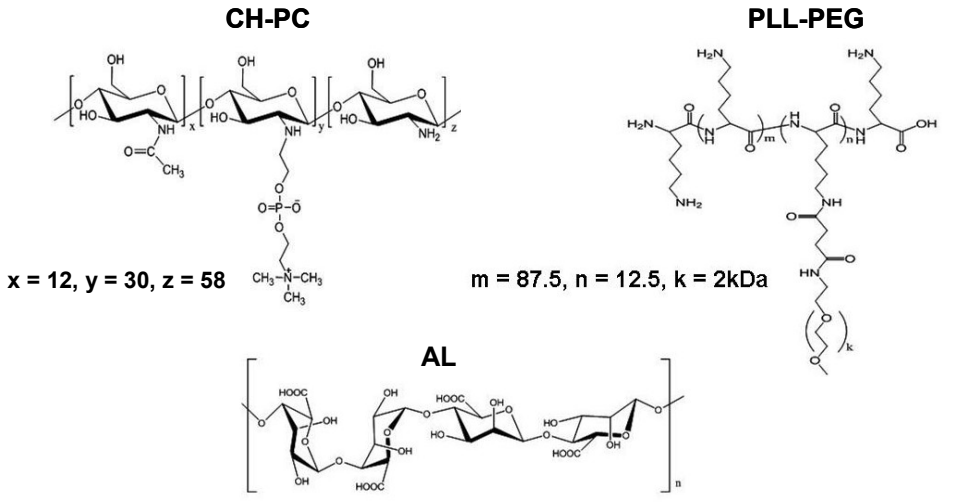

Figure 9.2. Chemical structures of the polyelectrolytes used for red blood cell encapsulation.

Polyelectrolytes self-assembly parameters, such as polyelectrolytes concentration, the amount of cells in suspension, and the rinsing method were varied to achieve optimized shell features and process yields Cell integrity was confirmed by optical microscopy after each layer deposition. Quartz crystal

microbalance with dissipation factor (QCM-D), zeta potential measurements, and transmission electron microscopy (TEM) were used to monitor multilayer build-up and to determine the final shell thickness. A hemolysis assay was performed to determine the viability and integrity of the coated RBCs. The functionality of RBCs before and after coating was assessed by measuring the oxygen uptake. Finally, the successful camouflage of RBCs was demonstrated by an agglutination assay.

9.3 Materials and methods

9.3.1 Materials

All solutions were prepared using deionized water (ρ = 18 MΩ cm^{-1}, Nanopure Diamond system, Barnstead International, Iowa, USA). The pH was maintained at 6.2 with a phosphate buffer saline (PBS) (0.01 M phosphate, 0.137 M NaCl, 0.027 M KCl) (Sigma-Aldrich, Oakville, Canada). Ultra pure Alginate (sodium salt MW 200,000-300,000 g mol^{-1}) from Novamatrix, (Norway) was a gift from Dr Alain Halle (Maisonneuve-Rosement Hospital, Montreal, Canada). Drabkin's reagent, glutaraldehyde, sodium cacodylate buffer, osmium tetroxide and epoxy (Epon) resin were purchased from Sigma-Aldrich (Oakville, Canada). Acid citrate dextrose was obtained from Baxter Corporation (Mississauga, Canada). Human fibronectin (HFN) was provided by Chemicon International (Temecula, USA). Poly-L-lysine (PLL) in the hydrobromide form, (MW 15,000 to 30,000 g mol^{-1}, polydispersity index; 1.1 to 1.5) was supplied by Sigma-Aldrich. PLL-PEG was prepared as previously described, using methoxy-terminated poly(ethylene glycol) (PEG, MW 2,000 g mol^{-1}) purchased from RAPP

Polymere, (Germany). CH (degree of deacetylation (DDA) 88%, Mn = 75,000 g mol^{-1}, determined by gel permeation chromatography (GPC) was obtained from Fisher Scientific Inc (Ottawa, Canada). Phosphorylcholine modified CH (CH-PC) was prepared by reaction of CH with phosphorylcholine glyceraldehydes as described previously.[108] The grafting ratio (GR), defined as the percentage of amine functions of PLL or CH modified by PEG and PC, respectively, was 12.5 mol % for PLL-PEG and 30 mol % for CH-PC, as determined by ^{1}H NMR spectroscopy. Anti-A, anti-B and anti-D (Rh) sera are from Carolina Biological Supply Company (Burlington, USA).

9.3.2 Preparation of RBCs samples

Blood samples were collected from healthy volunteers in accordance with the guidelines of the ethical committee of the Montreal Heart Institute. The blood withdrawn from the antecubital vein through a 19-gauge butterfly needle was collected in syringes containing acid citrate dextrose (Baxter Corporation, Mississauga, Canada) acting as an anticoagulant. The blood/acid citrate dextrose part ratio was 5/1. The collected blood was centrifuged at 3,000 rpm with the Beckmann Coulter centrifuge (Mississauga, Canada) for 15 min at room temperature. The plasma and the buffy coat were removed by aspiration. The RBCs were washed three times with a PBS buffer (10 mM, pH 7.4).

9.3.3 QCM-D measurements

A silica-covered quartz crystal (QSX-303), cleaned by treatment in a UV-ozone chamber (Biofore Nanosciences, Inc, Ames, USA) for 10 min, was mounted in the measurement chamber stabilized at 24.00 ± 0.02 ºC of a QCM-D D300

device (Biolin AB, Västra Frölunda, Sweden), operating at the fundamental resonance frequency of 5 MHz. Polyelectrolytes solutions (1.0 mg mL^{-1}) were prepared by dissolution of the AL, CH-PC and PLL-PEG, in aqueous PBS at pH 6.2. They were filtered through 0.45 µm Millipore PVDF filters prior to use. The silica surface was treated with an HFN solution (50 µg/mL) for 30 min[241] and rinsed with PBS (pH 7.4) after which a suspension of 10 millions RBCs/mL was injected. After 2 hours, the QCM-D cell was rinsed with PBS (pH 6.2) and a solution of AL was injected, kept for 10 min and rinsed again with PBS solution (pH 6.2). This protocol was repeated with the cationic CH-PC polyelectrolyte. The deposition steps were repeated until a coating of $(AL/CH\text{-}PC)_4$-$(AL/PLL\text{-}PEG)_2$/AL bilayers was achieved on the RBCs.

9.3.4 Investigation of RBCs aggregation

RBCs at a concentration of 10, 20, 50, 100 and 150 million cells/mL were incubated with CH-PC at a constant concentration of 1 mg mL^{-1} for 20 min under mild stirring. RBCs were examined under light microscope (Nikon Eclipse, NY, USA) and images were collected at 20x magnification. The concentration of free cells was calculated with a hematocytometer. The results are reported as the percentage of free cells as follow:

$$\frac{\text{number of free cells} \times 100}{\text{Total cells number before polymer addition}} = \text{Percentage of free cells} \qquad (9.1)$$

9.3.5 Polymers charge saturation assessment

RBCs were coated with several concentrations of CH-PC as first layer and AL as a second layer for the assessment of overcharge compensation. Briefly, 0, 0.005,

0.01, 0.250, 0.5, 0.75 and 1 mg°mL^{-1} of CH-PC or AL were incubated with 10 million cells/mL of RBCs for 10 min under mild stirring. The ξ-potential of the treated RBCs was determined with a ZetaPALS instrument (Brookhaven Instruments Corporation, USA).

9.3.6 Multilayer assembly on RBCs

Polyelectrolytes solutions (1.0 mg mL^{-1}) for multilayer assembly were prepared by dissolution of a polyelectrolyte in PBS (10 mM, pH 6.2). The solutions were filtered through 0.45 µm Millipore PVDF filters prior to use. After a rinsing step with PBS buffer (10 mM, pH 7.4), a suspension of 10 million RBCs/mL was treated with AL for 10 min. The resulting suspension was rinsed with a PBS solution at pH 6.2 using membrane filtration.[156] The RBCs/AL suspension was treated with CH-PC following the same protocol. This procedure was repeated with alternating polycation and polyanion solution until a coating made of [(AL/CH-PC)$_4$-(AL/PLL-PEG)$_2$-AL] was achieved on RBCs.

9.3.7 Transmission electron microscopy

A JEOL JEM-2000-FX transmission electron microscope (TEM) operated at 80 kV and the JEOL JEM-2100F field emission TEM (FE-TEM) operated at 200 kV was used for imaging. RBC were fixed with 2.5% glutaraldehyde in 0.01 M PBS buffer (pH 6.2), washed with sodium cacodylate buffer, and treated with 1% osmium tetroxide. The fixed samples were dehydrated through a graded series of ethanol/water solutions (from 30 to 100%). They were embedded in epoxy (Epon) resin. Serial, ultrathin sections were cut with a diamond knife using a Reichert-Jung Ultracut E ultramicrotome. The sections were transferred

onto copper TEM grids, conventionally stained with uranyl acetate and lead citrate, prior to imaging.

9.3.8 Optical microscopy analysis

RBCs were examined before and after LbL coating, under light microscope (Nikon Eclipse, Melville, USA). Images were collected at 20x magnification.

9.3.9 Cell hemolysis assay

After coating with every layer, RBCs were centrifuged for 7 s at 11,750 *g* (Eppendorf, Mississauga, Canada) and the supernatant (50 µl) was treated with Drabkin's reagent (1 ml) for 15 min. The amount of leaked hemoglobin in the supernatant was determined by UV-Vis spectroscopy based on the solution absorbance at 540 nm with a µQuant spectrophotometer (Bio-Tek Instruments, Winooski, USA). To validate the results, the hemoglobin amount inside the remaining cells was also measured as follow. Coated cells with every layer were lysed by dropping the pH to 5. The released hemoglobin was quantified by the Drabkin's reagent as mentioned above. The results were reported as the percentage of lysis as follow:

$$\frac{\text{Released hemoglobin in supernatant} \times 00}{\text{Total hemoglobin}} = \text{Percentage of lysis} \qquad (9.2)$$

The reported result is the average per coated layer of the released hemoglobin for a total of 13 layers made of $[(AL/CH\text{-}PC)_4/(AL/PLL\text{-}PEG)_2/AL]$.

9.3.10 Adenosine 5'-triphosphate assay

After coating with every layer, RBCs were centrifuged for 7 s at 11,750 *g*, and the supernatant (100 µL) was removed and quantified by the adenosine 5'-triphosphate (ATP) bioluminescent luciferase assay as described by the manufacturer (Biovision, California, USA). Briefly, ATP mix solution (100 µL) was added to samples (100 µL) and the solution was allowed to stand for 3 min before reading the amount of light produced by a Luminoskan Ascent luminometer (Thermo Labsystems, Franklin, USA). To validate the results, the ATP quantity inside the remaining cells was also measured. Coated cells with every layer were lysed by dropping the pH to 5. The released ATP was quantified by the bioluminescent luciferase assay by measuring the emitted light. The results are reported as the percentage of ATP found in the supernatant.

$$\frac{\text{Released ATP in supernatant} \times 00}{\text{Total ATP}} = \text{Percentage of released ATP} \qquad (9.3)$$

The reported result is the average per coated layer of the released ATP for a total of 13 layers made of $[(AL/CH\text{-}PC)_4/(AL/PLL\text{-}PEG)_2/AL]$.

9.3.11 Oxygen uptake measurement

The decrease of the dissolved oxygen was monitored in real-time by ArrowLabb™ plotting system (Lazar research, Los Angeles, USA) consisting of the DO-166MT-1SXS (Lazar research, Los Angeles, USA) electrode calibrated in air at 21% of oxygen. The electrode was immersed in a tube containing a 10 mL PBS solution (10 mM, pH 6.2) which was purged with oxygen to reach a

percentage of dissolved oxygen around 50%. The PBS solution was then transferred into two equal parts in new sealed tubes where the electrode was immersed in the tube and the concentration of the dissolved oxygen was recorded. After 2 min, a suspension of either uncoated or coated RBCs with $[(AL/CH\text{-}PC)_4/(AL/PLL\text{-}PEG)_2/AL]$ (0.1 mL, 500 x 10^6 cells) was added to the oxygenated PBS solution (5 mL). The oxygen concentration was then recorded until the signal stabilized.

9.3.12 Agglutination assay

RBC coated with 13 layers $[(AL/CH\text{-}PC)_4/(AL/PLL\text{-}PEG)_2/AL]$ were tested for blockage of the blood group antigens by the standard blood typing test with antibodies against antigens that includes A, B and D (Rh). The agglutination was evaluated by visualization under light microscope (Nikon Eclipse, Melville, USA)

9.3.13 Statistical analysis

All experiments were repeated three times and carried out in triplicate. Results are reported as the mean ± standard deviation.

9.4 Results and discussion

9.4.1 RBCs encapsulation and characterization

Based on our previous study of LbL construction on live RBCs adhered to a human fibronectin (HFN) coated substrate, we set up to coat RBCs maintained in suspension with two sets of polyelectrolyte pairs, first (CH-PC/HA) and, second, PLL-PEG/AL). However, it quickly became apparent that HA could not be used,

since it induced irreversible cell aggregation. Thus, it was necessary to redesign the protective polyelectrolyte shell and to replace HA to build the protecting-shell (P-shell).[255] AL was chosen in view of its chemical similarity with HA and its non-toxic, biocompatible characteristics. To establish the suitability of AL in LbL assembly on live RBCs, we was monitored by QCM-D, using a HFN-coated substrate on which a monolayer of RBCs was adhered, the layer build-up of AL/CH-PC as innermost layer, followed by 2 bilayers of AL/PLL-PEG and topped by a layer of AL. Monitoring the frequency and dissipation shifts confirmed the successful LbL construction on the RBCs monolayer with both HA and AL for the formation of $[(AL/CH\text{-}PC)_4\text{-}(AL/PLL\text{-}PEG)_2\text{-}AL]$ or $[(HA/CH\text{-}PC)_4\text{-}(AL/PLL\text{-}PEG)_2\text{-}AL]$ films (Figure 9.3). Larger frequency and dissipation shifts were observed in the case of an AL/CH-PC multilayer, compared to HA/CH-PC, indicating the formation of a thicker and more viscoelastic shell on RBCs in comparison to HA/CH-PC.[256] Having demonstrated that multilayer build-up with AL, instead of HA, is possible and leads to hydrogel-like coatings, we set about to pursue our main goal and to perform the LbL construction on live RBCs in suspension. Since the gel-like films are generally preferred over stiff films for a multilayer build-up on functional cells where the cell membrane is continuously in movement, the inescapable polyanion substitution turned out to be an asset.[101,105]

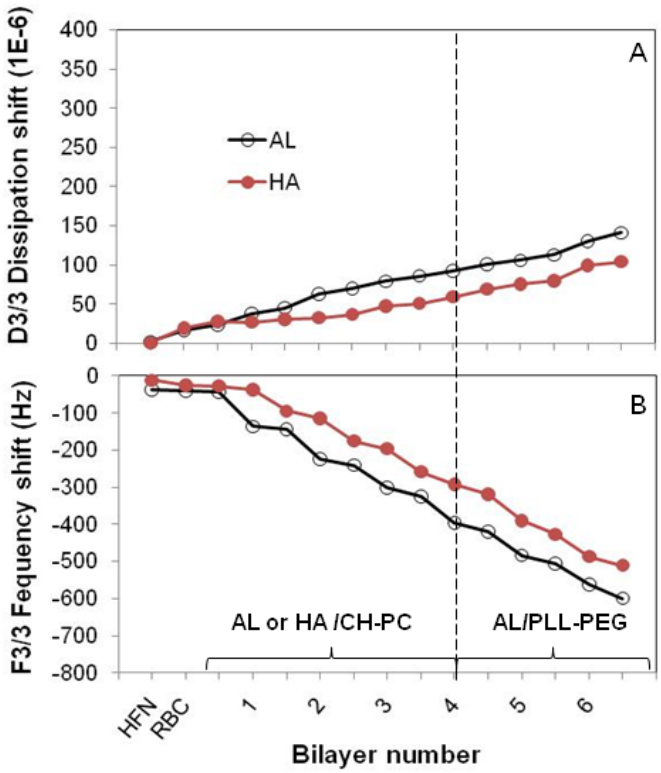

Figure 9.3. Evolution of dissipation and frequency shifts during the LbL build-up of AL (open circle) or HA (full circle) and CH-PC for bilayer 1 to layer 4 followed by the alternation between AL and PLL-PEG from bilayer 5 to 6 on RBCs' surface.

9.4.2 Coating live RBCs in suspension

During the LbL self-assembly, the average distance between the cells, which is governed by their concentration in suspension, by the ionic strength of the medium, and by the nature of the polyelectrolytes, plays a major role in cell aggregation, which must be avoided at all cost since it induces cell lysis and dramatically decreases the yield of cell encapsulation. The distance between particles (or cells) was adjusted by optimizing cell concentration. Figure 9.4 shows the percentage of non-aggregated cells along with the corresponding optical microscopy images of incubated RBCs for different concentrations of

CH-PC, which was determined by the percentage of non-aggregated cells after the addition of CH-PC. The least degree of RBCs aggregation, ~ 95% non aggregated cells, occurred in the case of manipulations carried out with a RBC concentration of 10 million cells/mL. As the RBCs concentration increased, the aggregation was more pronounced.

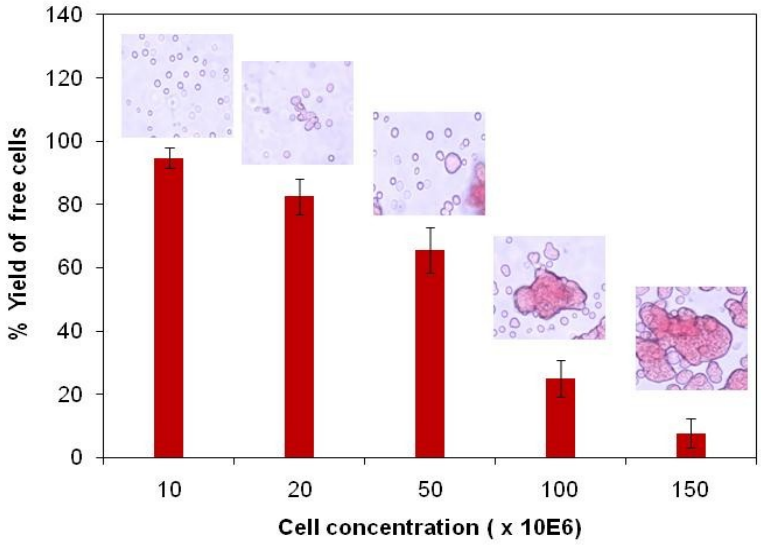

Figure 9.4. Percentage of none-aggregated cells along with the corresponding optical microscopy images of incubated RBCs at different concentrations of CH-PC.

Once the optimum RBC concentration was determined, it was important to find the concentration of the polymer required to induce overcharging after the first coated layer. Schneider and Decher found that there is one distinct regime in terms of charge stoichiometry between particles and polyelectrolytes for which aggregation tends to decrease.[257] Figure 9.5 shows the ζ-potential of coated RBCs with different concentrations of CH-PC and AL. At a concentration of 0.1 mg mL^{-1} of CH-PC as the first layer, an overcompensation charge was reached. The charge overcompensation was found to be the same for AL used

for building of the subsequent layer. The concentration of CH-PC, AL and PLL-PEG was therefore set at 1 mg mL^{-1} to insure polymer excess when incubated with RBCs at a concentration of 10 million cells/mL.

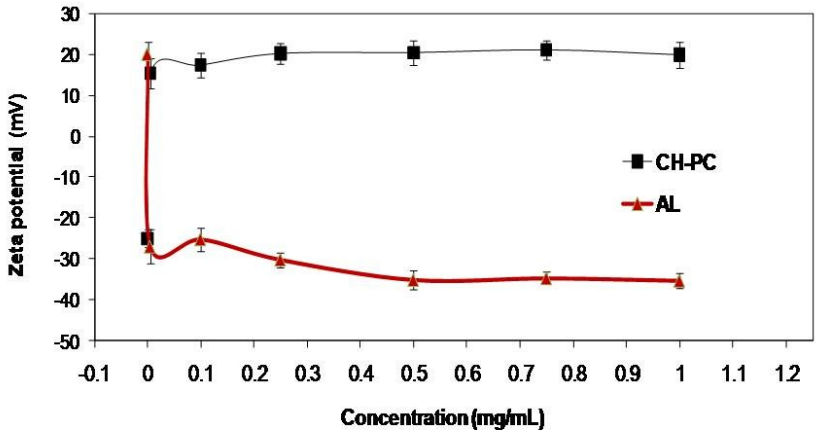

Figure 9.5. Zeta potential of coated RBCs with different concentrations of CH-PC and AL.

Since the LbL process is based on the alternating deposition of oppositely charged polyelectrolytes, following the deposition of each polyelectrolyte, the suspension is left in the presence of a large excess of polyelectrolyte chains that has to be removed prior to the adsorption of the following layer.[148] Therefore, a rinsing step is required to remove the free polyelectrolyte from the suspension and to avoid flocculation and coagulation. This purification step was very challenging, given the inherent fragility of RBCs and their sensitive to slight environmental changes. The most effective removal of polyelectrolyte excess was achieved by using a membrane filtration method with a continuous flow of PBS buffer throughout the filtration.[156] This procedure maintained the RBCs in suspension and ascertained the maintenance of RBCs integrity. It also led to a significantly decrease of cell aggregation and flocculation compared to the

purification by centrifugation. The observation of the cells under light microscope confirmed the absence of cell aggregation. The morphology of the cells was preserved upon LbL construction of $[(AL/CH\text{-}PC)_4\text{-}(AL/PLL\text{-}PEG)_2\text{-}AL]$ shell, as seen by comparin optical micrographs of bare and coated RBCs (Figure 9.6). The ratio of the released hemoglobin to total hemoglobin concentration calculated by measuring the changes in the absorbance at 540 nm indicated negligible level of cell lysis (about 3.4%) after each coating step (Figure 9.6).

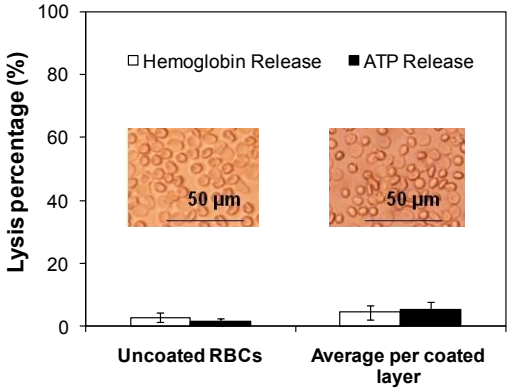

Figure 9.6. Percentage of lysis (released hemoglobin or released ATP) of uncoated RBCs and the average of lysis per coated layer. Optical microscopy images corresponding to uncoated cells and coated cells with $[(AL/CH\text{-}PC)_5\text{-}(A/PLL\text{-}PEG)_2\text{-}AL]$.

The successful build up of LbL assembly was followed by ζ-potential measurements. Sequential polyelectrolyte deposition was confirmed by charge reversal upon deposition of each layer. Initial polyelectrolyte deposition with negatively charged AL ensured homogenous dispersion of negative charge on RBCs, given that the RBC membrane possessed a total charge of around -

25 mV. Following the addition of the AL layer, the ζ-potential reached a value of - 30 mV. During multilayer growth, the ξ-potential varied between - 30 mV and + 10 mV (See supporting information). The charge of coated RBCs with a total of 13 layers containing [(AL/CH-PC)$_4$-(AL/PLL-PEG)$_2$-AL] was -25 mV, a value in the same range as the charge of uncoated RBCs. Preserving the overall negative charge of RBC upon coating is of critical importance in order to prevent undesirable and potentially catastrophic interactions of RBCs with other biological substances in the bloodstream.

Visualization of uncoated and coated RBCs with [(AL/CH-PC)$_4$-(AL/PLL-PEG)$_2$-AL] was performed by TEM (Figure 9.7). The TEM micrograph showed the complete coverage of the RBCs membrane by the multilayered shell, while preserving the initial morphology. The film thickness evaluated from the TEM micrographs was ~ 300 nm. This thickness is consistent with the value reported for similar multilayers coated on solid flat substrates determined by a scratch test using atomic force microscopy (574 ± 247 nm for [(CH-PC/HA)$_5$-(PLL-PEG/AL)$_2$/PLL-PEG)].[255] The deposition of this thin and spongy multilayer was assumed not to affect significantly the physical and mechanical properties of the coated RBCs since the average diameter of a normal RBC ranges between 6 and 8 μm.

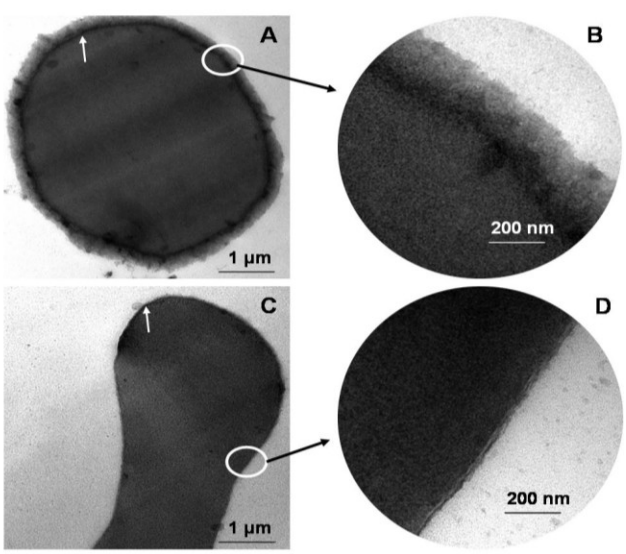

Figure 9.7. TEM images of: A) coated RBC with $[(AL/CH\text{-}PC)_4\text{-}(AL/PLL\text{-}PEG)_2\text{-}AL]$, C) uncoated RBC, B) Higher magnification of the circled area in (A) and D) Higher magnification of the circled area in (C). White arrows point to the cell membrane.

9.4.3 Viability and functionality of coated RBCs

To determine the RBC viability, we determined the percentage of released ATP upon construction of $[(CH\text{-}PC/HA)_5\text{-}(PLL\text{-}PEG/AL)_2/PLL\text{-}PEG]$ layers on RBCs using a bioluminescence assay. RBCs contain millimolar (mM) quantities of ATP produced primarily by membrane-bound glycolytic pathways within circulating RBC. The function of this large pool of ATP is generally considered to be a source for the metabolic energy required for the maintenance of cellular homeostasis and deformability. The ratio of released ATP to total ATP concentration indicated that only 4.9% of cells were lysed after deposition of a polyelectrolyte layer (Figure 9.6). A control group comprised of normal cells subjected to the same manipulations but without polyelectrolyte, exhibited an ATP release of 6%. This difference was not significant and most probably was

due to cell membrane damage and cell death during the multiple rinsing steps performed throughout the LbL build-up.

Since the essential function of RBCs in the body is to transport oxygen, it was critical to confirm that the LbL shell was permeable to oxygen. The ability of coated RBCs to uptake oxygen was investigated with a micro-oxygen electrode by measuring the amount of dissolved oxygen in solution. No significant difference in oxygen uptake was recorded in suspension of coated RBCs, compared to uncoated RBCs (12% versus 15%) (Figure 9.8). This implies that the LbL shell was permeable to oxygen. Since the multilayer affects only the surface of the RBCs, and not the hemoglobin inside, it should not alter the hemoglobin function. This was demonstrated by the fact that the hemoglobin in the coated RBCs was capable of oxygen uptake in the same manner as the hemoglobin from uncoated RBCs. It has been shown previously, that the kinetics of O_2 uptake by RBCs are limited by the size of the RBC size and by the diffusion of O_2 through the RBCs membrane.[258-260] Since the percentage of dissolved oxygen curves of coated and uncoated RBCs had similar shape, one can conclude that the multilayered shell did not affect the diffusion and the kinetics of O_2 uptake in the coated RBCs compared to uncoated RBCs. This result, together with the optical microscopy observation and low lysis percentage, confirmed that the viability, integrity and function of coated RBCs were well-preserved upon coating.

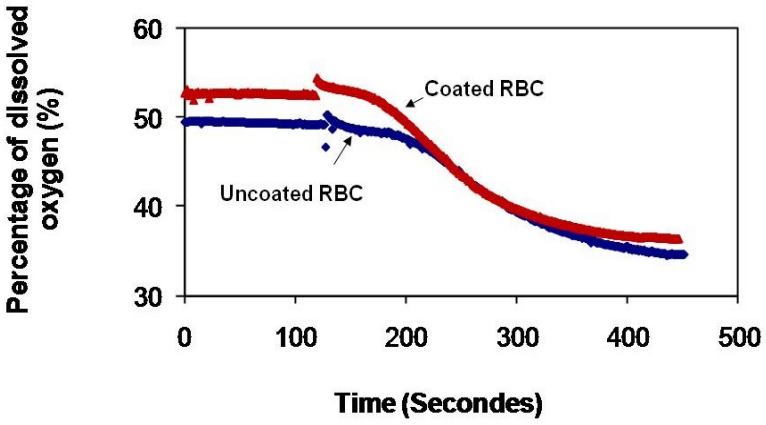

Figure 9.8. Percentage of oxygen uptake by uncoated RBCs and by coated RBCs with $[(AL/CH\text{-}PC)_4\text{-}(AL/PLL\text{-}PEG)_2\text{-}AL]$.

9.4.4 Investigation of immune recognition of encapsulated cells

The immunocamouflage of RBCs takes place when antigen recognition by the respective antibody is prevented. Agglutination assays of anti-A, anti-B and anti-D (Rh) sera with normal and coated RBCs were used to assess the effectiveness of the $[(AL/CH\text{-}PC)_4\text{-}(AL/PLL\text{-}PEG)_2\text{-}AL]$ coating in preventing the recognition of antigenic sites on coated cells. Figure 9 shows the optical microscopy micrographs of the agglutination assay performed on uncoated and coated RBCs with $(AL/CH\text{-}PC)_4\text{-}(AL/PLL\text{-}PEG)_2\text{-}AL$ incubated with anti-A, anti-B and anti-D (Rh) sera. The absence of agglutination indicated that the polyelectrolytes multilayer on RBCs inhibited the accessibility of antigens to the respective antibody. Thus, the coated cells provided RBCs with a serologic behaviour comparable to group O cells toward the assessed antibodies. The results presented here establish that the multilayer shell on RBCs was an effective camouflaging material capable of preventing the activation of the immune system which can allow the survival of foreign RBCs. The choice and the design of polyelectrolyte system was the prime consideration in achieving the

immunocamouflage. The multilayered shell composed of 13 biocompatible polyelectrolyte layers of $(AL/CH\text{-}PC)_4$-$(AL/PLL\text{-}PEG)_2$-AL formed an efficient barrier against antibody recognition in order to induce immunocamouflage.

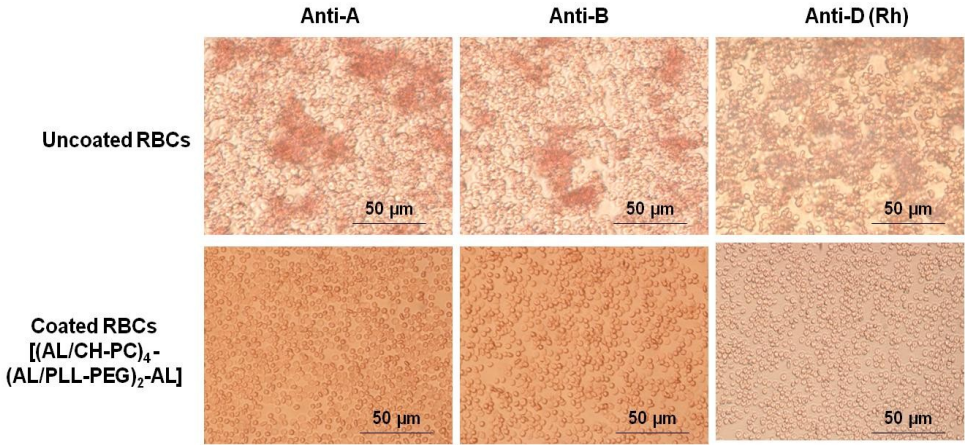

Figure 9.9. Agglutination assay of uncoated and coated RBCs with 13 layers of $(AL/CH\text{-}PC)_4$-$(AL/PLL\text{-}PEG)_2$-AL incubated with anti-A, anti-B and anti-D (Rh) sera. The agglutination is showed by RBCs agglomeration while free cells show absence of agglutination.

9.5 Conclusions

The main advantage of immunocamouflage is to physically modify the inherent immunogenicity of cells. It was achieved in this study by modification of the RBCs membrane surface with a multilayered contruct of non-immunogenic polyelectrolytes that form a barrier that prevents the recognition of antigenic sites by antibodies. Moreover the LbL self-assembly of polyelectrolytes on RBCs preserved the RBCs viability and functionality. The main challenge resided in avoiding cells aggregation in suspension during the LbL build-up. An optimal balance had to be found between the concentration of cells and that of the

adsorbing polyelectrolyte in order to attain full cell coverage while avoiding cell aggregation. The multilayered coat consisted of an inner protective shell made of 4 (CH-PC/AL) bilayers to prevent RBCs lysis and an outer shell composed of 2 bilayers of (AL/PLL-PEG) ending by the deposition of a negatively charged AL layer as the final protein repulsive layer. We demonstrated that the multilayer on RBCs can be used as a means to induce immunocamouflage of blood group antigens. The outstanding immunocamouflage property of our polyelectrolyte systems has been attributed to its unique design that might provide a new paradigm toward the production of universal RBCs for medical transfusion.

9.6 Acknowledgments

The authors thank the Fonds de la Recherche en Santé du Québec for the scholarship, Natural Sciences and Engineering Council of Canada-discovery grant, the Canadian Institutes for Health Research-regenerative medicine nano-medicine grant and FQRNT-Centre for Biorecognition and Biosensors for their financial support. The authors aknowlege Dr J-F. Théorêt for RBCs' purification, Dr F. Azari for her help with TEM sample preparation and imaging and Dr Z. Miao for CH-PC synthesis.

9.7 Supporting information

9.7.1 Zeta-potential measurements

The ξ-potential of the multilayers was determined with a ZetaPlus instrument (Brookhaven Instruments Corporation, UK). Multilayer assembly was performed by sequential deposition of the polyelectrolytes following the protocol

described above, starting with AL. The ξ-potential of each layer was measured after rinsing with 10 mM PBS pH 6.2.

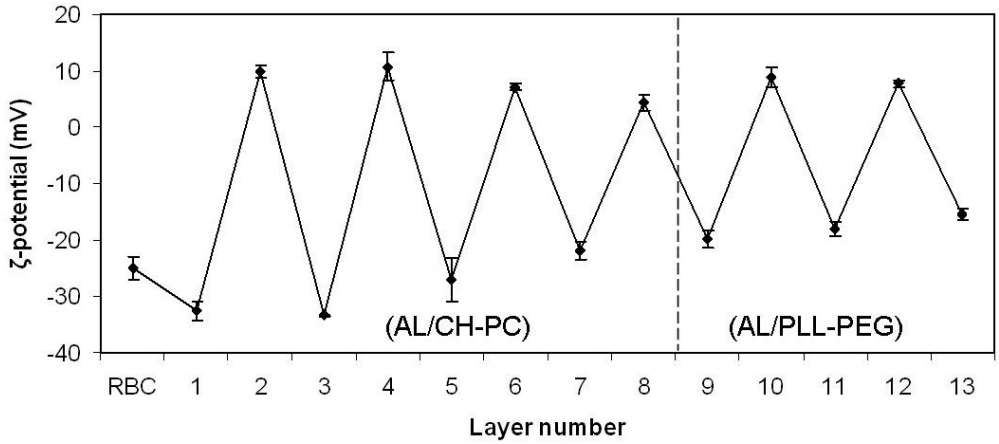

Figure 9.10. Zeta-potential as a function of layer number of the alternation between AL and CH-PC for layer 1 to layer 8 and the alternation between AL and PLL-PEG from 9 to 13.

CHAPTER 10: IMMUNOCAMOUFLAGE OF RBCS IN SUSPENSION

This chapter presents the immunocamouflage of the coated RBCS developed in chapter 9. We extended the immunocamouflage investigation through several techniques and antibodies. Moreover, a preliminary *in vivo* assay is presented in this chapter. The results show the survival of the coated mice RBCs in mice of a different strand.

The results are presented in an article entitled "Immunocamouflage of red blood cells through the layer-by-layer self-assembly technique: A step towards the production of universal red blood cells" presents the fulfillment of the third objective outlined in this theses and it will be submitted for publication in Transfusion journal. (Manuscript ID: Trans-2011-0076)

Immunocamouflage of red blood cells through the layer-by-layer self-assembly technique: A step towards the production of universal red blood cells

Sania Mansouri[†], Yahye Merhi[§], Françoise M. Winnik[‡], Maryam Tabrizian[†,*]

[†]Department of Biomedical Engineering, [*]Faculty of Dentistry, McGill University, H3A 2B, [‡]Faculté de Pharmacie and Département de Chimie, Université de Montréal, H3C 3J7, and [§] Montreal Heart Institute, H1T 1C8, Montreal, Canada

*Corresponding author: Maryam Tabrizian: PhD, MBA; Associate Professor
Phone: +1- 514-398-8129
Fax: +1-514-398-7461
Email: maryam.tabrizian@mcgill.ca

10.1 Abstract

BACKGROUND: *Shortages in the blood supply have potential life-threatening consequences for patients requiring rapid and urgent blood transfusion. This study reports the immunocamouflage of red blood cells (RBCs) by means of multilayered polymeric shell.*

STUDY DESIGN AND METHODS: *The immoucamouflage of RBCs) was achieved through the deposition of a polyelectrolyte multilayer comprising chitosan-graft-phosphorylcholine (CH-PC), poly-L-lysine-graft-polyethyleneglycol (PLL-PEG) and alginate (AL) via Layer-by-layer (LbL) self-assembly technique. The coated RBCs were exposed to anti-A, anti-B, anti-Lewis y and anti-CD44 antibodies in concert with agglutination assay, fluorescence microscopy and flow cytometry to assess their interactions with their respective antigens. As a preliminary step, toward the clinical application of such universal RBCs, an in vivo study was conducted to evaluate the safety and integrity of coated mice RBCs by allogenic transfusion in mice.*

RESULTS: *The antigens-antibodies interactions wereblocked upon treatment of coated RBCs with antibodies. No clumps of the coated RBCs cells were found after the incubation with antibodies suggesting no recognition of antigens was*

occurred. The "stealth" properties of coated RBCs toward the antigens assessed confirm that the multilayer covering the RBCs surface effectively prevents the antigens access to the respective antibodies. Moreover, the coated mice RBCs survived in bloodstream and did not trigger the immune response.

CONCLUSION: *The immunocamouflage assessment revealed the complete silencing of RBC antigens. These findings represent a significant step toward the potential use of the LbL coated RBCs as a universal blood in medical transfusion.*

Keywords: Layer-by-layer self-assembly of polyelectrolyte, Coated red blood cells, Antibody recognition, Immunocamouflage, RBC integrity. *In vivo* biocompatibility

10.2 Introduction

Despite tremendous progress in modern medicine, blood shortage still poses a serious concern and a bottleneck in many surgical interventions with lethal consequences for patients requiring rapid blood transfusions. Several alternatives for blood transfusion are being investigated as both, population and demand are on the rise.[51,52,54,55,57,58] Nevertheless, the production of large scale artificial blood or universal red blood cells (RBCs) has been limited by the preservation of the RBCs metabolism and functionality for a desired period of time. The most recently investigated technique is the production of RBCs by harvesting stem cells. This method relies on the production of a normal RBC which expresses the blood group antigens on its surface and as such, it does not prevent their recognition by the immune system.[83,84,86] Consequently, at the end of the production process of RBCs from stem cells, an additional step should be

considered to produce universal RBCs. In addition, this technique is limited due to several challenges in the large scale production of RBCs.[84] Conversely, two less controversial approaches have also been explored to date and are based on a gentle chemistry in order to modify the RBC membranes. Both methods, however, experience certain limitations, as they often induce complications in case of repeated transfusions. The first technique involves the cleaving of the antigenic groups from the surface of RBCs using specific enzymes, thus requiring the use of hundreds of different enzymes specific to each antigen on the RBCs.[55-58] In the second method, the prevention of RBCs recognition by the immune system is achieved through the application of cellular "immunocamouflage"[50,54,64,73] induced by modifying the membrane surface with polyethylene glycol (PEG). This modification of the cell membrane surface with non-immunogenic molecules aims to create a barrier that prevents the recognition of allogenic sites by circulating cells and antibodies of the recipient.[64,73] The main advantage of immunocamouflage lies in the direct modification of the inherent immunogenicity of the donor tissue itself, by employing the means that are strictly physicochemical in nature, which do not rely on the details of activation pathways, leaving the immune system of the recipient intact. The most recent immunocamouflage approaches were successful in producing universal RBCs and in decreasing the risk of transfusion. Nevertheless, complications with patients who have had previous transfusions still remain very common.

We report here a new method of inducing the immunocamouflage of RBCs using a Layer-by-Layer (LbL) deposition of polyelectrolytes onto functional RBCs. The feasibility of LbL deposition on *non-fixed and functional* RBCs as a template has been demonstrated recently by our group. [255] Therein, we applied the principle of the LbL polyelectrolyte multilayer deposition on live RBCs in order to produce universal RBCs. The proof of concept for immunocamouflage has been demonstrated in a two-dimensional model with RBCs coated with 10 layers of chitosan-graft-phosphorylcholine (CH-PC) and hyaluronic acid (HA) as a first set and 10 layers of alginate (AL) and Poly-L-lysine-graft-polyethylene glycol (PLL-PEG) as a second set of multilayered polyelectrolytes.[255] AL, extracted from seaweed, is a block copolymer of two monosaccharides linked (1 →4), β-D mannuronic acid and its C-5 epimer α-L-guluronic acid. Matrices formed from alginate have been employed for pancreatic islet encapsulation.[235] They were shown to exhibit extended longevity within the body without provoking immunogenic responses.[236,237] Similar to CH itself, CH-PC is also able to form multilayers with AL, provided that the degree of PC incorporation remains low (~ 30 % mol PC groups/glucosamine units).[108] Finally, PLL-PEG has the potential to adsorb spontaneously from aqueous solution onto negatively charged surfaces, resulting in a stable polymeric monolayer that renders the surfaces protein-resistant.[136] In a subsequent study, we fully characterized the LbL build-up on non fixed coated RBCs in suspension. We have shown that 13 layers of above mentioned polyelectrolytes shell ordered as $[(AL/CH\text{-}PC)_4$-

$(AL/PLL\text{-}PEG)_2$-AL] were necessary in order to prevent RBC agglutination with anti-A, anti-B and anti-D (Rh) antibodies.

Both previous studies demonstrated that by manipulating the LbL build-up conditions with protein repulsive polyelectrolytes, and by tuning the film thickness, the cell recognition by antibodies can be prevented. This work presents a step further where the immunocamouflage of RBCs coated in suspension with a film made of $[(AL/CH\text{-}PC)_4$-$(AL/PLL\text{-}PEG)_2$-AL] is demonstrated. Fully functional RBCs were coated by means of LbL assembly using AL, CH-PC and PLL-PEG as polyelectrolyte to form $[(AL/CH\text{-}PC)_4$-$(AL/PLL\text{-}PEG)_2$-AL] shell on RBCs. The blocking effect the coating was determined by agglutination tests along with fluorescence microscopy and flow cytometry using fluorescently-labeled antibodies. The immunocamouflage against (i) the ABO blood group which represents the only blood with pre-existing antibodies in the body, (ii) the Lewis y, a minor blood group, and (iii) the CD44, a membrane marker of the RBCs was investigated. The stability of the coated RBCs was compared to the non-coated RBCs for the duration of 15 days. Finally, an *in vivo* study was performed on mice RBCs in order to assess the hemocompatibility of allogenic coated RBCs with polymeric multilayers.

10.3 Materials and methods

10.3.1 Materials

All solutions were prepared using deionized water (ρ = 18 MΩ cm^{-1}, Nanopure Diamond system, Barnstead International, Iowa, USA). The pH was maintained at 6.2 with a phosphate buffer saline (PBS) (0.01 M phosphate, 0.137 M NaCl,

0.027 M KCl) (Sigma-Aldrich, Oakville, Canada). Bovine serum albumin (BSA), Drabkin`s reagent, somnotol, and Poly-L-lysine (PLL) in the hydrobromide form, (MW 15,000 to 30,000 g mol^{-1}, polydispersity index; 1.1 to 1.5, as stated by the supplier) were all purchased from Sigma-Aldrich (Oakville, Canada). PLL-PEG was prepared as previously described, using methoxy-terminated poly (ethylene glycol) (PEG, MW 2,000 g mol^{-1}) purchased from RAPP Polymere (Germany).[136] CH (degree of deacetylation (DDA) 88%, Mn = 75,000 g mol^{-1}, determined by gel permeation chromatography (GPC) [261] was obtained from Fisher Scientific Inc (Ottawa, Canada). Phosphorylcholine modified CH (CH-PC) was prepared by reaction of CH with phosphorylcholine glyceraldehydes as described previously.[108] The grafting ratio (GR), defined as the percentage of amine functions of PLL or CH modified by PEG and PC, respectively, was 12.5 mol % for PLL-PEG and 30 mol % for CH-PC, as determined by ^{1}H NMR spectroscopy. Antibody anti-blood group A-FITC (fluorescein isothiocyanate), and anti-human IgG-FITC were purchased from BD Biosciences (Mississauga, Canada). Antibody anti-B, Lewis y, CD44-FITC were obtained from Abcam (Cambridge, USA).

10.3.2 Red blood cell isolation

Blood samples were collected from healthy volunteers in accordance with the guidelines of the ethical committee of the Montreal Heart Institute. The blood withdrawn from the antecubital vein through a 19-gauge butterfly needle was collected in syringes containing acid citrate dextrose acting as an anticoagulant. The blood/acid citrate dextrose part ratio was 5/1. The collected blood was

centrifuged at 3,000 rpm with the Beckmann Coulter centrifuge (Mississauga, Canada) for 15 min at room temperature. The plasma and the buffy coat were removed by aspiration. The RBCs were washed three times with a PBS buffer pH 7.4.

10.3.3 Polyelectrolytes multilayer assembly

Polyelectrolytes solutions (1.0 mg mL^{-1}) for multilayer assembly were prepared by dissolution of a polyelectrolyte in PBS (10 mM, pH 6.2). The solutions were filtered through 0.45 µm Millipore PVDF filters prior to use. Following a rinsing step with PBS buffer (10 mM, pH 7.4), a suspension of 10 million RBCs/mL was treated with AL for 10 min. The resulting suspension was rinsed with a PBS solution at pH 6.2 using membrane filtration.[156] Subsequently, the RBCs/AL suspension was treated with CH-PC using the same protocol. This procedure was repeated with alternating polycation and polyanion solutions until a coating made of $[(AL/CH\text{-}PC)_4\text{-}(AL/PLL\text{-}PEG)_2\text{-}AL]$ on RBCs.was achieved.

10.3.4 Fluorescence microscopy imaging

Multilayer assembly was performed in suspension at room temperature following the protocol described above in order to prepare $(AL/CH\text{-}PC)_4/(AL/PLL\text{-}PEG)_2/AL$ coated RBCs. Coated and uncoated RBCs were incubated with BSA (2% in PBS pH 7.4) for 30 min followed by 1 hr incubation with FITC-Anti-A antibody (1 µg mL^{-1} of BSA 2%) or anti-B (0.75 µg mL^{-1} of BSA 2%) or Lewis y (3 µg mL^{-1} of BSA 2%) or FITC-CD44 (5 µg mL^{-1} of BSA 2%) and washed with a PBS buffer pH 7.4 prior to imaging by fluorescence microscopy (Nikon Eclipse TE2000U microscope, Melville, USA).

10.3.5 Flow cytometry

Coated RBCs were analyzed with a Coulter Epics XL flow cytometer (Coulter Corp., Hialeah, U.S.A.) using single immunofluorescence staining. Light scatter and fluorescence channels were set on a logarithmic scale. An appropriately labeled isotype matching negative control IgG was set in the corresponding fluorescence channel and gated in order to assess the nonspecific binding. This gate was used as a threshold to determine the proportion of cells exhibiting a greater fluorescence. Next, both, RBCs and coated RBCs with AL/CH-PC)$_4$/(AL/PLL-PEG)$_2$/AL bilayers were incubated for 1 hr with FITC-anti-A antibody (1 μg mL^{-1} of BSA 2%) or anti-B (0.75 μg mL^{-1} of BSA 2%) or Lewis y (3 μg mL^{-1} of BSA 2%) or FITC-CD44 (5 μg mL^{-1} of BSA 2%) and washed with a PBS buffer pH 7.4. Subsequently, they were identified and gated by their characteristic forward and side scatter properties. Antibody binding was determined by the percentage of the fluorescent cells obtained from 5,000 events in each sample.

10.3.6 Complement activation assay

The alternative (fragment Bb) and classical (C4d) pathway were quantified using an appropriate immunoassay kit (Quidel Bb plus EIA kit, San Diego, USA). Briefly, the immunoassay consisted of a three step procedure utilising a microassay plate coated with a mouse monoclonal antibody that binds specifically to human Bb or to human C4d, a horseradish peroxidase (HRP)-conjugated murine anti-human Bb or HRP-conjugated goat anti-human C4d, and a chromogenic substrate. Prior to starting the immunoassay, samples including,

coated RBCs, CH-PC, PLL-PEG and AL were added to plasma in equal quantity and then diluted at a 1:10 ratio for the alternative pathway and a 1:70 ratio for the classical pathway using the provided complement specimen diluents. A 100 µl of standards, controls and samples were added to the microassay wells and incubated for 30 min, followed by the addition of HRP-conjugated murine anti-Bb antibody or HRP-conjugated goat anti-human C4d. After a 30 min incubation time, a wash cycle was performed to remove any unbound, excess conjugate. Finally, a chromogenic enzyme substrate was added to each microassay well. The bound HRP-conjugate reacted with the substrate forming a color. After 15 min incubation for the alternative pathway and 30 minutes for the classical pathway, the enzyme reaction was stopped chemically., The sample color changed to yellow, and the measurement of the color intensity as an indication of Bb concentration or C4d concentration in samples was performed using a spectrophotometer operating at 450 nm in the alternative pathway or 405 nm in the classical pathway (Bio-Tek Instruments, Winooski, USA).

10.3.7 Stability assay

Uncoated and coated RBCs with $[(AL/CH\text{-}PC)_4/(AL/PLL\text{-}PEG)_2/AL]$ were stored at 4°C. A hemolysis assay was performed using the Drabkin's reagent on samples of uncoated and coated RBCs at day 1, 3, 5, 7, 9, 11, 13, and 15. Briefly, uncoated and coated RBCs were centrifuged for 7 s at 11,750 *g*, and the supernatant (50 µl) was mixed with Drabkin's reagent (1 ml) for 15 min. The amount of leaked hemoglobin in the supernatant was determined by UV-Vis spectroscopy based on the solution absorbance at 540 nm (µQuant

spectrophotometer, Bio-Tek Instruments, Winooski, USA). Results validation was performed using cell lysis by dropping the pH to 5, which allowed the quantitative measurements of the amount of hemoglobin inside the remaining uncoated and coated cells. The released hemoglobin was quantified by the Drabkin's reagent as mentioned above. The results were reported as the percentage of lysis:

$$\frac{\text{Released hemoglobin in supernatant} \times 00}{\text{Total hemoglobin}} = \text{Percentage of lysis} \qquad (10.1)$$

10.3.8 In vivo protocol study

Eight mice of Strain Balb/c and 4 mice of strain C57BL/6 underwent the general anaesthesia by intraperitoneal injection of somnotol 65mg/kg according to the Montreal heart institute guidelines for the care and use of laboratory animals. As a control, two mice of strain Balb/c (defined as RBC-C) and two mice of strain C57BL/6 (defined as RBC-NT) were sacrificed and the blood was withdrawn. Another two C57BL/6 mice were sacrificed for the preparation of coated RBCs with $(AL/CH\text{-}PC)_4$-$(AL/PLL\text{-}PEG)_2$-AL, defined as the RBC-T. The mice RBCs were then purified by 3 washes with PBS 10 mM, pH 7.4 before transfusion and before treatment with the multilayer assembly. RBCs from Balb/c (RBC-C) were then injected to two Balb/c mice as a control. Unmodified RBC-NT from C57BL/6 (0.5 mL, 25% hematocrit) were injected to two Balb/c mice, and modified RBC-T from C57BL/6 (0.5 mL, 25% hematocrit) were injected to two other Balb/c mice (see Fig.10.1).

The vital sign of the mice were observed for the next 10 minutes after injection. The animals were then sacrificed and the collected blood was analyzed for changes in hematologic parameters using an automated cell counter (T890, Beckman Coulter, Inc., Fullerton, USA)

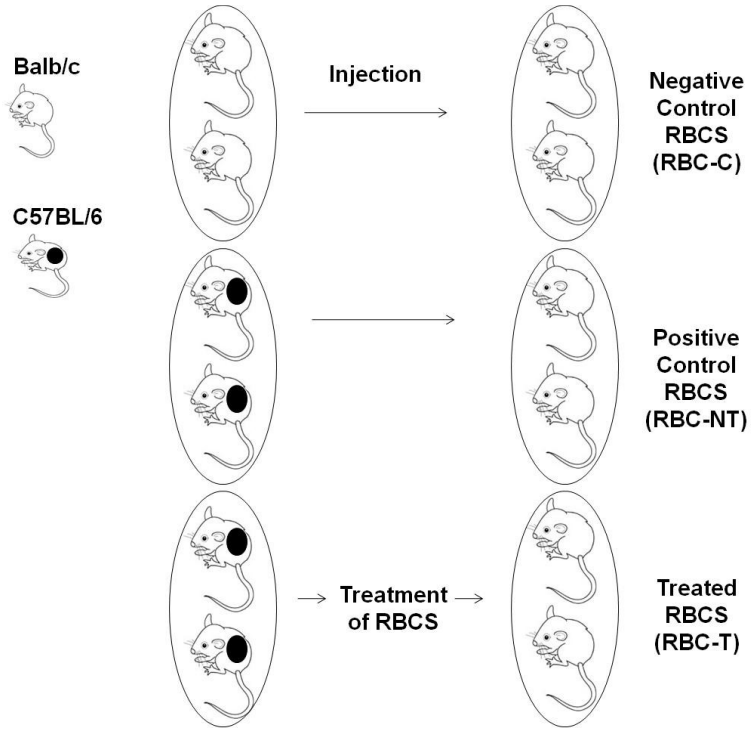

Figure 10.1. *In vivo* study description, 2 mice of Balb/c were injected in 2 mice Balb/c as the negative control (RBC-C), , 2 mice of C57BL/6 were injected in 2 mice Balb/c as non-treated RBCs(RBC-NT and 2 mice of C57BL/6 were injected in 2 mice Balb/c as treated RBCs (RBC-T).

10.3.9 Statistical analysis

All experiments were carried out in triplicate. Results are reported as the mean value ± standard deviation.

10.4 Results

10.4.1 Immunocamouflage of coated RBCs with polymeric multilayer

Modified non-fixed and functional coated RBCs with [(AL/CH-PC)$_4$-(AL/PLL-PEG)$_2$-AL] multilayer were assessed by three different techniques: agglutination assay, fluorescence microscopy and flow cytometry. Uncoated and coated RBCs carrying A, B, Lewis y and CD44 antigens were tested for agglutination with their respective antibody. Results showed that the agglutination of these coated cells was completely inhibited compared to uncoated cells (Fig. 10.2).

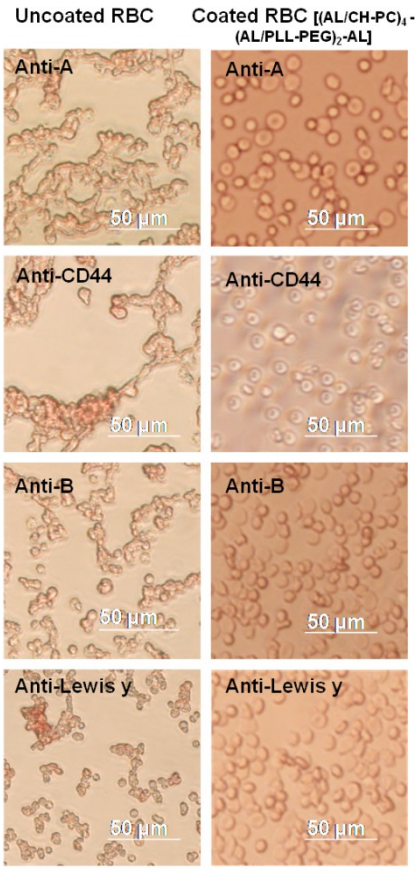

Figure 10.2. Optical microscopy micrographs of uncoated and coated RBCs with (AL/CH-PC)$_4$-(AL/PLL-PEG)$_2$-AL incubated with anti-A, anti-B, anti-lewis y and anti-CD44 antibodies.

The absence of fluorescence in fluorescence micrographs (Fig. 10.3) for the coated RBCs incubated with anti-A, anti-B, anti-Lewis y and anti-CD44 antibodies confirmed the results obtained by agglutination assay. Further, flow cytometry analysis allowed for determination of the percentage of fluorescently labeled uncoated and coated RBCs following their treatment with anti-A, anti-B, anti-Lewis y and anti-CD44 fluorescently labeled antibodies. Approximately 5% of the coated cells were detected to be fluorescent for antigen A, B, Lewis y and 1% for antigen CD44 (Fig. 10.4).

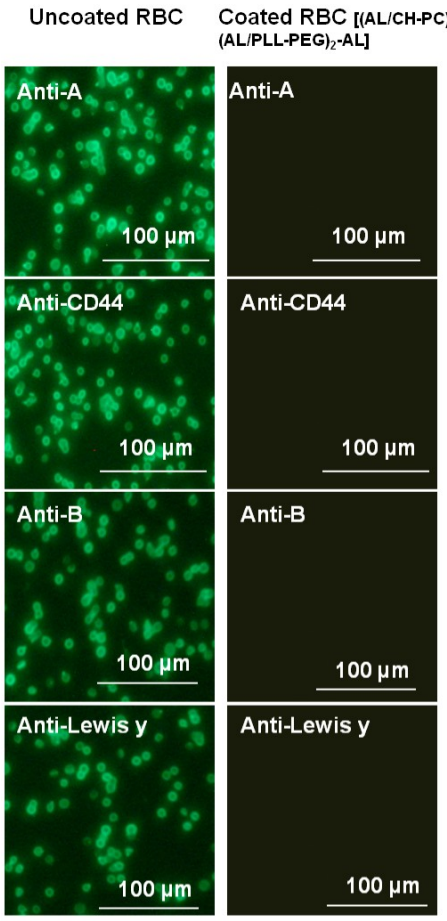

Figure 10.3. Fluorescence micrographs of uncoated and coated RBCs. The binding of anti-A (at 1000x dilution) anti-B (1500x dilution), anti-lewis y (350x dilution) and anti-CD44 (at 200x dilution) to uncoated and coated RBCs with 13 layers of $(AL/CH\text{-}PC)_4$-$(AL/PLL\text{-}PEG)_2$-AL.

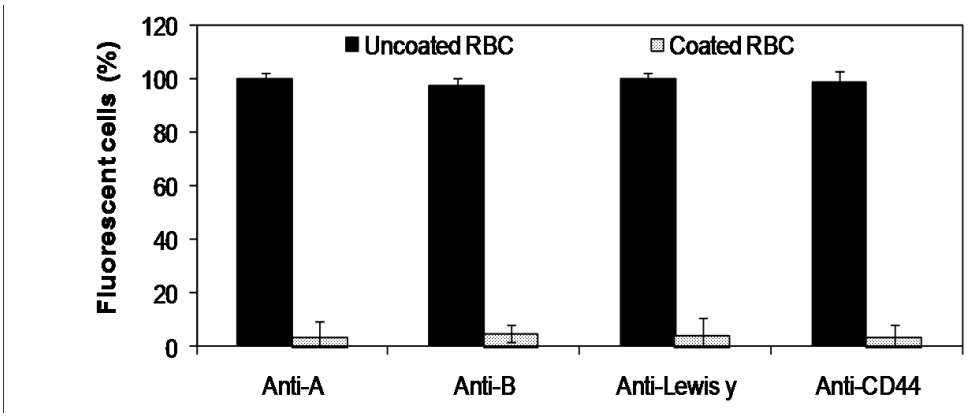

Figure 10.4. Flow cytometric analysis of Coated RBCs. The binding of anti-A (at 1000x dilution) anti-B (500x dilution), anti-lewis y (350x dilution) and anti-CD44 (at 200x dilution) to uncoated and coated RBCs with 13 layers of $(AL/CH\text{-}PC)_4$-$(AL/PLL\text{-}PEG)_2$-AL.

10.4.2 Complement activation assay

The C4d fragment resulting from the classical complement pathway activation was quantified by immunoassay. The results demonstrated a very low, almost inexistent, level of C4d in the samples (Fig. 10.5). The result of the alternative pathway showed the absence of the Bb factor in the coated RBCs and in the polymers samples namely CH-PC, PLL-PEG and AL samples.

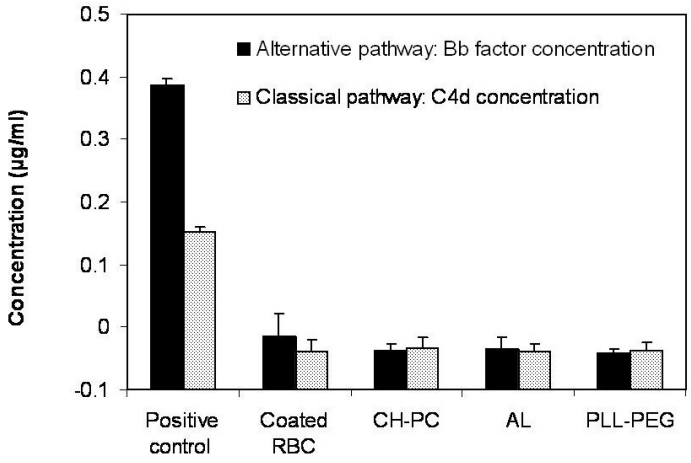

Figure 10.5. Complement activation assay after incubation with control, coated RBCs, AL, CH-PC and PLL-PEG in human serum. Factor C4d is the result of classical pathway activation, while the factor Bb is the result of the alternative pathway activation.

10.4.3 Stability assay

The stability of the coated RBCs was assessed by measuring the percentage of lysis upon storage for 15 days. As shown in Fig. 10.6, the percentage of lysed coated RBCs remained below 41 %, confirming that at least 60% of the cells remained intact whereas uncoated cells showed a lower lysis percentage of approximately 15 % after 15 days stored in the same conditions. The optical microscopy images showed that the remaining coated RBCs had similar shapes to uncoated RBCs. In addition, they did not interact with anti-A antibody as shown by the absence of fluorescence (Fig.10.6 insert) demonstrating that the immunocamouflage effect could be maintained over 15 days.

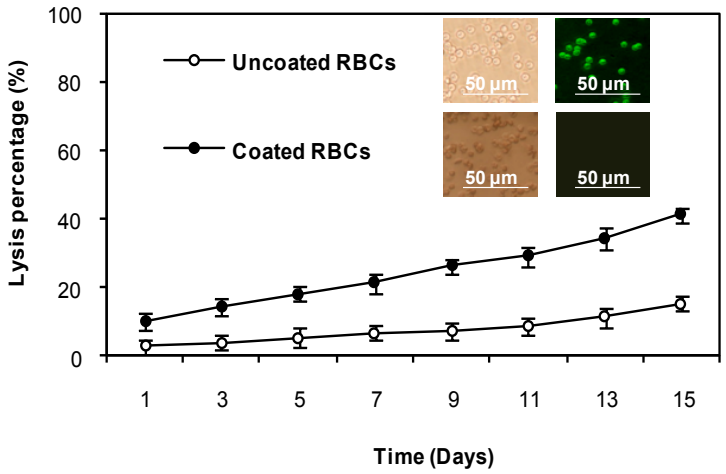

Figure 10.6. Stability study of the coated RBCs with (AL/CH-PC)4-(AL/PLL-PEG)2/AL compared to uncoated RBCs presented by the lysis percentage over 15 days. Optical microscopy and fluorescence microscopy with antibody anti-A with uncoated and coated RBCs stored for 15 days.

10.4.4 Multilayer shell biocompatibility of coated mice RBCs In vivo

The untreated mice RBCs were investigated for the hemocompatibility of the multilayered polymeric shell. C57BL/6 mice survived after the injection of

Balb/c RBCs, demonstrating the compatibility of Balb/c and C57BL/6 RBCs. Moreover, the hematologic parameters including the number of RBCs, white blood cells and hemoglobin were similar to normal mice blood values (Fig. 10.7). Thereafter, the treated C57BL/6 mice RBCs with the polymeric multilayer were injected in Balb/c mice. The Balb/c mice remained alive and the hematologic parameters including the numbers of RBCs, white blood cells and hemoglobin were again similar to normal cells (Fig. 10.7)

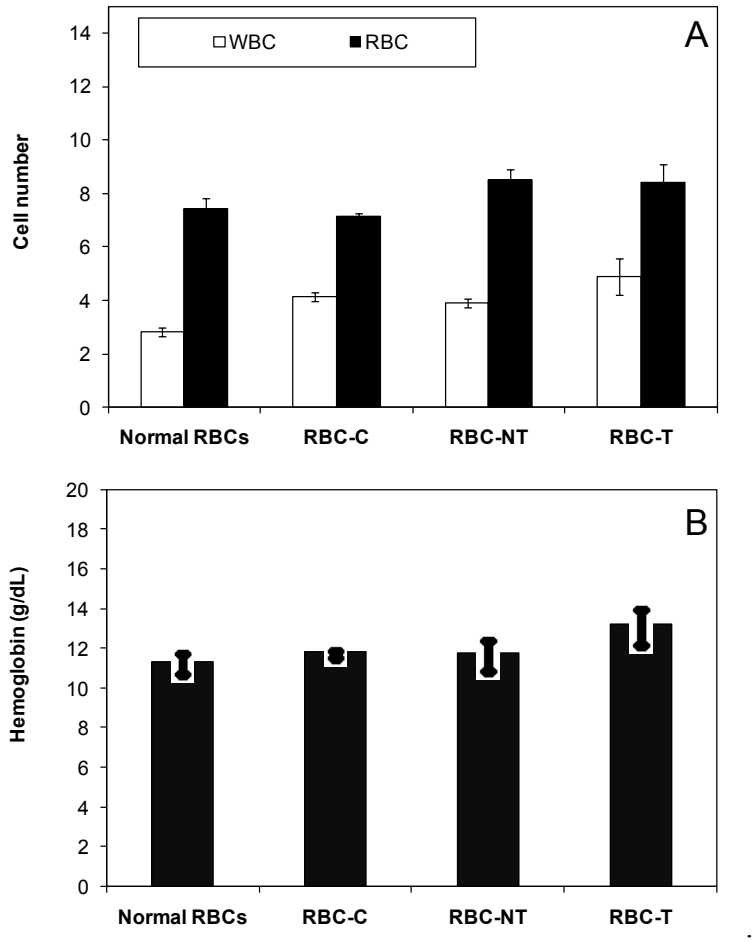

Figure 10.7. (A) White blood cells (WBC) ($x10^9$) and RBCs ($x10^{12}$) count in normal blood, RBC-C, RBC-NT and RBC-T. (B) Hemoglobine (Hbg)(g/dL) count in normal blood, RBC-C, RBC-NT and RBC-T

10.5 Discussion

Masking of blood group antigens on RBCs by polymeric coating via LbL technique was the strategy utilized in order to produce universal RBCs. The immunocamouflage of RBCs takes place when antibody recognition is prevented in cells, while the cells retain their integrity and functionality.[48,52,73] Unlike previously assessed approaches to the universal blood production, the immunocamouflage by means of the LbL technique provides a complete coverage of the RBCs membrane surface. The results presented herein establish that the polymeric multilayer covering the RBC surface inhibited the accessibility of antigens A, B, Lewis y and CD44. The hollow capsules formed with sodium cellulose sulfate/CH multilayer do not permeate molecules bigger than 70 kDa demonstrating the capability of such layers to block the diffusion of macromolecules in and out of the capsules.[262] This is in agreement with our findings since the multilayered shell prevented the permeation of the antibodies which have a molecular weight of 150 kDa.[255] The polymeric multilayer on RBCs containing the protein repulsive PEG masked the antigen A, B, Lewis y and CD44 to an appropriate level from their respective antibodies. This level of inhibition is important for achieving the universal cells for medical transfusion. To date, the coated RBCs behaved as stealth cells toward the assessed antibodies.

The immune system is composed of the adaptive immune scheme that requires antibodies and memory cells acquired through previous immunization, and the

innate immune system. The complement system which is a biochemical cascade consisting of a number of small proteins circulating in the blood as inactive precursors is part of the innate system that "complements" the ability of antibodies to clear pathogens and foreign bodies. When stimulated by one of several triggers, proteases in the system cleave specific proteins to release cytokines and initiate an amplifying cascade of further cleavages. The end-result of this activation cascade is massive amplification of the response and activation of the cell-killing membrane attack complex. The complement system can be activated through the classical complement pathway or the alternative complement pathway. It is therefore important to demonstrate that the polymeric shell built on RBCs polymer do not trigger the complement activation. Previous reports showed that the low molecular weight CH can activate C3.[263] However, above the molecular weight of 70 kDa, CH is a weaker activator of the complement, which explains the results obtained herein using a 75 kDa molecular weight CH-PC. Ward et al. showed that PLL activates the alternative pathway of the complement; in contrast, the complement is not activated when PLL is linked to a radiolabelled probe. In our case, it seems that the cytolytic effects of the complement activation could be prevented by covalently binding the PEG to PLL.[264] These results together with previous findings indicate that the polyelectrolyte multilayer provided the coated RBCs with an immunocamouflage against the complement activation.

In an extreme case, the multilayer shell on the RBCs could cause cell destruction, increasing the hemoglobin concentration and decreasing the RBCs concentration

causing death in short time.[265] However, our results showed that the coated RBCs remained intact after 15 days storage and suggested that the design of polyelectrolyte shell has greatly contributed to preserve cells over this period. Interestingly, in our case, the multilayered shell not only remained attached on the RBCs after 15 days *in vitro* storage, but also maintained the immunocamouflage effect after this period. Moreover, coated RBCs from C57BL/6 mice did not trigger the immune system when they have been injected into Balb/c. The white blood cell count which is an indicator of the body reaction to foreign materials and infectious bodies, was normal. All hematologic parameters remained stable in mice received allogenic RBCs transfusion. The injected mice with modified RBCs survived with normal vital signs. These overall observations would indicate that the coated RBCs could withstand the pressure and the mechanical restraint conditions during their circulation in the bloodstream.

The approach taken in this work is therefore effective with a potential application in the production of universal red blood cells. Nano-shell composed of [AL/CH-PC)$_4$-(AL/PLL-PEG)$_2$-AL] built on fully functional RBCs through LbL self-assembly technique prevented the antibody interactions with antigens A, B, Lewis y and CD44 on the RBC surfaces. The polymeric multilayered shell does not seem to introduce adverse effects once used on mice RBCs and could be carried on in the bloodstream. While much more work is required prior to clinical application of the technique, this breakthrough has a great scale-up

potential and might provide a safe solution of allogenic blood transfusion for many patients with massive blood loss.

10.6 Acknowledgments

The authors thank Dr Jean-François Théorêt for red blood cell purification. This work is supported by Natural Sciences and Engineering Research Council of Canada-Discovery grant, the Canadian Institutes of Health Research-Regenerative Medicine and Nanomedicine grant and Fonds de la Recherche en Santé du Québec scholarship.

CHAPTER 11: CONCLUSIONS AND FUTURE PERSPECTIVES

This thesis presented an original approach to the encapsulation of red blood cells through the LbL self-assembly technique for effective immunocamouflage with potential application in blood transfusion, thus confirming the main hypothesis as stated in chapter 2. The results of this thesis have led to one published original paper, one paper accepted for publication and one submitted manuscripts. A published comprehensive review on the LbL principles for coating flat surfaces and colloidal system was also presented in the introduction. The summary of the main findings regarding the thesis objectives and accomplishments are outlined in the following sections.

11.1 Objective 1: Development of two-dimension model and optimization of RBCs coating and immunocamouflage

The first objective was to demonstrate the ability of a polymeric multilayer to induce immunocamouflage. The strategy undertaken was based on the polymeric multilayer assembly on a monolayer of RBCs adhered to silica surface in order to circumvent the aggregation and hemolysis issues which arose during the LbL build-up in suspension. The choice of adequate polymers has been extensively investigated and optimized for the immunocamouflage induction to finally reside in CH-PC, HA, PLL-PEG and AL polyelectrolytes.. These polyelectrolytes were successfully assembled in a well-designed multilayer system on non-fixed RBCs in a 2-D model. The CH was grafted to PC in order to allow a better solubility at neutral pH while keeping the polymer positively

charged. PEG grafted to PLL provided an effective protein repulsive barrier of the multilayer thus prohibiting antibody recognition. HA and AL being negatively charged, have the property to form viscoelastic films. A thorough study of constructs formed by the two pairs of oppositely charged biocompatible polyelectrolytes has been performed. Five bilayers of CH-PC/HA were constructed as a first set followed by a second set of five bilayers of PLL-PEG/AL. The PLL-PEG was a part of the second set of polymers in order to prevent potential hemolysis which could occur if used in the early stages of the LbL build-up. The polymeric multilayer was characterized by complementary techniques including the zeta-potential measurements, QCM-D and AFM.

To assess the multilayers' effect on RBCs behavior, in view of the absence of nucleus and mitochondria in RBCs, the measurement of the released hemoglobin was performed and taken as indication of cell viability and integrity. The hemoglobin amount measurement, following the multilayer build-up, was also used to study the permeability of anti-A antibody through the multilayer film, since the antibody anti-A causes agglutination and hemolysis when in contact with RBCs expressing anti-A antigens.

QCM-D was used to study the adhesion of antibodies on the multilayer. The obtained results were then confirmed by fluorescence microscopy. The immunocamouflage was assessed through the recognition of the antigen A which is the most difficult antigen to mask in comparison to the other minor groups.[48,60,64] Therefore, it is expected that if the antigen A can be masked, the biorecognition of other antigens should be prevented as well. In summary, we

have demonstrated that by modulating the LbL film composition, the build-up conditions, the film thickness and the multilayer permeability, cell recognition by the Anti-A antibody can be prevented. The «permeability», in this thesis, is referred to as the diffusion of antibody anti-A through the polymeric multilayer shell without the application of pressure.

11.2 Objective 2: Development and optimization of RBCs coating in suspension

Once the immunocamouflage optimization was achieved in a 2-D model, the second objective consisted of developing a protocol for the coating of RBCs in suspension. The design and optimization of the LbL system using extensive physicochemical characterization was required in order to achieve an effective and uniform coating of unfixed RBCs in suspension. The functionality and viability of coated RBCs were assessed to demonstrate the ability of the polymeric multilayer to permeate oxygen.

While the ultimate goal was to reproduce the LbL coating on non-fixed RBCs in suspension, the challenge of avoiding cells aggregation during the LbL build-up remained. Specifically, the balance had to be achieved between the concentration of cells and the adsorbing polyelectrolytes in order to provide saturation conditions for full cell coverage while avoiding their aggregation. The RBCs concentration during the LbL build-up was set at 10 million cells·mL^{-1} and the polyelectrolyte concentration was set in excess of 1mg·mL^{-1}. The excess of the polymers was removed via membrane filtration, by keeping the RBCs always in suspension and thus avoiding aggregation. The multilayered shell consisted of

an inner protective shell made of 4 (CH-PC/AL) bilayers to prevent RBCs lysis and an outer camouflaging shell composed of 2 bilayers of (AL/PLL-PEG) ending by the deposition of AL as the final negatively charged layer. Initially used HA was replaced by AL because the HA induced aggregation in the early stages of LbL build-up in suspension. TEM micrographs have shown the multilayer thickness to be ~ 300 nm.

The viability and the functionality of the coated RBCs were examined in order to allow their use in blood transfusion. Since RBCs lack cell nucleus and mitochondria, the standard viability assays, such as the MTT test, could not be employed. Instead, the viability of the coated RBCs was assessed by quantifying the release of hemoglobin and ATP in suspension. Additionally, the functionality of the coated RBCs in terms of their ability to transport oxygen was also assessed, since the transportation of oxygen to the cells is crucial in blood transfusion in order to avoid major harms that cause organs failure and ultimately patient's death. The oxygen uptake by the coated RBCs was investigated using an oxygen electrode. The results showed that the coated RBCs remained viable and functional following their coating with a multilayered shell.

11.3 Objective 3: Assessment of the coated RBCs Immunocamouflage

The third objective was to demonstrate the immunocamouflage properties of the multilayered shell. As known, the immune system is divided into the adaptive immune system that requires antibodies and memory cells and the innate immune system which eliminates foreign bodies through the activation of the complement

system. Therefore, the approach for immunocamouflage relied on the modification of the RBCs membrane surface with non-immunogenic polyelectrolytes in order to create a barrier that prevents the recognition of antigenic sites. The immunocamouflage was first demonstrated by a simple agglutination test where the coated RBCs were incubated in the presence of antibodies. The antibody-repulsive property of the multilayer was also demonstrated in more depth using immunofluorescence and flow cytometry with antibodies specific to A, B, CD44 and Lewis y antigens. We have demonstrated that the multilayer RBC coating was capable of inducing immunocamouflage of blood group antigens. Moreover, the coated RBCs and the polymers used to perform the coating did not induce the complement activation.

Finally, a preliminary *in vivo* study was conducted in order to demonstrate the biocompatibility of the polymeric multilayered shell in the bloodstream. In this study, RBCs from C57BL/6 mice were coated and injected into Balb/c to investigate the biocompatibility of the polymeric coating and its effect on the hematologic parameters. The injected Balb/c mice remained live and the hematologic parameters including the numbers of the hemoglobin, RBCs and white blood cells were similar to normal Balb/c mice.

11.4 Future perspectives

The manuscripts included in this thesis provide a proof-of-principle for the LbL strategy used in order to induce the immunocamouflage of the red blood cells coated with a nano-organized shell. The feasibility of the LbL build-up based on electrostatic adhesion on the red blood cells was demonstrated. The viability and

the functionality of the coated RBCs as well as the immunocamouflage of the A, B, Lewis y and CD44 antigens was confirmed for their potential application in blood transfusion. Prior to the clinical application of the proposed technique, higher-level investigations should be completed, including: (i) Improvement of the LbL fabrication for the self-assembly in a large scale production settings, (ii) An extensive *in vitro* study, and finally (iii) An *in vivo* study to validate the blood transfusion application of these coated cells.

Other than incubation of the RBCs with the polyelectrolytes, the coating system is based on a simple filtration through a membrane to remove the free polyelectrolyte to allow the next deposition step. The filtration system should be redesigned to optimize the LbL build-up conditions. A custom made filtration system composed of a low pressure vacuum suction and a mixing apparatus capable of maintaining all the RBCs in suspension could considerably reduce the deposition time, while allowing higher yield of RBCs coating. A limitation of the filtration technique is the buffer volume that is needed to remove the free polyelectrolytes between the polyelectrolyte's adsorption. This limitation should be solved before moving to clinical studies by increasing the concentration of coated cells. For now, the concentration of coated cells is 10 million cells per/ mL, a higher concentration of coated RBCs is necessary to increase the yield of RBCs coating per buffer volume used during the washing periods. Following the coating process of the entire polymeric multilayered shell, the concentration of the coated cells should be optimized to have similar concentration to the RBCs found in the bloodstream to conduct proper clinical studies.

Thorough *in vitro* investigations in relation with the mechanical stability and biodegradability of the multilayer on the RBCs should be conducted. The mechanical stability investigations will demonstrate the capability of the coated multilayer to pass through small capillaries. Moreover, the coated RBCs have to be tested in conditions equivalent to blood pressure in order to study the stability of the multilayer on the RBCs. Since the life span of the RBCs is 120 days, it's primordial to study the biodegradability of the multilayer in order to have a similar time log. Since the enzymes degrade the polymers under physiological conditions in the living body, the degradation of the multilayered shell by enzymes, namely chitosanase and lysosyme could be quantitatively analyzed by QCM-D. The biodegradability of the polymeric multilayered shell could be modulated by its cross-linking with appropriate agents but preliminary assays are necessary to keep the polymeric multilayer deformability character. Moreover, the relation between the mechanical properties of the membrane and its biodegradability expected to occur should be studied prior to clinical studies.

To fully validate the biocompatibility and the survival of the coated RBCs in the bloodstream, a xeno-transfusion of coated human red blood cells into the animal should be performed. The heart rate, as well as the hematologic parameters of the transfused animal should be monitored for a specific period of time. Finally, the animal should be sacrificed and the heart, liver, kidney and spleen should be removed to study the signs of agglutination and polymer accumulation. This can be evaluated by immunohistochemistry.

11.5 Final conclusion

According to the FDA estimates, over ten companies have Blood substitute products publicly disclosed and under development in preclinical and clinical trials. Their main concern is how to provide maximum oxygen delivery to cells with minimal concentration of the oxygen carrier. In parallel with developing hemoglobin-based oxygen carriers and perfluorochemical compounds to replace RBCs, the strategies for universal blood development have shifted to investigate the new processes involving cell surface modification with polymers to prevent alloimmune recognition of the allogenic RBCs antigens. The main advantage of this new process, so-called “immunocamouflage”, is that it physically modifies the inherent immunogenicity of cells. A number of diseases, including thalassemia, that require many repeated blood transfusions are often complicated by the development of antibodies to "minor" red cell antigens. This "allosensitization" can render the transfusion impossible for the affected patients. In this regard, we have presented our approach for immunocamouflage which has relied on the modification of the RBCs membrane surface with non-immunogenic polyelectrolytes through the LbL self-assembly technique which creates a barrier that prevents the recognition of antigenic sites by cells. LbL self-assembly of polyelectrolytes on RBCs preserved the RBCs viability and functionality in suspension. The main challenge resided in avoiding cells aggregation during the LbL build-up which was surmounted by careful optimization of cell concentration and the concentration of adsorbing polyelectrolytes. The outstanding immunocamouflage property of our

polyelectrolyte systems on unfixed RBCs in suspension has been attributed to its unique design. The multilayered shell consisted of an inner protective shell made of 4 (CH-PC/AL) bilayers to prevent RBCs lysis and outer shell composed of 2 bilayers of (AL/PLL-PEG) finished by the deposition of an AL layer as the final protein repulsive layer providing a negative charge. The modified cells, while structurally and functionally normal, also remained antigenically "silent". This technique may provide a new paradigm toward the production of universal RBCs for medical transfusion.

CUMULATIVE REFERENCES

1. Greenwalt, T. J. A short history of transfusion medicine. *Transfusion* **1997,** *37* (5), 550-563.

2. Myhre, B. A. The 1St Recorded blood-transfusions - 1656 to 1668. *Transfusion* **1990,** *30* (4), 358-362.

3. Custer, B.; Hoch, J. S. Cost-Effectiveness Analysis: What It Really Means for Transfusion Medicine Decision Making. *Transfusion Medicine Reviews* **2009,** *23* (1), 1-12.

4. Klein, H. G.; Anderson, D.; Bernardi, M. J.; Cable, R.; Carey, W.; Hoch, J. S.; Robitaille, N.; Sivilotti, M. L. A.; Smaill, F. Pathogen inactivation: making decisions about new technologies - Report of a consensus conference. *Transfusion* **2007,** *47* (12), 2338-2347.

5. Amin, M.; Fergusson, D.; Wilson, K.; Tinmouth, A.; Aziz, A.; Coyle, D.; Hebert, P. The societal unit cost of allogenic red blood cells and red blood cell transfusion in Canada. *Transfusion* **2004,** *44* (10), 1479-1486.

6. Goodnough, L. T. What is a transfusion medicine specialist? *Transfusion* **1999,** *39* (9), 1031-1033.

7. Nakao, M. New insights into regulation of erythrocyte shape. *Current Opinion of Hematology* **2002,** *9* (2), 127-132.

8. Kabanova, S.; Kleinbongard, P.; Volkmer, J.; Andree, B.; Kelm, M.; Jax, T. W. Gene expression analysis of human red blood cells. *International Journal of Medicine Science* **2009,** *6* (4), 156-159.

9. Bieber, E. Erythropoietin, the biology of erythropoiesis and epoetin alfa - An overview. *Journal of Reproductive Medicine* **2001,** *46* (5), 521-530.

10. Foller, M.; Huber, S. M.; Lang, F. Erythrocyte programmed cell death. *Iubmb Life* **2008,** *60* (10), 661-668.

11. Hardison, R. C. A brief history of hemoglobins: plant, animal, protist, and bacteria. *Proceedings of the National Academy of Sciences of the United States of America* **1996,** *93* (12), 5675-5679.

12. Matteucci, E.; Giampietro, O. Electron Pathways through Erythrocyte Plasma Membrane in Human Physiology and Pathology: Potential Redox Biomarker? *Biomark. Insights.* **2007,** *2*, 321-329.

13. Marcus, R. L.; Smith, S.; Morrell, G.; Addison, O.; Dibble, L. E.; Wahoff-Stice, D.; LaStayo, P. C. Comparison of Combined Aerobic and High-Force Eccentric Resistance Exercise With Aerobic Exercise Only for People With Type 2 Diabetes Mellitus. *Physical Therapy* **2008,** *88* (11), 1345-1354.

14. Landsteiner, K.; Witt, D. H. Observations on the human blood groups - Irregular reactions. Isoagglutinins in sera of group IV. The factor A. *Journal of Immunology* **1926,** *11* (3), 221-247.

15. Giraud, C.; Korach, J. M.; Andreu, G.; Lacaze, C.; Vaicle, M.; Schooneman, F.; Guillevin, L. The immunological basics of transfusion. *Transfusion Clinique et Biologique* **2002,** *9* (3), 163-167.

16. Rouger, P. Impact of blood group antigens in transplantation. *Transfusion Clinique et Biologique* **2005,** *12* (5), 403-408.

17. Berg, J. M.; Tymoczko, J. L.; Stryer, L. *Biochemistry;* 5th edition ed.; 2002.

18. Joneckis, C. C.; Ackley, R. L.; Orringer, E. P.; Wayner, E. A.; Parise, L. V. Integrin-alpha-4-beta-1 and glycoprotein-iv (Cd36) are expressed on circulating reticulocytes in sickle-cell-anemia. *Blood* **1993,** *82* (12), 3548-3555.

19. Yawata, Y.; Miyashima, K.; Sugihara, T.; Murayama, N.; Hosoda, S.; Nakashima, S.; Iida, H.; Nozawa, Y. Self-adaptive modification of red-cell membrane-lipids in lecithin - cholesterol acyltransferase deficiency - lipid analysis and spin labeling. *Biochimica et Biophysica Acta* **1984,** *769* (2), 440-448.

20. Yawata, Y.; Sugihara, T.; Mori, M.; Nakashima, S.; Nozawa, Y. Lipid Analyses and fluidity studies by electron-spin resonance of red-cell membranes in hereditary high red-cell membrane phosphatidylcholine hemolytic-anemia. *Blood* **1984,** *64* (5), 1129-1134.

21. Carlton, R. http://www.rbcarlton.com/membrane.jpg. 2010.

22. Lowe, J. B. Glycosylation, immunity, and autoimmunity. *Cell* **2001,** *104* (6), 809-812.

23. Bevers, E. M.; Comfurius, P.; Dekkers, D. W. C.; Zwaal, R. F. A. Lipid translocation across the plasma membrane of mammalian cells. *Biochimica et Biophysica Acta-Molecular and Cell Biology of Lipids* **1999,** *1439* (3), 317-330.

24. Dolis, D.; Moreau, C.; Zachowski, A.; Devaux, P. F. Aminophospholipid translocase and proteins involved in transmembrane phospholipid traffic. *Biophyical Chemistry* **1997,** *68* (1-3), 221-231.

25. Daleke, D. L.; Lyles, J. V. Identification and purification of aminophospholipid flippases. *Biochimica et Biophysica Acta-* **2000,** *1486* (1), 108-127.

26. Kuypers, F. A. Phospholipid asymmetry in health and disease. *Current Opinion of Hematology* **1998,** *5* (2), 122-131.

27. Dekkers, D. W.; Comfurius, P.; Schroit, A. J.; Bevers, E. M.; Zwaal, R. F. Transbilayer movement of NBD-labeled phospholipids in red blood cell membranes: outward-directed transport by the multidrug resistance protein 1 (MRP1). *Biochemistry* **1998,** *37* (42), 14833-14837.

28. Fukuda, M. Molecular genetics of the glycophorin A gene cluster. *Seminar of Hematology* **1993,** *30* (2), 138-151.

29. Cartron, J. P.; Le Van, K. C.; Colin, Y. Glycophorin C and related glycoproteins: structure, function, and regulation. *Seminar of Hematology* **1993,** *30* (2), 152-168.

30. Zon, L. I. Developmental Biology of Hematopoiesis. *Blood* **1995,** *86* (8), 2876-2891.

31. Orkin, S. H.; Zon, L. I. Hematopoiesis: An evolving paradigm for stem cell biology. *Cell* **2008,** *132* (4), 631-644.

32. Johnson, G. R.; Moore, M. A. S. Role of Stem-Cell Migration in initiation of mouse fetal liver hematopoiesis. *Nature* **1975,** *258* (5537), 726-728.

33. Ledouarin, N. M.; Dieterlenlievre, F.; Oliver, P. D. Ontogeny of primary lymphoid organs and lymphoid stem-cells. *American Journal of Anatomy* **1984,** *170* (3), 261-299.

34. Rebel, V. I.; Miller, C. L.; Eaves, C. J.; Lansdorp, P. M. The repopulation potential of fetal liver hematopoietic stem cells in mice exceeds that of their adult bone marrow counterparts. *Blood* **1996,** *87* (8), 3500-3507.

35. Rebel, V. I.; Miller, C. L.; Thornbury, G. R.; Dragowska, W. H.; Eaves, C. J.; Lansdorp, P. M. A comparison of long-term repopulating hematopoietic stem cells in fetal liver and adult bone marrow from the mouse. *Experimental Hematology* **1996,** *24* (5), 638-648.

36. Harrison, D. E.; Zhong, R. K.; Jordan, C. T.; Lemischka, I. R.; Astle, C. M. Relative to adult marrow, fetal liver repopulates nearly five times more effectively long-term than short-term. *Experimental Hematology* **1997,** *25* (4), 293-297.

37. Zanjani, E. D.; Ascensao, J. L.; Tavassoli, M. Liver-derived fetal hematopoietic stem-cells selectively and preferentially home to the fetal bone-marrow. *Blood* **1993,** *81* (2), 399-404.

38. Brown, G.; Hughes, P. J.; Michell, R. H.; Rolink, A. G.; Ceredig, R. The sequential determination model of hematopoiesis. *Trends in Immunology* **2007,** *28* (10), 442-448.

39. Weissman, I. L. Stem cells: Units of development, units of regeneration, and units in evolution. *Cell* **2000,** *100* (1), 157-168.

40. Palis, J. Ontogeny of erythropoiesis. *Current Opinion in Hematology* **2008,** *15* (3), 155-161.

41. Adams, G. B.; Chabner, K. T.; Alley, I. R.; Olson, D. P.; Szczepiorkowski, Z. M.; Poznansky, M. C.; Kos, C. H.; Pollak, M. R.; Brown, E. M.; Scadden, D. T. Stem cell engraftment at the endosteal niche is specified by the calcium-sensing receptor. *Nature* **2006,** *439* (7076), 599-603.

42. Metcalf, D. Hematopoietic cytokines. *Blood* **2008,** *111* (2), 485-491.

43. Tsiftsoglou, A. S.; Vizirianakis, I. S.; Strouboulis, J. Erythropoiesis: Model systems, molecular regulators, and developmental programs. *Iubmb Life* **2009,** *61* (8), 800-830.

44. Kim, S. I.; Bresnick, E. H. Transcriptional control of erythropoiesis: emerging mechanisms and principles. *Oncogene* **2007,** *26* (47), 6777-6794.

45. Fearon, D. T.; Locksley, R. M. The instructive role of innate immunity in the acquired immune response. *Science* **1996,** *272* (5258), 50-53.

46. Parkin, J.; Cohen, B. An overview of the immune system. *Lancet* **2001,** *357* (9270), 1777-1789.

47. Thompson, C. B. New Insights Into V(D)J Recombination and its role in the evolution of the immune-system. *Immunity* **1995,** *3* (5), 531-539.

48. Scott, M. D.; Murad, K. L.; Koumpouras, F.; Talbot, M.; Eaton, J. W. Chemical camouflage of antigenic determinants: Stealth

erythrocytes. *Proceedings of the National Academy of Sciences of the United States of America* **1997,** *94* (14), 7566-7571.

49. Murad, K. T.; Mahany, K. L.; Brugnara, C.; Kuypers, F. A.; Eaton, J. W.; Scott, M. D. Structural and functional consequences of antigenic modulation of red blood cells with methoxypoly(ethylene glycol). *Blood* **1999,** *93* (6), 2121-2127.

50. Murad, K. L.; Gosselin, E. J.; Eaton, J. W.; Scott, M. D. Stealth cells: Prevention of major histocompatibility complex class II-mediated T-cell activation by cell surface modification. *Blood* **1999,** *94* (6), 2135-2141.

51. Scott, M. D.; Murad, K. L. Cellular camouflage: Fooling the immune system with polymers. *Current Pharmaceutical Design* **1998,** *4* (6), 423-438.

52. Scott, M. D.; Bradley, A. J.; Murad, K. L. Camouflaged blood cells: Low-technology bioengineering for transfusion medicine? *Transfusion Medicine Reviews* **2000,** *14* (1), 53-63.

53. Eugene, M. Polyethyleneglycols and immunocamouflage of the cells tissues and organs for transplantation. *Cellular and Molecular Biology* **2004,** *50* (3), 209-215.

54. Scott, M. D.; Murad, K. L.; Mahany, K. L.; Kuypers, F. A.; Brugnara, C.; Eaton, J. W. Antigenic and immunogenic attenuation of erythrocytes by cell surface modification with methoxy (polyethylene glycol). *Blood* **1997,** *90* (10), 1933.

55. Goldstein, J.; Siviglia, G.; Hurst, R.; Lenny, L.; Reich, L. Group-B erythrocytes enzymatically converted to group-O survive normally in A, B, and O individuals. *Science* **1982,** *215* (4529), 168-170.

56. Lenny, L. L.; Hurst, R.; Goldstein, J.; Benjamin, L. J.; Jones, R. L. Single-Unit Transfusions of rbc enzymatically converted from group-B to group-O to group-A and group-O Normal Volunteers. *Blood* **1991,** *77* (6), 1383-1388.

57. Lenny, L. L.; Hurst, R.; Zhu, A.; Goldstein, J.; Galbraith, R. A. Multiple-unit and second transfusions of red cells enzymatically converted from group B to group O: Report on the end of Phase 1 trials. *Transfusion* **1995,** *35* (11), 899-902.

58. Zhu, A.; Leng, L.; Monahan, C.; Zhang, Z. F.; Hurst, R.; Lenny, L.; Goldstein, J. Characterization of recombinant alpha-galactosidase for use in seroconversion from blood group B to O of human

erythrocytes. *Archives of Biochemistry and Biophysics* **1996,** *327* (2), 324-329.

59. Chen, A. M.; Scott, M. D. Current and future applications of immunological attenuation via pegylation of cells and tissue. *BioDrugs* **2001,** *15* (12), 833-847.

60. Jeong, S. T.; Byun, S. M. Decreased agglutinability of methoxy-polyethylene glycol attached red blood cells : Significance as a blood substitute. *Artificial Cells Blood Substitutes and Immobilization Biotechnology* **1996,** *24* (5), 503-511.

61. Hortin, G. L.; Huang, S. T. Surface-pegylated red cells as potential universal donor red cells. *Blood* **1996,** *88* (10), 713.

62. Hortin, G. L.; Lok, H. T.; Huang, S. T. Progress toward preparation of universal donor red cells. *Artificial Cells Blood Substitutes and Immobilization Biotechnology* **1997,** *25* (5), 487-491.

63. Armstrong, J. K.; Meiselman, H. J.; Fisher, T. C. Covalent binding of poly(ethylene glycol) (PEG) to the surface of red blood cells inhibits aggregation and reduces low shear blood viscosity. *American Journal of Hematology* **1997,** *56* (1), 26-28.

64. Nacharaju, P.; Boctor, F. N.; Manjula, B. N.; Acharya, S. A. Surface decoration of red blood cells with maleimidophenyl-polyethylene glycol facilitated by thiolation with iminothiolane: an approach to mask A, B, and D antigens to generate universal red blood cells. *Transfusion* **2005,** *45* (3), 374-383.

65. Garratty, G.; Leger, R.; Arndt, P.; Armstrong, J. K.; Meiselman, H. J.; Fisher, T. C. Polyethylene glycol treatment of RBCs can mask blood group antigens, but may also cause non-specific protein uptake. *Blood* **1997,** *90* (10), 2102.

66. Ong, K.; Dimacali, K.; Quintos, R. Decreased agglutinability of human erythrocytes by attachment of methoxy polyethylene glycol and the effect on erythrocyte oxygen-carrying ability. *Clin. Hemorheol. Microcirc.* **2003,** *29* (3-4), 401-407.

67. Garratty, G. Progress in modulating the RBC membrane to produce transfusable universal/stealth donor RBCs. *Transfusion Medicine Reviews* **2004,** *18* (4), 245-256.

68. Huang, S. T.; Huang, Z.; Marques, M. B.; Prchal, J. T. Adding methoxy polyethylene glycol to red blood cells coated with crosslinked polyethylene glycol-albumin prevents reaction with naturally

occurring antibodies while preserving red cell oxygen carrying capacity. *Transfusion* **1999,** *39* (10), 80S.

69. Armstrong, J. K.; Arndt, P. A.; Leger, R. M.; Meiselman, H. J.; Fisher, T. C. Reduction of autologous IgG uptake by poly(ethylene glycol)-coated red blood cells. *Transfusion* **2000,** *40* (10), 121S.

70. Bradley, A. J.; Murad, K. L.; Regan, K. L.; Scott, M. D. Biophysical consequences of linker chemistry and polymer size on stealth erythrocytes: size does matter. *Biochimica et Biophysica Acta-Biomembranes* **2002,** *1561* (2), 147-158.

71. Fisher, T. C.; Armstrong, J. K.; Meiselman, H. J.; Leger, R. M.; Garratty, G. Second generation poly(ethylene glycol) surface coatings for red blood cells. *Transfusion* **2000,** *40* (10), 119S.

72. Bradley, A. J.; Test, S. T.; Murad, K. L.; Mitsuyoshi, J.; Scott, M. D. Interactions of IgM ABO antibodies and complement with methoxy-PEG-modified human RBCs. *Transfusion* **2001,** *41* (10), 1225-1233.

73. Tan, Y.; Qiu, Y.; Xu, H.; Ji, S.; Li, S.; Gong, F.; Zhang, Y. Decreased immunorejection in unmatched blood transfusions by attachment of methoxypolyethylene glycol on human red blood cells and the effect on D antigen. *Transfusion* **2006,** *46* (12), 2122-2127.

74. Morgan, W. T. J. The human abo blood group substances. *Experientia* **1947,** *3* (7), 257-267.

75. Watkins, W. M.; Morgan, W. T. J. Inactivation of the H-receptors on human erythrocytes by an enzyme obtained from trichomonas-foetus. *British Journal of Experimental Pathology* **1954,** *35* (2), 181-190.

76. Zarnitz, M. L.; Kabat, E. A. Immunochemical studies on blood groups .25. the action of coffee bean alpha-galactosidase on blood group-B and group-Bp1 substances. *Journal of the American Chemical Society* **1960,** *82* (15), 3953-3957.

77. Yatziv, S.; Flowers, H. M. Action of -galactosidase on glycoprotein from human B-erythrocytes. *Biochem. Biophys. Res. Commun.* **1971,** *45* (2), 514-518.

78. Harpaz, N.; Flowers, H. M.; Sharon, N. Studies on B-antigenic sites of human erythrocytes by use of coffee bean alpha-galactosidase. *Archives of Biochemistry and Biophysics* **1975,** *170* (2), 676-683.

79. Lenny, L. L.; Hurst, R.; Goldstein, J.; Galbraith, R. A. Transfusions to group-O subjects of 2 units of red-cells enzymatically converted from group-B to group-O. *Transfusion* **1994,** *34* (3), 209-214.

80. Kruskall, M. S.; AuBuchon, J. P.; Anthony, K. Y.; Herschel, L.; Pickard, C.; Biehl, R.; Horowitz, M.; Brambilla, D. J.; Popovsky, M. A. Transfusion to blood group A and O patients of group B RBCs that have been enzymatically converted to group O. *Transfusion* **2000,** *40* (11), 1290-1298.

81. Goldstein, J. Conversion of ABO blood groups. *Transfusion Medicine Reviews* **1989,** *3* (3), 206-212.

82. Liu, Q. P.; Sulzenbacher, G.; Yuan, H.; Bennett, E. P.; Pietz, G.; Saunders, K.; Spence, J.; Nudelman, E.; Levery, S. B.; White, T.; Neveu, J. M.; Lane, W. S.; Bourne, Y.; Olsson, M. L.; Henrissat, B.; Clausen, H. Bacterial glycosidases for the production of universal red blood cells. *Nature Biotechnology* **2007,** *25* (4), 454-464.

83. Ehnert, S.; Glanemann, M.; Schmitt, A.; Vogt, S.; Shanny, N.; Nussler, N. C.; Stockle, U.; Nussler, A. The possible use of stem cells in regenerative medicine: dream or reality? *Langenbecks Archives of Surgery* **2009,** *394* (6), 985-997.

84. Timmins, N. E.; Nielsen, L. K. Blood cell manufacture: current methods and future challenges. *Trends in Biotechnology*. **2009,** *27* (7), 415-422.

85. Neildez-Nguyen, T. M. A.; Wajcman, H.; Marden, M. C.; Bensidhoum, M.; Moncollin, V.; Giarratana, M. C.; Kobari, L.; Thierry, D.; Douay, L. Human erythroid cells produced ex vivo at large scale differentiate into red blood cells in vivo. *Nature Biotechnology* **2002,** *20* (5), 467-472.

86. Douay, L. Cell culture for transfusion purposes: The concept of "cultured red blood cells". *Transfusion Clinique et Biologique* **2009,** *16* (2), 134-137.

87. Burke, S. E.; Barrett, C. J. pH-responsive properties of multilayered poly(L-lysine)/hyaluronic acid surfaces. *Biomacromolecules.* **2003,** *4* (6), 1773-1783.

88. Schonhoff, M. Self-assembled polyelectrolyte multilayers. *Current Opinion in Colloid & Interface Science* **2003,** *8* (1), 86-95.

89. Lvov, Y. M.; Sukhorukov, G. B. Protein architecture: Assembly of ordered films by means alternated adsorption of opposite charged

macromolecules. *Biologicheskie Membrany* **1997,** *14* (3), 229-250.

90. Chluba, J.; Voegel, J. C.; Decher, G.; Erbacher, P.; Schaaf, P.; Ogier, J. Peptide hormone covalently bound to polyelectrolytes and embedded into multilayer architectures conserving full biological activity. *Biomacromolecules* **2001,** *2* (3), 800-805.

91. Sukhorukov, G. B.; Susha, A. S.; Davis, S.; Leporatti, S.; Donath, E.; Hartmann, J.; Mohwald, H. Precipitation of inorganic salts inside hollow micrometer-sized polyelectrolyte shells. *Journal of Colloid and Interface Science* **2002,** *247* (1), 251-254.

92. Sukhorukov, G. B.; Donath, E.; Lichtenfeld, H.; Knippel, E.; Knippel, M.; Budde, A.; Mohwald, H. Layer-by-layer self assembly of polyelectrolytes on colloidal particles. *Colloids and Surfaces A-Physicochemical and Engineering Aspects* **1998,** *137* (1-3), 253-266.

93. Caruso, F.; Caruso, R. A.; Mohwald, H. Nanoengineering of inorganic and hybrid hollow spheres by colloidal templating. *Science* **1998,** *282* (5391), 1111-1114.

94. Donath, E.; Moya, S.; Neu, B.; Sukhorukov, G. B.; Georgieva, R.; Voigt, A.; Baumler, H.; Kiesewetter, H.; Mohwald, H. Hollow polymer shells from biological templates: Fabrication and potential applications. *Chemistry-A European Journal* **2002,** *8* (23), 5481-5485.

95. Farhat, T. R.; Schlenoff, J. B. Ion filtering by polyelectrolyte multilayers. *Abstracts of Papers of the American Chemical Society* **2001,** *221*, U380.

96. Farhat, T. R.; Schlenoff, J. B. Ion transport and equilibria in polyelectrolyte multilayers. *Langmuir* **2001,** *17* (4), 1184-1192.

97. Lösche, M.; Schmitt, j.; Decher, G.; Bouwman, W. G.; Kjaer, K. Detailed structure of molecularly thin polyelectrolyte multilayer films on solid substrates as revealed by neutron reflectometry. *Macromolecules* **1998,** *31*, 8893-8906.

98. Hubsch, E.; Ball, V.; Senger, B.; Decher, G.; Voegel, J. C.; Schaaf, P. Controlling the growth regime of polyelectrolyte multilayer films: Changing from exponential to linear growth by adjusting the composition of polyelectrolyte mixtures. *Langmuir* **2004,** *20* (5), 1980-1985.

99. DeLongchamp, D. M.; Kastantin, M.; Hammond, P. T. High-contrast electrochromism from layer-by-layer polymer films. *Chemistry of Materials* **2003,** *15* (8), 1575-1586.

100. Schoeler, B.; Poptoschev, E.; Caruso, F. Growth of multilayer films of fixed and variable charge density polyelectrolytes: Effect of mutual charge and secondary interactions. *Macromolecules* **2003,** *36* (14), 5258-5264.

101. Picart, C.; Mutterer, J.; Richert, L.; Luo, Y.; Prestwich, G. D.; Schaaf, P.; Voegel, J. C.; Lavalle, P. Molecular basis for the explanation of the exponential growth of polyelectrolyte multilayers. *Proceedings of the National Academy of Sciences of the United States of America* **2002,** *99* (20), 12531-12535.

102. Richert, L.; Lavalle, P.; Payan, E.; Shu, X. Z.; Prestwich, G. D.; Stoltz, J. F.; Schaaf, P.; Voegel, J. C.; Picart, C. Layer by layer buildup of polysaccharide films: Physical chemistry and cellular adhesion aspects. *Langmuir* **2004,** *20* (2), 448-458.

103. Kujawa, P.; Badia, A.; Winnik, F. M. Layer-by-layer self-assembly of hyaluronan and chitosan as viewed by SPR, fluorescence, and AFM. *Abstracts of Papers of the American Chemical Society* **2004,** *227*, U506.

104. Richert, L.; Boulmedais, F.; Lavalle, P.; Mutterer, J.; Ferreux, E.; Decher, G.; Schaaf, P.; Voegel, J. C.; Picart, C. Improvement of stability and cell adhesion properties of polyelectrolyte multilayer films by chemical cross-linking. *Biomacromolecules* **2004,** *5* (2), 284-294.

105. Kujawa, P.; Moraille, P.; Sanchez, J.; Badia, A.; Winnik, F. M. Effect of molecular weight on the exponential growth and morphology of hyaluronan/chitosan multilayers: A surface plasmon resonance spectroscopy and atomic force microscopy investigation. *Journal of the American Chemical Society* **2005,** *127* (25), 9224-9234.

106. Illum, L. Chitosan and its use as a pharmaceutical excipient. *Pharmaceutical Research* **1998,** *15* (9), 1326-1331.

107. Claesson, P. M.; Ninham, B. W. Ph-dependent interactions between adsorbed chitosan layers. *Langmuir* **1992,** *8* (5), 1406-1412.

108. Tiera, M. J.; Qiu, X. P.; Bechaouch, S.; Shi, Q.; Fernandes, J. C.; Winnik, F. M. Synthesis and characterization of phosphorylcholine-substituted chitosans soluble in physiological pH conditions. *Biomacromolecules* **2006,** *7* (11), 3151-3156.

109. Iwasaki, Y.; Aiba, Y.; Morimoto, N.; Nakabayashi, N.; Ishihara, K. Semi-interpenetrating polymer networks composed of biocompatible phospholipid polymer and segmented polyurethane. *Journal of Biomedical Materials Research* **2000,** *52* (4), 701-708.

110. Ishihara, K.; Oshida, H.; Endo, Y.; Ueda, T.; Watanabe, A.; Nakabayashi, N. Hemocompatibility of human whole-blood on polymers with a phospholipid polar group and its mechanism. *Journal of Biomedical Materials Research* **1992,** *26* (12), 1543-1552.

111. Sugano, M.; Watanabe, S.; Kishi, A.; Izume, M.; Ohtakara, A. Hypocholesterolemic action of chitosans with different viscosity in rats. *Lipids* **1988,** *23* (3), 187-191.

112. Lim, B. O.; Yamada, K.; Nonaka, M.; Kuramoto, Y.; Hung, P.; Sugano, M. Dietary fibers modulate indices of intestinal immune function in rats. *Journal of Nutrition* **1997,** *127* (5), 663-667.

113. Miyazaki, S.; Ishii, K.; Nadai, T. The use of chitin and chitosan as drug carriers. *Chemical & Pharmaceutical Bulletin* **1981,** *29* (10), 3067-3069.

114. Tomihata, K.; Ikada, Y. In vitro and in vivo degradation of films of chitin and its deacetylated derivatives. *Biomaterials* **1997,** *18* (7), 567-575.

115. Muzzarelli, R. A. A. Biochemical significance of exogenous chitins and chitosans in animals and patients. *Carbohydrate Polymers* **1993,** *20* (1), 7-16.

116. Benesch, J.; Tengvall, P. Blood protein adsorption onto chitosan. *Biomaterials* **2002,** *23* (12), 2561-2568.

117. Remminghorst, U.; Rehm, B. H. A. Bacterial alginates: from biosynthesis to applications. *Biotechnology Letters* **2006,** *28* (21), 1701-1712.

118. Ertesvag, H.; Valla, S. Biosynthesis and applications of alginates. *Polymer Degradation and Stability* **1998,** *59* (1-3), 85-91.

119. Jain, S.; Mondal, K.; Gupta, M. N. Applications of alginate in bioseparation of proteins. *Artificial Cells Blood Substitutes and Biotechnology* **2006,** *34* (2), 127-144.

120. Skjakbraek, G.; Grasdalen, H.; Smidsrod, O. Inhomogeneous polysaccharide ionic gels. *Carbohydrate Polymers* **1989,** *10* (1), 31-54.

121. Grant, G. T.; Morris, E. R.; Rees, D. A.; Smith, P. J. C.; Thom, D. Biological interactions between polysaccharides and divalent cations - Egg-Box model. *Febs Letters* **1973,** *32* (1), 195-198.

122. Smidsrod, O.; Haug, A. Dependence Upon Uronic Acid Composition of Some Ion-Exchange Properties of Alginates. *Acta Chemica Scandinavica* **1968,** *22* (6), 1989-&.

123. Brownlee, I. A.; Allen, A.; Pearson, J. P.; Dettmar, P. W.; Havler, M. E.; Atherton, M. R.; Onsoyen, E. Alginate as a source of dietary fiber. *Critical Reviews in Food Science and Nutrition* **2005,** *45* (6), 497-510.

124. Jones, V.; Grey, J. E.; Harding, K. G. ABC of wound healing - Wound dressings. *British Medical Journal* **2006,** *332* (7544), 777-780.

125. Chen, H. M.; Wei, O. Y.; Jones, M.; Metz, T.; Martoni, C.; Haque, T.; Cohen, R.; Lawuyi, B.; Prakash, S. Preparation and characterization of novel polymeric microcapsules for live cell encapsulation and therapy. *Cell Biochemistry and Biophysics* **2007,** *47* (1), 159-167.

126. Haque, T.; Chen, H.; Ouyang, W.; Martoni, C.; Lawuyi, B.; Urbanska, A.; Prakash, S. Investigation of a new microcapsule membrane combining alginate, chitosan, polyethylene glycol and poly-L-lysine for cell transplantation applications. *International Journal of Artificial Organs* **2005,** *28* (6), 631-637.

127. Tam, S. K.; Dusseault, J.; Polizu, S.; Menard, M.; Halle, J. P.; Yahia, L. Impact of residual contamination on the biofunctional properties of purified alginates used for cell encapsulation. *Biomaterials* **2006,** *27* (8), 1296-1305.

128. Ciofani, G.; Raffa, V.; Menciassi, A.; Micera, S.; Dario, P. A drug delivery system based on alginate microspheres: Mass-transport test and in vitro validation. *Biomedical Microdevices* **2007,** *9* (3), 395-403.

129. Zhao, Q. H.; Han, B. S.; Wang, Z. H.; Gao, C. Y.; Peng, C. H.; Shen, J. C. Hollow chitosan-alginate multilayer microcapsules as drug delivery vehicle: doxorubicin loading and in vitro and in vivo studies. *Nanomedicine-Nanotechnology Biology and Medicine* **2007,** *3* (1), 63-74.

130. Qurrat, u. A.; Sharma, S.; Khuller, G. K.; Garg, S. K. Alginate-based oral drug delivery system for tuberculosis: pharmacokinetics and therapeutic effects. *Journal of Antimicrobial Chemotherapy* **2003,** *51* (4), 931-938.

131. Aggarwal, N.; HogenEsch, H.; Guo, P. X.; North, A.; Suckow, M.; Mittal, S. K. Biodegradable alginate microspheres as a delivery system for naked DNA. *Canadian Journal of Veterinary Research-Revue Canadienne de Recherche Veterinaire* **1999,** *63* (2), 148-152.

132. Kakiuchi, K.; Akutsu, H. Hydrodynamic behavior and molecular-conformation of poly(L-Lysine Hbr) in carbonate buffer solution. *Biopolymers* **1981,** *20* (2), 345-357.

133. Wagner, M. S.; Pasche, S.; Castner, D. G.; Textor, M. Characterization of poly(L-lysine)-graft-poly(ethylene glycol) assembled monolayers on niobium pentoxide substrates using time-of-flight secondary ion mass spectrometry and multivariate analysis. *Analytical Chemistry* **2004,** *76* (5), 1483-1492.

134. Yoshida, T.; Nagasawa, T. epsilon-Poly-L-lysine: microbial production, biodegradation and application potential. *Applied Microbiology and Biotechnology* **2003,** *62* (1), 21-26.

135. Huang, N. P.; Michel, R.; Voros, J.; Textor, M.; Hofer, R.; Rossi, A.; Elbert, D. L.; Hubbell, J. A.; Spencer, N. D. Poly(L-lysine)-g-poly(ethylene glycol) layers on metal oxide surfaces: Surface-analytical characterization and resistance to serum and fibrinogen adsorption. *Langmuir* **2001,** *17* (2), 489-498.

136. Pasche, S.; De Paul, S. M.; Voros, J.; Spencer, N. D.; Textor, M. Poly(L-lysine)-graft-poly(ethylene glycol) assembled monolayers on niobium oxide surfaces: A quantitative study of the influence of polymer interfacial architecture on resistance to protein adsorption by ToF-SIMS and in situ OWLS. *Langmuir* **2003,** *19* (22), 9216-9225.

137. Wattendorf, U.; Koch, M. C.; Walter, E.; Voeroes, J.; Textor, M.; Merkle, H. P. Phagocytosis of poly(L-lysine)-graft-poly(ethylene glycol) coated microspheres by antigen presenting cells: Impact of grafting ratio and poly(ethylene glycol) chain length on cellular recognition. *Biointerphases* **2006,** *1* (4), 123-133.

138. Laurent, T. C. Biochemistry of hyaluronan. *Acta Oto-Laryngologica* **1987,** 7-24.

139. Fraser, J. R. E.; Laurent, T. C.; Laurent, U. B. G. Hyaluronan: Its nature, distribution, functions and turnover. *Journal of Internal Medicine* **1997,** *242* (1), 27-33.

140. Fraser, J. R. E.; Pertoft, H.; Alstonsmith, J.; Laurent, T. C. Uptake of Hyaluronan in hepatic endothelial-cells is not directly affected by

endotoxin and associated cytokines. *Experimental Cell Research* **1991,** *197* (1), 8-11.

141. Presti, D.; Scott, J. E. Hyaluronan-mediated protective effect against cell-damage caused by enzymatically produced hydroxyl (oh-center-dot) radicals is dependent on hyaluronan molecular-mass. *Cell Biochemistry and Function* **1994,** *12* (4), 281-288.

142. Xu, H. P.; Ito, T.; Tawada, A.; Maeda, H.; Yamanokuchi, H.; Isahara, K.; Yoshida, K.; Uchiyama, Y.; Asari, A. Effect of hyaluronan oligosaccharides on the expression of heat shock protein 72. *Journal of Biological Chemistry* **2002,** *277* (19), 17308-17314.

143. Decher, G. and Schneider, A. Multilayer thin films.Sequential assembly of nanocomposite materials. Wiley-VCH Verlag GmbH & Co. KGaA. **2002**

144. Sauerbrey, G. Verwendung Von Schwingquarzen Zur Wagung Dunner Schichten und Zur Mikrowagung. *Zeitschrift fur Physik* **1959,** *155* (2), 206-222.

145. Voinova, M. V.; Rodahl, M.; Jonson, M.; Kasemo, B. Viscoelastic acoustic response of layered polymer films at fluid-solid interfaces: Continuum mechanics approach. *Physica Scripta* **1999,** *59* (5), 391-396.

146. Voinova, M. V.; Jonson, M.; Kasemo, B. 'Missing mass' effect in biosensor's QCM applications. *Biosensors & Bioelectronics* **2002,** *17* (10), 835-841.

147. Decher, G.; Hong, J. D.; Schmitt, J. Buildup of ultrathin multilayer films by a self-assembly process. 3. Consecutively alternating adsorption of anionic and cationic polyelectrolytes on charged surfaces. *Thin Solid Films* **1992,** *210* (1-2), 831-835.

148. Decher, G. Fuzzy nanoassemblies: Toward layered polymeric multicomposites. *Science* **1997,** *277* (5330), 1232-1237.

149. Forzani, E. S.; Otero, M.; Perez, M. A.; Teijelo, M. L.; Calvo, E. J. The structure of layer-by-layer self-assembled glucose oxidase and Os(Bpy)(2)ClPyCH2NH-Poly(allylamine) multilayers: Ellipsometric and quartz crystal microbalance studies. *Langmuir* **2002,** *18* (10), 4020-4029.

150. Krasemann, L.; Tieke, B. Selective ion transport across self-assembled alternating multilayers of cationic and anionic polyelectrolytes. *Langmuir* **2000,** *16* (2), 287-290.

151. Khopade, A. J.; Caruso, F. Stepwise self-assembled poly(amidoamine) dendrimer and poly(styrenesulfonate) microcapsules as sustained delivery vehicles. *Biomacromolecules* **2002,** *3* (6), 1154-1162.

152. Decher, G.; Hong, J. D. Buildup of ultrathin multilayer films by a self-assembly process. 2. consecutive adsorption of anionic and cationic bipolar amphiphiles and polyelectrolytes on charged surfaces. *Berichte der Bunsen-Gesellschaft-Physical Chemistry Chemical Physics* **1991,** *95* (11), 1430-1434.

153. Lvov, Y.; Decher, G.; Sukhorukov, G. Assembly of thin-films by means of successive deposition of alternate layers of DNA and poly(Allylamine). *Macromolecules* **1993,** *26* (20), 5396-5399.

154. Lvov, Y.; Decher, G.; Mohwald, H. Assembly, Structural characterization, and thermal-behavior of layer-by-layer deposited ultrathin films of poly(vinyl sulfate) and poly(allylamine). *Langmuir* **1993,** *9* (2), 481-486.

155. Bertrand, P.; Jonas, A.; Laschewsky, A.; Legras, R. Ultrathin polymer coatings by complexation of polyelectrolytes at interfaces: suitable materials, structure and properties. *Macromolecular Rapid Communications* **2000,** *21* (7), 319-348.

156. Voigt, A.; Lichtenfeld, H.; Sukhorukov, G. B.; Zastrow, H.; Donath, E.; Baumler, H.; Mohwald, H. Membrane filtration for microencapsulation and microcapsules fabrication by layer-by-layer polyelectrolyte adsorption. *Industrial & Engineering Chemistry Research* **1999,** *38* (10), 4037-4043.

157. Shiratori, S. S.; Rubner, M. F. pH-dependent thickness behavior of sequentially adsorbed layers of weak polyelectrolytes. *Macromolecules* **2000,** *33* (11), 4213-4219.

158. Shen, L.; Hu, N. Electrostatic adsorption of heme proteins alternated with polyamidoamine dendrimers for layer-by-layer assembly of electroactive films. *Biomacromolecules* **2005,** *6* (3), 1475-1483.

159. Vinogradova, O. I.; Lebedeva, O. V.; Vasilev, K.; Gong, H. F.; Garcia-Turiel, J.; Kim, B. S. Multilayer DNA/poly(allylamine hydrochloride) microcapsules: Assembly and mechanical properties. *Biomacromolecules* **2005,** *6* (3), 1495-1502.

160. Kleinfeld, E. R.; Ferguson, G. S. Stepwise formation of multilayered nanostructural films from macromolecular precursors. *Science* **1994,** *265* (5170), 370-373.

161. Yoon, H. C.; Hong, M. Y.; Kim, H. S. Functionalization of a poly(amidoamine) dendrimer with ferrocenyls and its application to the construction of a reagentless enzyme electrode. *Anal. Chem.* **2000,** *72* (18), 4420-4427.

162. Kotov, N. A.; Dekany, I.; Fendler, J. H. Layer-by-layer self-assembly of polyelectrolyte-semiconductor nanoparticle composite films. *Journal of Physical Chemistry* **1995,** *99* (35), 13065-13069.

163. Cheng, L.; Dong, S. J. A novel potentiodynamic method of electrochemical growth for layer-by-layer film formation based on electrostatic interaction. *Electrochemistry Communications* **1999,** *1* (5), 159-162.

164. Caruso, F. Hollow inorganic capsules via colloid-templated layer-by-layer electrostatic assembly. *Colloid Chemistry Ii* **2003,** *227*, 145-168.

165. Tong, W. J.; Gao, C. Y. Layer-by-layer assembled microcapsules: Fabrication, stimuli-responsivity, loading and release. *Chemical Journal of Chinese Universities-Chinese* **2008,** *29* (7), 1285-1298.

166. Kwon, I. C.; Bae, Y. H.; Kim, S. W. Electrically erodible polymer gel for controlled release of drugs. *Nature* **1991,** *354* (6351), 291-293.

167. Hillberg, A. L.; Tabrizian, M. Biorecognition through layer-by-layer polyelectrolyte assembly: In-situ hybridization on living cells. *Biomacromolecules* **2006,** *7* (10), 2742-2750.

168. Veerabadran, N. G.; Goli, P. L.; Stewart-Clark, S. S.; Lvov, Y. M.; Mills, D. K. Nanoencapsulation of stem cells within polyelectrolyte multilayer shells. *Macromolecular Bioscience* **2007,** *7* (7), 877-882.

169. vonKlitzing, R.; Mohwald, H. A realistic diffusion model for ultrathin polyelectrolyte films. *Macromolecules* **1996,** *29* (21), 6901-6906.

170. Harris, J. J.; Bruening, M. L. Electrochemical and in situ ellipsometric investigation of the permeability and stability of layered polyelectrolyte films. *Langmuir* **2000,** *16* (4), 2006-2013.

171. Antipov, A. A.; Sukhorukov, G. B.; Mohwald, H. Influence of the ionic strength on the polyelectrolyte multilayers' permeability. *Langmuir* **2003,** *19* (6), 2444-2448.

172. Johnston, A. P. R.; Caruso, F. A molecular beacon approach to measuring the DNA permeability of thin films. *Journal of the American Chemical Society* **2005,** *127* (28), 10014-10015.

173. Angelatos, A. S.; Johnston, A. P. R.; Wang, Y. J.; Caruso, F. Probing the permeability of polyelectrolyte multilayer capsules via a molecular beacon approach. *Langmuir* **2007,** *23* (8), 4554-4562.

174. Steitz, R.; Leiner, V.; Siebrecht, R.; von Klitzing, R. Influence of the ionic strength on the structure of polyelectrolyte films at the solid/liquid interface. *Colloids and Surfaces A-Physicochemical and Engineering Aspects* **2000,** *163* (1), 63-70.

175. Fery, A.; Scholer, B.; Cassagneau, T.; Caruso, F. Nanoporous thin films formed by salt-induced structural changes in multilayers of poly(acrylic acid) and poly(allylamine). *Langmuir* **2001,** *17* (13), 3779-3783.

176. Lu, H.; Hu, N. Salt-induced swelling and electrochemical property change of hyaluronic acid/myoglobin multilayer films. *J. Phys. Chem. B* **2007,** *111* (8), 1984-1993.

177. Shenoy, D. B.; Antipov, A. A.; Sukhorukov, G. B.; Mohwald, H. Layer-by-layer engineering of biocompatible, decomposable core-shell structures. *Biomacromolecules* **2003,** *4* (2), 265-272.

178. Kujawa, P.; Sanchez, J.; Badia, A.; Winnik, F. M. Probing the stability of biocompatible sodium hyaluronate/chitosan nanocoatings against changes in salinity and pH. *Journal of Nanoscience and Nanotechnology* **2006,** *6* (6), 1565-1574.

179. Zhang, J. T.; Chua, L. S.; Lynn, D. M. Multilayered thin films that sustain the release of functional DNA under physiological conditions. *Langmuir* **2004,** *20* (19), 8015-8021.

180. Minagawa, M.; Tanioka, A.; Ramirez, P.; Mafe, S. Amino acid transport through cation exchange membranes: Effects of pH on interfacial transport. *Journal of Colloid and Interface Science* **1997,** *188* (1), 176-182.

181. Minagawa, M.; Tanioka, A. Leucine transport through cation exchange membranes, effects of HCl concentration on interfacial transport. *Journal of Colloid and Interface Science* **1998,** *202* (1), 149-154.

182. Jimbo, T.; Tanioka, A.; Minoura, N. Characterization of an amphoteric-charged layer grafted to the pore surface of a porous membrane. *Langmuir* **1998,** *14* (25), 7112-7118.

183. Ramirez, P.; Alcaraz, A.; Mafe, S.; Pellicer, J. pH and supporting electrolyte concentration effects on the passive transport of cationic and anionic drugs through fixed charge membranes. *Journal of Membrane Science* **1999,** *161* (1-2), 143-155.

184. Ramirez, P.; Mafe, S.; Alcaraz, A.; Cervera, J. Modeling of pH-switchable ion transport and selectivity in nanopore membranes with fixed charges. *Journal of Physical Chemistry B* **2003,** *107* (47), 13178-13187.

185. Nishizawa, M.; Menon, V. P.; Martin, C. R. Metal nanotubule membranes with electrochemically switchable ion-transport selectivity. *Science* **1995,** *268* (5211), 700-702.

186. Martin, C. R.; Nishizawa, M.; Jirage, K.; Kang, M. S.; Lee, S. B. Controlling ion-transport selectivity in gold nanotubule membranes. *Advanced Materials* **2001,** *13* (18), 1351-1362.

187. Lee, S. B.; Martin, C. R. Controlling the transport properties of gold nanotubule membranes using chemisorbed thiols. *Chemistry of Materials* **2001,** *13* (10), 3236-3244.

188. Lee, S. B.; Martin, C. R. pH-switchable, ion-permselective gold nanotubule membrane based on chemisorbed cysteine. *Analytical Chemistry* **2001,** *73* (4), 768-775.

189. Balogh, L. P.; Redmond, S. M.; Balogh, P.; Tang, H.; Martin, D. C.; Rand, S. C. Self assembly and optical properties of dendrimer nanocomposite multilayers. *Macromolecular Bioscience* **2007,** *7* (8), 1032-1046.

190. Elzieciak, A.; Zapotoczny, S.; Nowak, P.; Krastev, R.; Nowakowska, M.; Warszynski, P. Influence of pH on the structure of multilayer films composed of strong and weak polyelectrolytes. *Langmuir* **2009,** *25* (5), 3255-3259.

191. Harris, J. J.; Derose, P. M.; Bruening, M. L. Synthesis of passivating, nylon-like coatings through cross-linking of ultrathin polyelectrolyte films. *Journal of the American Chemical Society* **1999,** *121* (9), 1978-1979.

192. Harris, J. J.; Stair, J. L.; Bruening, M. L. Layered polyelectrolyte films as selective, ultrathin barriers for anion transport. *Chemistry of Materials* **2000,** *12* (7), 1941-1946.

193. Stair, J. L.; Harris, J. J.; Bruening, M. L. Enhancement of the ion-transport selectivity of layered polyelectrolyte membranes through cross-linking and hybridization. *Chemistry of Materials* **2001,** *13* (8), 2641-2648.

194. Bruening, M. L.; Sullivan, D. M. Enhancing the ion-transport selectivity of multilayer polyelectrolyte membranes. *Chemistry-A European Journal* **2002,** *8* (17), 3833-3837.

195. Dai, J. H.; Jensen, A. W.; Mohanty, D. K.; Erndt, J.; Bruening, M. L. Controlling the permeability of multilayered polyelectrolyte films through derivatization, cross-linking, and hydrolysis. *Langmuir* **2001,** *17* (3), 931-937.

196. Dai, J. H.; Balachandra, A. M.; Lee, J. I.; Bruening, M. L. Controlling ion transport through multilayer polyelectrolyte membranes by derivatization with photolabile functional groups. *Macromolecules* **2002,** *35* (8), 3164-3170.

197. Park, M. K.; Deng, S. X.; Advincula, R. C. pH-sensitive bipolar ion-permselective ultrathin films. *Journal of the American Chemical Society* **2004,** *126* (42), 13723-13731.

198. Ibarz, G.; Dahne, L.; Donath, E.; Mohwald, H. Resealing of polyelectrolyte capsules after core removal. *Macromolecular Rapid Communications* **2002,** *23* (8), 474-478.

199. Qiu, X. P.; Donath, E.; Mohwald, H. Permeability of ibuprofen in various polyelectrolyte multilayers. *Macromolecular Materials and Engineering* **2001,** *286* (10), 591-597.

200. Antipov, A. A.; Sukhorukov, G. B.; Mohwald, H. Influence of the ionic strength on the polyelectrolyte multilayers' permeability. *Langmuir* **2003,** *19* (6), 2444-2448.

201. Ai, H.; Jones, S. A.; De Villiers, M. M.; Lvov, Y. M. Nano-encapsulation of furosemide microcrystals for controlled drug release. *Journal of Controlled Release* **2003,** *86* (1), 59-68.

202. Qiu, X. P.; Leporatti, S.; Donath, E.; Mohwald, H. Studies on the drug release properties of polysaccharide multilayers encapsulated ibuprofen microparticles. *Langmuir* **2001,** *17* (17), 5375-5380.

203. Pargaonkar, N.; Lvov, Y. M.; Li, N.; Steenekamp, J. H.; De Villiers, M. M. Controlled release of dexamethasone from microcapsules produced by polyelectrolyte layer-by-layer nanoassembly. *Pharmaceutical Research* **2005,** *22* (5), 826-835.

204. Chen, Y.; Lin, X. Studies on the drug release properties of nano-encapsulated indomethacin microparticles. *Journal of Microencapsulation* **2005,** *22* (1), 47-55.

205. Thierry, B.; Kujawa, P.; Tkaczyk, C.; Winnik, F. M.; Bilodeau, L.; Tabrizian, M. Delivery platform for hydrophobic drugs: Prodrug approach combined with self-assembled multilayers. *Journal of the American Chemical Society* **2005,** *127* (6), 1626-1627.

206. Ren, K. F.; Ji, J.; Shen, J. C. Construction of polycation-based non-viral DNA nanoparticles and polyanion multilayers via layer-by-layer self-assembly. *Macromolecular Rapid Communications* **2005,** *26* (20), 1633-1638.

207. Haidar, Z. S.; Hamdy, R. C.; Tabrizian, M. Protein release kinetics for core-shell hybrid nanoparticles based on the layer-by-layer assembly of alginate and chitosan on liposomes. *Biomaterials* **2008,** *29* (9), 1207-1215.

208. Antipov, A. A.; Sukhorukov, G. B.; Donath, E.; Mohwald, H. Sustained release properties of polyelectrolyte multilayer capsules. *Journal of Physical Chemistry B* **2001,** *105* (12), 2281-2284.

209. An, Z. H.; Lu, G.; Mohwald, H.; Li, J. B. Self-assembly of human serum albumin (HSA) and L-alpha-dimyristoylphosphatidic acid (DMPA) microcapsules for controlled drug release. *Chemistry-A European Journal* **2004,** *10* (22), 5848-5852.

210. Fan, Y. F.; Wang, Y. N.; Fan, Y. G.; Ma, J. B. Preparation of insulin nanoparticles and their encapsulation with biodegradable polyelectrolytes via the layer-by-layer adsorption. *International Journal of Pharmaceutics* **2006,** *324* (2), 158-167.

211. Haidar, Z.; Hamdy, R.; Tabrizian, M. A novel OP-1 delivery system for the potential acceleration of regenerate formation and consolidation in distraction osteogenesis. *Bone* **2008,** *43*, S51.

212. An, Z.; Mohwald, H.; Li, J. pH controlled permeability of lipid/protein biomimetic microcapsules. *Biomacromolecules* **2006,** *7* (2), 580-585.

213. Olivieri, J. R.; Craievich, A. F. The subdomain structure of human serum albumin in solution under different pH conditions studied by small angle X-ray scattering. *Eur. Biophys. J.* **1995,** *24* (2), 77-84.

214. Wang, C. Y.; He, C. Y.; Tong, Z.; Liu, X. X.; Ren, B. Y.; Zeng, F. Combination of adsorption by porous CaCO3 microparticles and encapsulation by polyelectrolyte multilayer films for sustained drug delivery. *International Journal of Pharmaceutics* **2006,** *308* (1-2), 160-167.

215. Picart, C.; Schneider, A.; Etienne, O.; Mutterer, J.; Schaaf, P.; Egles, C.; Jessel, N.; Voegel, J. C. Controlled degradability of polysaccharide multilayer films in vitro and in vivo. *Advanced Functional Materials* **2005,** *15* (11), 1771-1780.

216. Antipov, A. A.; Sukhorukov, G. B.; Leporatti, S.; Radtchenko, I. L.; Donath, E.; Mohwald, H. Polyelectrolyte multilayer capsule permeability control. *Colloids and Surfaces A-Physicochemical and Engineering Aspects* **2002,** *198*, 535-541.

217. Damge, C.; Vranckx, H.; Balschmidt, P.; Couvreur, P. Poly(alkyl cyanoacrylate) nanospheres for oral administration of insulin. *Journal of Pharmaceutical Sciences* **1997,** *86* (12), 1403-1409.

218. Pecheur, E. I.; Hoekstra, D.; SainteMarie, J.; Maurin, L.; Bienvenue, A.; Philippot, J. R. Membrane anchorage brings about fusogenic properties in a short synthetic peptide. *Biochemistry* **1997,** *36* (13), 3773-3781.

219. Caruso, F. Nanoengineering of particle surfaces. *Advanced Materials* **2001,** *13* (1), 11-+.

220. Peyratout, C. S.; Dahne, L. Tailor-made polyelectrolyte microcapsules: From multilayers to smart containers. *Angewandte Chemie-International Edition* **2004,** *43* (29), 3762-3783.

221. Haynie, D. T.; Balkundi, S.; Palath, N.; Chakravarthula, K.; Dave, K. Polypeptide multilayer films: Role of molecular structure and charge. *Langmuir* **2004,** *20* (11), 4540-4547.

222. Serizawa, T.; Yamaguchi, M.; Akashi, M. Alternating bioactivity of polymeric layer-by-layer assemblies: Anticoagulation vs procoagulation of human blood. *Biomacromolecules* **2002,** *3* (4), 724-731.

223. Ye, S. Q.; Wang, C. Y.; Liu, X. X.; Tong, Z. Deposition temperature effect on release rate of indomethacin microcrystals from microcapsules of layer-by-layer assembled chitosan and alginate multilayer films. *Journal of Controlled Release* **2005,** *106* (3), 319-328.

224. Wang, C. Y.; Ye, S. Q.; Dai, L.; Liu, X. X.; Tong, Z. Enhanced resistance of polyelectrolyte multilayer microcapsules to pepsin erosion and release properties of encapsulated indomethacin. *Biomacromolecules* **2007,** *8* (5), 1739-1744.

225. Berth, G.; Voigt, A.; Dautzenberg, H.; Donath, E.; Mohwald, H. Polyelectrolyte complexes and layer-by-layer capsules from chitosan/chitosan sulfate. *Biomacromolecules* **2002,** *3* (3), 579-590.

226. vonKlitzing, R.; Mohwald, H. Transport through ultrathin polyelectrolyte films. *Thin Solid Films* **1996,** *285*, 352-356.

227. Choi, J. W.; Nam, Y. S.; Fujihira, M. Nanoscale fabrication of biomolecular layer and its application to biodevices. *Biotechnology and Bioprocess Engineering* **2004,** *9* (2), 76-85.

228. Chinnayelka, S.; McShane, M. J. Microcapsule biosensors using competitive binding resonance energy transfer assays based on apoenzymes. *Analytical Chemistry* **2005,** *77* (17), 5501-5511.

229. Antipov, A. A.; Sukhorukov, G. B. Polyelectrolyte multilayer capsules as vehicles with tunable permeability. *Adv. Colloid Interface Sci.* **2004,** *111* (1-2), 49-61.

230. Scott, M. D.; Murad, K. L. Reproducibility of red cell pegylation on the immunocamouflage of non-ABO antigens. *Blood* **2000,** *96* (11), 110B.

231. Neu, B.; Voigt, A.; Mitlohner, R.; Leporatti, S.; Gao, C. Y.; Donath, E.; Kiesewetter, H.; Mohwald, H.; Meiselman, H. J.; Baumler, H. Biological cells as templates for hollow microcapsules. *Journal of Microencapsulation* **2001,** *18* (3), 385-395.

232. Hargittai, I.; Hargittai, M. Molecular structure of hyaluronan: an introduction. *Structural Chemistry* **2008,** *19* (5), 697-717.

233. Schneider, A.; Vodouhe, C.; Richert, L.; Francius, G.; Le Guen, E.; Schaaf, P.; Voegel, J. C.; Frisch, B.; Picart, C. Multifunctional polyelectrolyte multilayer films: Combining mechanical resistance, biodegradability, and bioactivity. *Biomacromolecules* **2007,** *8* (1), 139-145.

234. Szarpak, A.; Pignot-Paintrand, I.; Nicolas, C.; Picart, C.; Auzely-Velty, R. Multilayer assembly of hyaluronic acid/poly(allylamine): Control of the buildup for the production of hollow capsules. *Langmuir* **2008,** *24* (17), 9767-9774.

235. Krol, S.; del Guerra, S.; Grupillo, M.; Diaspro, A.; Gliozzi, A.; Marchetti, P. Multilayer nanoencapsulation. New approach for immune protection of human pancreatic islets. *Nano Letters* **2006,** *6* (9), 1933-1939.

236. Orive, G.; Carcaboso, A. M.; Hernandez, R. M.; Gascon, A. R.; Pedraz, J. L. Biocompatibility evaluation of different alginates and alginate-based microcapsules. *Biomacromolecules* **2005,** *6* (2), 927-931.

237. Devos, P.; DeHaan, B.; VanSchilfgaarde, R. Effect of the alginate composition on the biocompatibility of alginate-polylysine microcapsules. *Biomaterials* **1997,** *18* (3), 273-278.

238. Mansouri, S.; Lavigne, P.; Corsi, K.; Benderdour, M.; Beaumont, E.; Fernandes, J. C. Chitosan-DNA nanoparticles as non-viral vectors in gene therapy: strategies to improve transfection efficacy. *European Journal of Pharmaceutics and Biopharmaceutics* **2004,** *57* (1), 1-8.

239. Carrigan, S. D.; Scott, G.; Tabrizian, M. Real-time QCM-D immunoassay through oriented antibody immobilization using cross-linked hydrogel biointerfaces. *Langmuir* **2005,** *21* (13), 5966-5973.

240. Carrigan, S. D.; Scott, G.; Tabrizian, M. Rapid three-dimensional biointerfaces for real-time immunoassay using hIL-18BPa as a model antigen. *Biomaterials* **2005,** *26* (35), 7514-7523.

241. Fatisson, J.; Merhi, Y.; Tabrizian, M. Quantifying blood platelet morphological changes by dissipation factor monitoring in multilayer shells. *Langmuir* **2008,** *24* (7), 3294-3299.

242. Tooney, N. M.; Mosesson, M. W.; Amrani, D. L.; Hainfeld, J. F.; Wall, J. S. Solution and Surface Effects on Plasma Fibronectin Structure. *Journal of Cell Biology* **1983,** *97* (6), 1686-1692.

243. Scott, M. D.; Mahany, K. L.; Bradley, A. J.; Murad, K. L. Size does matter: Immunocamouflage of erythrocyte antigens by methoxypoly(ethylene glycol). *Blood* **2000,** *96* (11), 64A.

244. Kujawa, P.; Schmauch, G.; Viitala, T.; Badia, A.; Winnik, F. M. Construction of viscoelastic biocompatible films via the layer-by-layer assembly of hyaluronan and phosphorylcholine-modified chitosan. *Biomacromolecules* **2007,** *8* (10), 3169-3176.

245. Kakita, H.; Kamishima, H. Some properties of alginate gels derived from algal sodium alginate. *Journal of Applied Phycology* **2008,** *20* (5), 543-549.

246. Lecak, J.; Scott, K.; Young, C.; Hannon, J.; Acker, J. P. Evaluation of red blood cells stored at-80 degrees C in excess of 10 years. *Transfusion* **2004,** *44* (9), 1306-+.

247. Salloum, D. S.; Schlenoff, J. B. Protein adsorption modalities on polyelectrolyte multilayers. *Biomacromolecules* **2004,** *5* (3), 1089-1096.

248. Galeska, I.; Chattopadhyay, D.; Moussy, F.; Papadimitrakopoulos, F. Calcification-resistant nafion/Fe3+ assemblies for implantable biosensors. *Biomacromolecules* **2000,** *1* (2), 202-207.

249. Miyazawa, K.; Winnik, F. M. Solution properties of phosphorylcholine-based hydrophobically modified polybetaines in water and mixed solvents. *Macromolecules* **2002,** *35* (25), 9536-9544.

250. Boehm, D.; Murphy, W. G.; Al Rubeai, M. The potential of human peripheral blood derived CD34+ cells for ex vivo red blood cell production. *J. Biotechnol.* **2009**.

251. Fakhrullin, R. F.; Zamaleeva, A. I.; Morozov, M. V.; Tazetdinova, D. I.; Alimova, F. K.; Hilmutdinov, A. K.; Zhdanov, R. I.; Kahraman, M.; Culha, M. Living fungi cells encapsulated in polyelectrolyte shells doped with metal nanoparticles. *Langmuir* **2009,** *25* (8), 4628-4634.

252. Semenov, O. V.; Malek, A.; Bittermann, A. G.; Voros, J.; Zisch, A. H. Engineered polyelectrolyte multilayer substrates for adhesion, proliferation, and differentiation of human mesenchymal stem cells. *Tissue Eng Part A* **2009,** *15* (10), 2977-2990.

253. Ai, H.; Fang, M.; Jones, S. A.; Lvov, Y. M. Electrostatic layer-by-layer nanoassembly on biological microtemplates: Platelets. *Biomacromolecules* **2002,** *3* (3), 560-564.

254. Kizilel, S.; Scavone, A.; Liu, X.; Nothias, J. M.; Ostrega, D.; Witkowski, P.; Millis, M. Encapsulation of Pancreatic Islets Within Nano-Thin Functional Polyethylene Glycol Coatings for Enhanced Insulin Secretion. *Tissue Eng Part A* **2010**.

255. Mansouri, S.; Fatisson, J.; Miao, Z.; Merhi, Y.; Winnik, F. M.; Tabrizian, M. Silencing Red Blood Cell Recognition toward Anti-A Antibody by Means of Polyelectrolyte Layer-by-Layer Assembly in a Two-Dimensional Model System (dagger). *Langmuir* **2009**.

256. Maurstad, G.; Morch, Y. A.; Bausch, A. R.; Stokke, B. T. Polyelectrolyte layer interpenetration and swelling of alginate-chitosan multilayers studied by dual wavelength reflection interference contrast microscopy. *Carbohydrate Polymers* **2008,** *71* (4), 672-681.

257. Schneider, G.; Decher, G. Functional core/shell nanoparticles via layer-by-layer assembly. investigation of the experimental parameters for controlling particle aggregation and for enhancing dispersion stability. *Langmuir* **2008,** *24* (5), 1778-1789.

258. Phu, D. N.; Yamaguchi, K.; Scheid, P.; Piiper, J. Kinetics of Oxygen-Uptake and Release by Red-Blood-Cells of Chicken and Duck. *Journal of Experimental Biology* **1986,** *125*, 15-27.

259. Yamaguchi, K.; Nguyenphu, D.; Scheid, P.; Piiper, J. Kinetics of O-2 uptake and release by human-erythrocytes studied by a stopped-flow technique. *Journal of Applied Physiology* **1985,** *58* (4), 1215-1224.

260. Piiper, J.; Nguyenphu, D.; Yamaguchi, K.; Scheid, P. Oxygen-transfer kinetics of avian red-blood-cells. *American Zoologist* **1986,** *26* (4), A48.

261. Kujawa, P.; Schmauch, G.; Viitala, T.; Badia, A.; Winnik, F. M. Construction of viscoelastic biocompatible films via the layer-by-layer assembly of hyaluronan and phosphorylcholine-modified chitosan. *Biomacromolecules* **2007,** *8* (10), 3169-3176.

262. Xie, Y. L.; Wang, M. J.; Yao, S. J. Preparation and characterization of biocompatible microcapsules of sodium cellulose sulfate/chitosan by means of layer-by-layer self-assembly. *Langmuir* **2009,** *25* (16), 8999-9005.

263. Bertholon, I.; Vauthier, C.; Labarre, D. Complement activation by core-shell poly(isobutylcyanoacrylate)-polysaccharide nanoparticles: Influences of surface morphology, length, and type of polysaccharide. *Pharmaceutical Research* **2006,** *23* (6), 1313-1323.

264. Rayat, G. R.; Rajotte, R. V.; Ao, Z. L.; Korbutt, G. S. Microencapsulation of neonatal porcine islets: Protection from human antibody/complement-mediated cytolysis in vitro and long-term reversal of diabetes in nude mice. *Transplantation* **2000,** *69* (6), 1084-1090.

265. Zou, S. M.; Wu, Y. Y.; Cable, R.; Dorsey, K.; Tang, Y. L.; Hapip, C. A.; Melmed, R.; Trouern-Trend, J.; Carrano, D.; Champion, M.; Fujii, K.; Fang, C.; Dodd, R. A prospective study of multiple donor exposure blood recipients: surveillance value and limitations for hemovigilance. *Transfusion* **2010,** *50* (1), 128-138.